Catchment Structure Regulates Hydrodynamic Drivers of Chemical Weathering in Shallow Forest Soils

Amanda Pennino

Dissertation submitted to the faculty of the Virginia Polytechnic Institute and State University in partial fulfillment of the requirements for the degree of

Doctor of Philosophy
In
Forest Resources and Environmental Conservation

Brian D. Strahm, Co-Chair
Kevin J. McGuire, Co-Chair
Scott W. Bailey
Madeline E. Schreiber
Benjamin C. Gill

May 3rd, 2023
Blacksburg, Virginia

Keywords: mineral weathering, forest soils, pedology, hydrology, catchment science, carbon, ecosystem science

Catchment Structure Regulates Hydrodynamic Drivers of Chemical Weathering in Shallow Forest Soils

Amanda Pennino

ABSTRACT

Determining where, when, and how subsurface flow affects soil processes and the resulting arrangement of soil development along flow paths is challenging. While hydrologic regime and soil solution acidity are known to influence weathering rates and soil transformation processes, an integrated understanding of these factors together is still lacking. This dissertation explores the effects of subsurface flow on the mobility and distribution of dissolved organic carbon (DOC) and base cations to explain spatial patterns in chemical weathering in a forested headwater catchment. In the first chapter, relationships between hydrologic behavior, fluxes of weathered elements, and the extent of soil elemental loss across landscape positions are established. The second chapter investigates what specific groundwater behavior best explains spatial patterns in solution DOC concentrations during storm events. Lastly, in the third chapter, near surface saturation dynamics are examined to determine when and where DOC mobilization might be enhanced by subsurface flow. Results show that weathering extent was greatest in the upper reaches of the catchment, where O horizon saturation frequency and DOC concentrations are highest. Annual base cation fluxes, which were also greatest in these positions, could indicate where weathering is likely still enhanced. Additionally, while O horizon saturation occurred across the catchment, spatial differences in DOC concentrations suggest there are other sources of acidity to groundwater solutions other than just leaching from O horizons. Shallow organic soils, near bedrock outcrops at the top of the catchment is likely this additional C source, in which drainage water is transported downslope to nearby mineral soils when water tables are high and hydrologic connectivity between soils is increased. Spring and fall storm events were identified as times when groundwater most frequently reached O horizons during the snow-free year, providing insight into the timing of these processes throughout the year. This dissertation highlights how catchment structure mediates DOC flushing events, which in turn,

influences the spatial architecture of soil development and chemical weathering processes across the landscape.

Catchment Structure Regulates Hydrodynamic Drivers of Chemical Weathering in Shallow Forest Soils

Amanda Pennino

GENERAL AUDIENCE ABSTRACT

This dissertation explores how the movement and chemistry of groundwater influences chemical weathering in forest soils. Chemical weathering is an important process in which rocks and soils are broken down into soil nutrients and water-soluble elements. The control of weathering processes by spatial and temporal differences in water behavior across landscapes is not well understood. To address these knowledge gaps, this dissertation measured groundwater fluctuations, solution chemistry, and nutrient fluxes across a mountainous forested landscape. Results from this work found that areas with more frequent flushing of organic matter-rich soil horizons (i.e., soil layers) increases groundwater acidity, which can enhance weathering processes. Flushing frequency of organic-rich horizons and soil nutrient fluxes were greatest in the highest elevation portions of the landscape, where soils were most weathered (greatest loss of soil nutrients). This study revealed that flushing events occurred most frequently in spring and fall storm events during the snow-free year, shedding light on the when weathering might be most enhanced. Overall, this research demonstrates that topographic graphic position described differences in catchment groundwater behavior and solution acidity, which contributes to predictable patterns of weathering and soil development across the landscape.

Acknowledgements

I want to thank all of those who have helped and supported me throughout my time at Virginia Tech.

First, I would like to thank my advisors Brian Strahm and Kevin McGuire for their invaluable guidance on this dissertation and continuous encouragement to make this research my own. I am grateful for their patience and support as I took a nontraditional route towards the finish line. Additionally, I cannot express enough how much I appreciate their excitement for science and mentoring- their enthusiasm is unmatched.

I would also like to extend my gratitude to my research committee (Scott Bailey, Madeline Schreiber, and Benjamin Gill) and Virginia Tech faculty (JP Gannon, Corey Green, and Angela Possinger) who have provided insightful comments, constructive feedback, and many thought-provoking discussions which have helped shape the development of this dissertation.

A huge thanks to the entire Lateral Weathering Across Gradients group (Jennifer Bower, Stephanie Duston, Joshua Benton) and to those who have helped me in the field and in the lab over many years (Delaney Peterson, Nathaniel Rasnake, Kara Crawford, Kaitlyn Hogarth, Tammy Wooster, Geoff Wilson, David Mitchem). It takes a village.

Last, but not least, I would like to thank my parents, Scott and Barbara Pennino who have always encouraged me to always chase my dreams, even if it meant playing in the dirt. And of course, to my husband Eric Bronnenkant, who has been a constant source of patience and support through these years.

This research was supported by the National Science Foundation Geobiology and Low Temperature Geochemistry Program (EAR 1643327) and Long-Term Ecological Research Network (LTER, DEB 1637685). Additional support was provided by the Global Change Center at Virginia Tech and the Edna Bailey Sussman Foundation.

Table of contents

List of Figures

Figure 4. Relationship between bedrock-weighted Upslope Accumulated Area (UAAb) and Topographic Wetness Index (TWI) and elevation at the location of each well.

Figure 5. Groundwater response rates by A) season and B) season by well group (Q1-Q4). A groundwater response was determined by a rise in the water level at least 2 cm above the maximum recording depth. The number of responses were divided by total responses + non-responses to arrive a response rate percentage (%).

Figure 6. Boxplots of peak water level for all storm event groundwater responses between groundwater groups. Lower case letters above each box denote significant differences between well groups ($p < 0.001$). Boxplot lines display the range of minimums and maximum values, boxes represent the interquartile range, and dots show outliers.

Figure 7. Peak groundwater responses for all storm events characterized in this study across increasing storm precipitation. Trend lines within each panel are LOESS (locally weighted smoothing) lines. Dotted black horizontal lines denote the median and lower depths of the organic horizon, which was calculated from the lower depths of Oa horizons in 36 soil pits described in the catchment (Fig. 1).

Figure 8. Saturation frequency of organic horizons for all UAAb well groups (Q1-Q4) for storm events across all snow-free seasons (May-Nov). Saturation frequency was calculated as the number times the peak depth of the water table crossed over the threshold of the median catchment Oa horizon (14 cm) and deepest catchment Oa horizon (30 cm), divided by the total number of groundwater responses.

Figure 9. Median peak water level reached across all storm events for each well. Shapes indicate which well group (Q1-Q4) each well classified as. Top panel: shapes are colored by the average duration of time water levels sat at or above 30 cm (deepest Oa horizon lower boundary). Bottom panel: shapes are colored by average DOC concentration (mg/L) for all groundwater samples taken between the months of May and November. Gray colors indicate that no groundwater chemistry data was available for that well.

List of Tables

Introduction and Justification

The recovery of soil nutrient status following persistent nutrient leaching losses from acid rain remains an ongoing area of research (e.g., Cawley et al., 2014; Laudon et al., 2021). Decades of atmospheric deposition of sulfuric and nitric oxides from fossil fuel emissions has led to the acidification of soils and surface waters across northeast US forests (Driscoll et al., 2001; Johnson and Lindberg, 2013). Increased inputs of anions from acid rain have accelerated the removal, leaching, and export of base cations (e.g., Ca^{2+}) from soils thereby altering the forest nutrient availability and the composition and health of forests (Fahey et al., 1988; Hugget et al., 2007). Additionally, increased concentrations of inorganic aluminum concentrations mobilized to streams has significantly impacted aquatic species mortality in this region (Baker et al., 1996; Baldigo and Lawrence, 2001). Therefore, measuring controls on nutrient replenishment (e.g., base cations) to soils through mineral weathering processes in forested ecosystems affected by acid rain is critical (Oliva et al., 2003).

Mineral weathering, the physiochemical breakdown of rocks, is a significant long-term contributor of nutrients controlling the production and formation of soil landscapes, chemistry of surface waters, and regulation of atmospheric CO_2 levels (Amundson et al., 2007; Berner and Berner, 1997; Bluth and Kump, 1994; Likens et al., 1967; Miller and Drever, 1977; van Breemen and Buurman, 2002;). However, quantifying mineral weathering processes at the ecosystem scale is difficult due to obscuring signals of weathered elements by intrasystem nutrient cycling, which often happen at a more rapid pace (Bormann and Likens, 1967). Identifying key drivers of mineral weathering is also challenging due the inherent variability in soil properties and water availability. In addition, the measurement and prediction of many ecosystem processes, such as weathering, rely on constraining how these factors vary within soil profiles, and across landscapes, both spatially and temporally. Many approaches have been taken to measure and refine annual weathering fluxes (e.g., Bailey et al., 1996, Bailey et al., 2003; Millot et al., 2002; Augustin et al., 2018; Likens et al., 1998), though unfortunately, interpretations have become increasingly convoluted due to alterations of hydrologic and nutrient cycles from anthropogenic disturbances and climate change.

At the local scale (e.g., mineral, within-pedon), weathering rates from chemical dissolution are highly dependent on environment conditions such as temperature, pH, redox conditions, biotic activity and, solution ionic strength and saturation (Carroll, 1970; Langmuir, 1997; Lasaga et al., 1994). Lithologic properties affect resistance to chemical alteration, such as mineral composition, porosity, and grain size (Maher et al., 2004; White and Brantley, 2003). The solubility of mineral constituents leads to differential weathering rates for certain elements which, when scaled up, explains unique chemical signatures of river waters globally (Bluth and Kump, 1994; Pye, 1986).

The conventional trajectory of weathering through the regolith is thought to advance from the soil surface, where physiochemical denudation and biotic activity is known to be greatest, downward toward unweathered bedrock. The interaction of minerals with infiltrating acidic meteoric waters and the enhancement of pedoturbation processes (e.g., physical churning from freeze thaw, tree throw, biologic mixing), results in an upward advancement in regolith thickening and soil production (Bazilevskaya et al., 2013; Riebe, et al., 2017). In this conceptual model, solutes in solution move downward with percolating water and transported deeper in the soil profile. In pedology, these transformation and translocation processes lead to formation of vertical layering or subsurface soil horizons (e.g., albic, argillic, calcic, spodic horizons).

However, at the landscape scale, the unidirectional interpretation of the vertical weathering front discounts lateral water movement along hillslopes, which alter moisture conditions and transfer of solutes between pedons along subsurface flow paths. While lateral transport processes are well recognized in the context of sediment and solute transport mechanisms, only relatively recently has it been incorporated in models for deriving chemical weathering rates (Mudd and Furbish, 2006; Wen et al., 2022; Xiao et al., 2021; Yoo et al., 2007). It is well recognized that weathering accelerates with increasing solution acidity (Blum and Stillings, 1995; Huan and Kian, 1972; Welch and Ullman, 1996). Additionally, it is also known hydrologic conditions regulate the movement of dissolved organic carbon, which enhances solution acidity across landscapes (e.g., Musloff et al., 2018; Perdrial et al., 2018; Raymond et al., 2016; Sebestyen et al., 2008; Wen et al., 2020). Therefore, in landscapes where hydrological

and biogeochemical regimes vary greatly along across topographic gradients, establishing linkages between subsurface flow dynamics and weathering reactions is still needed.

Shallow subsurface flow hydrologically connects upland soils to streams and thus, is an important component of stormflow generation (Anderson and Burt, 1990; Shanley et al., 2015; Sidle et al., 2000) and nutrient export (Herndon et al., 2015; Keller et al., 2019; McGlynn and McDonnell, 2003). Studies have shown that in steep mountainous areas with permeable soils, topography plays a key role as a spatiotemporal organizer of water movement (Anderson and Burt, 1978; Hinton et al., 1993; McGuire et al., 2005; Tromp-van Meerveld and McDonnell, 2006). In areas where soils are shallow to bedrock, or a limiting layer is present, vertical water movement and storage is restricted and water flows downhill. Conversely, where soils are thicker and relief is low, water tends to accumulate and persist in soils. To describe groundwater behavior across catchments, topographic metrics derived from surface slope are often used as a representation of hydraulic gradient (Beven and Kirkby, 1979; Rinderer et at., 2016; Seibert and McGlynn, 2007; Thompson and Moore, 1996), even though it is recognized that underlying heterogeneity can obscure topographic controls (Benton et al., 2022).

At Hubbard Brook Experimental Forest (HBEF), interactions between soils and subsurface flow paths are necessary for understanding spatial variations in soil development across forested catchments. The HBEF is in the White Mountains of New Hampshire, USA, which is a humid glaciated landscape with soils classified primarily as Spodosols. Intensive soil characterization and mapping has led to the description of unique podzol types, regionally known as hydropedological units based on their associations with hydrologic regimes (Bailey et al., 2014; Gillin et al., 2015). The distribution in podzol expression, such as the presence or dominance of various spodic horizons (e.g., eluvial vs. illuvial horizons), is thought to have formed by variations in groundwater behavior and flow paths controlling the formation and lateral movement of spodic materials across the landscape (Bailey et al., 2014; Bourgault et al., 2017; Gannon et al., 2014; Gannon et al., 2017).

The prevailing hypothesis of soil formation at HBEF is that areas highest in the landscape near bedrock outcrops, which are interlaced with shallow organic soils, undergo frequent saturation with the rising of the transient water table during

precipitation events and act as sources of acidity to the catchment (Bailey et al., 2019). As organic-rich soils drain, groundwater with high concentrations of organic acidity (e.g., DOC) enhance mineral weathering processes to form soils that are predominantly E-horizons (eluvial) on top of bedrock. Chemical dissolution of primary minerals releases soluble metals that can chelate with organic acids to form Fe- and Al-complexes. These organometallic complexes are transported and immobilized along lateral flow paths downslope to where soils are thicker, and the transient water table tends to stay lower in the soil profile. Farther from bedrock outcrops, soils are characterized as being enriched in illuvial spodic materials (e.g., Bhs, Bs, Bh horizons).

Groundwater behavior, solution chemistry, and soil development are known to vary systematically across HBEF; however, a quantitative understanding of the hydrologic drivers controlling spatial variation in solution acidity is still lacking. Additionally, it must also be considered that current morphology may be relict, and instead represent hydrologic processes of a wetter climate on a younger (more chemically reactive) landscape of the past. If frequent flushing of organic acidity is a dominant driver of mineral weathering and the transport of weathered elements, then identifying when and where DOC mobilization occurs could be of importance for interpreting base cation replenishment to soils and downslope C-sequestration rates. The work presented in this dissertation aims to address many of these presented knowledge gaps.

Chapter 1 aims to characterize the spatial arrangement of base cation fluxes through the shallow soil zone. Annual estimations of base cation fluxes were measured using ion-exchange resins along topographic gradients. Relationships are drawn between flux magnitude and annual saturation dynamics (i.e., duration and frequency) at multiple soil depths. Established relationships are then used to draw conclusions between current-day annual solute flux dynamics and long-term weathering observations from profile elemental depletion calculations at each location. Based on what is already known about spatial variations in groundwater solution acidity at HBEF, any observed relationships between the physical flushing of groundwater mediating solute export from soils with patterns in mineral weathering is likely only part of the story. Therefore, further investigation into the spatiotemporal dynamics of groundwater behavior and solution acidity is warranted.

In Chapter 2, groundwater response metrics during storm events were examined as potential drivers of shallow groundwater DOC concentrations. Using terrain-based wetness metrics as organizing principles, groundwater responses were categorized into groups. Common groundwater behavior and DOC concentrations between each group was used to infer the role catchment topography has on mediating subsurface flow dynamics, and thus, where DOC flushing events occur. Although not specifically analyzed in this chapter, it is likely that the mobilization of DOC could be related to the degradation and saturation dynamics of the organic horizon, which is a primary DOC source within soil profiles.

To identify when DOC might be most often mobilized across the catchment, Chapter 3 explores the effects of precipitation magnitude and seasonality on organic horizon saturation across the catchment. Dynamics of saturation and DOC concentrations are compared between landscape positions to infer differences in DOC sources across the landscape. Interpretations presented in this dissertation aim to highlight how catchment structure mediates groundwater behavior and solution DOC chemistry, which in turn, could drive spatiotemporal patterns of present-day mineral weathering rates.

References

Amundson, R., Richter, D.D., Humphreys, G.S., Jobbágy, E.G. and Gaillardet, J., 2007. Coupling between biota and earth materials in the critical zone. *Elements*, *3*(5), pp.327-332.

Anderson, M.G. and Burt, T.P., 1978. The role of topography in controlling throughflow generation. *Earth Surface Processes*, *3*(4), pp.331-344.

Anderson, M.G. and Burt, T.P., 1990. Subsurface runoff. *Process studies in hillslope hydrology*. John Wiley & Sons. pp.365-400.

Augustin, F., Houle, D. and Courchesne, F., 2018. An approach at estimating present day base cation weathering rates: a case study for the Hermine watershed, Canada. *Biogeochemistry*, *140*, pp.127-144.

Baker, J.P., Van Sickle, J., Gagen, C.J., DeWalle, D.R., Sharpe, W.E., Carline, R.F., Baldigo, B.P., Murdoch, P.S., Bath, D.W., Krester, W.A. and Simonin, H.A., 1996. Episodic acidification of small streams in the northeastern United States: Effects on fish populations. *Ecological Applications*, *6*(2), pp.422-437.

Bailey, S.W., Hornbeck, J.W., Driscoll, C.T. and Gaudette, H.E., 1996. Calcium inputs and transport in a base-poor forest ecosystem as interpreted by Sr isotopes. *Water Resources Research*, *32*(3), pp.707-719.

Bailey, S.W., Buso, D.C. and Likens, G.E., 2003. Implications of sodium mass balance for interpreting the calcium cycle of a forested ecosystem. *Ecology*, *84*(2), pp.471-484.

Bailey, S.W., Brousseau, P.A., McGuire, K.J. and Ross, D.S., 2014. Influence of landscape position and transient water table on soil development and carbon distribution in a steep, headwater catchment. *Geoderma*, *226*, pp.279-289.

Bailey, S.W., McGuire, K.J., Ross, D.S., Green, M.B. and Fraser, O.L., 2019. Mineral weathering and podzolization control acid neutralization and streamwater chemistry gradients in upland glaciated catchments, northeastern United States. *Frontiers in Earth Science*, *7*, p.63.

Baldigo, B.P. and Lawrence, G.B., 2001. Effects of stream acidification and habitat on fish populations of a North American river. *Aquatic Sciences*, *63*, pp.196-222.

Bazilevskaya, E., Lebedeva, M., Pavich, M., Rother, G., Parkinson, D.Y., Cole, D. and Brantley, S.L., 2013. Where fast weathering creates thin regolith and slow weathering creates thick regolith. *Earth Surface Processes and Landforms*, *38*(8), pp.847-858.

Berner, R.A. and Berner, E.K., 1997. Silicate weathering and climate. *Tectonic uplift and climate change*, Springer Science & Business Media. pp.353-365.

Beven, K.J. and Kirkby, M.J., 1979. A physically based, variable contributing area model of basin hydrology/Un modèle à base physique de zone d'appel variable de l'hydrologie du bassin versant. *Hydrological sciences journal*, *24*(1), pp.43-69.

Bormann, F.H. and Likens, G.E., 1967. Nutrient Cycling: Small watersheds can provide invaluable information about terrestrial ecosystems. *Science*, *155*(3761), pp.424-429.

Bourgault, R.R., Ross, D.S., Bailey, S.W., Bullen, T.D., McGuire, K.J. and Gannon, J.P., 2017. Redistribution of soil metals and organic carbon via lateral flowpaths at the catchment scale in a glaciated upland setting. *Geoderma*, *307*, pp.238-252

Blum, A.E. and Stillings, L.L., 2018. Feldspar dissolution kinetics. In *Chemical weathering rates of silicate minerals* (pp. 291-352). De Gruyter.

Bluth, G.J. and Kump, L.R., 1994. Lithologic and climatologic controls of river chemistry. *Geochimica et Cosmochimica Acta*, *58*(10), pp.2341-2359.

Cawley, K.M., Campbell, J., Zwilling, M. and Jaffé, R., 2014. Evaluation of forest disturbance legacy effects on dissolved organic matter characteristics in streams at the Hubbard Brook Experimental Forest, New Hampshire. *Aquatic sciences*, *76*, pp.611-622.

Driscoll, C.T., Lawrence, G.B., Bulger, A.J., Butler, T.J., Cronan, C.S., Eagar, C., Lambert, K.F., Likens, G.E., Stoddard, J.L. and Weathers, K.C., 2001. Acidic Deposition in the Northeastern United States: Sources and Inputs, Ecosystem Effects, and Management Strategies: The effects of acidic deposition in the northeastern United States include the acidification of soil and water, which stresses terrestrial and aquatic biota. *BioScience*, *51*(3), pp.180-198.

Fahey, T.J., Battles, J.J. and Wilson, G.F., 1998. Responses of early successional northern hardwood forests to changes in nutrient availability. *Ecological Monographs*, *68*(2), pp.183-212.

Gannon, J.P., Bailey, S.W. and McGuire, K.J., 2014. Organizing groundwater regimes and response thresholds by soils: A framework for understanding runoff generation in a headwater catchment. *Water Resources Research*, *50*(11), pp.8403-8419.

Gannon, J.P., McGuire, K.J., Bailey, S.W., Bourgault, R.R. and Ross, D.S., 2017. Lateral water flux in the unsaturated zone: A mechanism for the formation of spatial soil heterogeneity in a headwater catchment. *Hydrological Processes*, *31*(20), pp.3568-3579.

Gillin, C.P., Bailey, S.W., McGuire, K.J. and Gannon, J.P., 2015. Mapping of hydropedologic spatial patterns in a steep headwater catchment. *Soil Science Society of America Journal*, *79*(2), pp.440-453.

Herndon, E.M., Dere, A.L., Sullivan, P.L., Norris, D., Reynolds, B. and Brantley, S.L., 2015. Landscape heterogeneity drives contrasting concentration–discharge relationships in shale headwater catchments. *Hydrology and Earth System Sciences*, *19*(8), pp.3333-3347.

Hinton, M.J., Schiff, S.L. and English, M.C., 1993. Physical properties governing groundwater flow in a glacial till catchment. *Journal of Hydrology*, *142*(1-4), pp.229-249.

Huang, W.H. and Kiang, W.C., 1972. Laboratory dissolution of plagioclase feldspars in water and organic acids at room temperature. *American Mineralogist: Journal of Earth and Planetary Materials*, *57*(11-12), pp.1849-1859.

Huggett, B.A., Schaberg, P.G., Hawley, G.J. and Eagar, C., 2007. Long-term calcium addition increases growth release, wound closure, and health of sugar maple (Acer saccharum) trees at the Hubbard Brook Experimental Forest. *Canadian Journal of Forest Research*, *37*(9), pp.1692-1700.

Johnson, D.W. and Lindberg, S.E. eds., 2013. *Atmospheric deposition and forest nutrient cycling: a synthesis of the integrated forest study* (Vol. 91). Springer Science & Business Media.

Keller, C.K., 2019. Carbon exports from terrestrial ecosystems: A critical-zone framework. *Ecosystems*, *22*(8), pp.1691-1705

Langmuir, D., 1997. Aqueous Environmental Geochemistry. Pearson Education. Prentice Hall: Upper Saddle River, NJ, 600.

Lasaga, A.C., Soler, J.M., Ganor, J., Burch, T.E. and Nagy, K.L., 1994. Chemical weathering rate laws and global geochemical cycles. *Geochimica et Cosmochimica Acta*, *58*(10), pp.2361-2386.

Laudon, H., Sponseller, R.A. and Bishop, K., 2021. From legacy effects of acid deposition in boreal streams to future environmental threats. *Environmental Research Letters*, *16*(1), p.015007.

Likens, G.E., Bormann, F.H., Johnson, N.M. and Pierce, R.S., 1967. The calcium, magnesium, potassium, and sodium budgets for a small forested ecosystem. *Ecology*, *48*(5), pp.772-785.

Likens, G.E., Driscoll, C.T., Buso, D.C., Siccama, T.G., Johnson, C.E., Lovett, G.M., Fahey, T.J., Reiners, W.A., Ryan, D.F., Martin, C.W. and Bailey, S.W., 1998. The biogeochemistry of calcium at Hubbard Brook. *Biogeochemistry*, *41*(2), pp.89-173.

Maher, K., 2011. The role of fluid residence time and topographic scales in determining chemical fluxes from landscapes. *Earth and Planetary Science Letters*, *312*(1-2), pp.48-58.

McGlynn, B.L. and McDonnell, J.J., 2003. Role of discrete landscape units in controlling catchment dissolved organic carbon dynamics. *Water Resources Research*, *39*(4).

McGuire, K.J., McDonnell, J.J., Weiler, M., Kendall, C., McGlynn, B.L., Welker, J.M. and Seibert, J., 2005. The role of topography on catchment-scale water residence time. *Water Resources Research*, *41*(5).

Miller, W.R. and Drever, J.I., 1977. Chemical weathering and related controls on surface water chemistry in the Absaroka Mountains, Wyoming. *Geochimica et cosmochimica acta*, *41*(12), pp.1693-1702.

Millot, Romain, et al. "The global control of silicate weathering rates and the coupling with physical erosion: new insights from rivers of the Canadian Shield." *Earth and Planetary Science Letters* 196.1-2 (2002): 83-98.

Mudd, S.M. and Furbish, D.J., 2004. Influence of chemical denudation on hillslope morphology. *Journal of Geophysical Research: Earth Surface*, *109*(F2).

Musolff, A., Fleckenstein, J.H., Opitz, M., Büttner, O., Kumar, R. and Tittel, J., 2018. Spatio-temporal controls of dissolved organic carbon stream water concentrations. *Journal of hydrology*, *566*, pp.205-215.

Oliva, P., Viers, J. and Dupré, B., 2003. Chemical weathering in granitic environments. *Chemical geology*, *202*(3-4), pp.225-256.

Perdrial, J., Brooks, P.D., Swetnam, T., Lohse, K.A., Rasmussen, C., Litvak, M., Harpold, A.A., Zapata-Rios, X., Broxton, P., Mitra, B. and Meixner, T., 2018. A net ecosystem carbon budget for snow dominated forested headwater catchments: linking water and carbon fluxes to critical zone carbon storage. *Biogeochemistry*, *138*, pp.225-243.

Pye, K., 1986. Mineralogical and textural controls on the weathering of granitoid rocks. *Catena*, *13*(1-2), pp.47-57.

Raymond, P.A., Saiers, J.E. and Sobczak, W.V., 2016. Hydrological and biogeochemical controls on watershed dissolved organic matter transport: Pulse-shunt concept. *Ecology*, *97*(1), pp.5-16.

Riebe, C.S., Hahm, W.J. and Brantley, S.L., 2017. Controls on deep critical zone architecture: A historical review and four testable hypotheses. *Earth Surface Processes and Landforms*, *42*(1), pp.128-156.

Rinderer, M., van Meerveld, I., Stähli, M. and Seibert, J., 2016. Is groundwater response timing in a pre-alpine catchment controlled more by topography or by rainfall?. *Hydrological Processes*, *30*(7), pp.1036-1051.

Chapter 1

Annual Variations in Dynamic Subsurface Stormflow and Base Cation Fluxes: Implications for Chemical Weathering in Shallow Forest Soils.

Abstract

Elemental mass balance approaches have long been used to estimate weathering rates; however, these estimates are often aggregated at a scale (i.e., catchment) that obscures the variation in weathering inputs across pedon to hillslope scales. In forested landscapes, smaller scales are often more important to our understanding of the patterns in species composition, productivity, and nutrient export. It is well known that catchment structure (e.g., topography, soil depth, minerology) can vary greatly, and at relatively short distances, leading to hypotheses that elemental fluxes will also vary greatly along hillslopes. This study measured annual base cation fluxes commonly associated with chemical weathering reactions (Ca^{2+}, Mg^{2+}, Na^{+}) within the shallow soil zone (<1 m depth), where the transient groundwater table frequently reaches near the soil surface. Fluxes were measured using a combination of ion-exchange resins placed in groundwater wells and hydrologic measurements of annual groundwater fluctuations. Base cation fluxes were positively correlated with spatial variations in the soil saturation frequency, which varied by topographic position, and was greatest in soil profiles that were most elementally depleted (highly weathered). Results from this study suggest that mineral weathering could be highest in soil profiles that are most frequently flushed during storm events, when groundwater is most responsive. These findings have broad implications for reinterpreting spatial variations in catchment chemical weathering, which replenishes nutrients back to nutrient-depleted forest soils following acid rain deposition.

Introduction

Across northeast US forests, decades of acid deposition have fundamentally altered soil chemistry, fueling important questions regarding rates and controls on base cation replenishment (Lawrence et al. 2015; Siemion et al. 2018; Johnson et al., 1981). Even prior to this disturbance, the soils in this region that are not underlain by calcareous bedrock typically have low base saturation, defined as the proportion of cation exchange sites occupied by Ca^{2+}, Na^{+}, Mg^{2+}, and K^{+}, and have limited capacity to neutralize inputs of acidity as a result. Consequently, significant changes in precipitation chemistry across acid-sensitive forests in northern Europe and eastern North America has led to widespread soil acidification and elevated concentrations of toxic inorganic forms of aluminum in soil and stream waters (Cronan and Schofield, 1990; Driscoll et al., 2001). Long-term data has shown elevated concentrations of acidic compounds in stream water during this time correlated with the rapid export of base cations, likely relinquished from the soil exchange complex, which has resulted in the depletion of nutrients in forest ecosystems still prevalent today (Likens et al., 1996; Driscoll et al., 2001; Lawrence et al., 2016; Johnson et al., 2018). Mineral weathering provides a long-term replenishment of base cations to soils and surface waters; however, scaling laboratory and observational chemical weathering rates is still a great challenge (White and Brantley, 2003). Therefore, increasing our understanding of the spatial and temporal variation in processes that regulate weathering rates within acid-affected ecosystems is important for measuring the replenishment of base cation pools.

Precipitation is a primary rate-controlling factor affecting chemical weathering reactions (Brantley et al., 2008; White and Blum, 1995), especially in systems where the effects of physical erosion (Millot et al., 2002; Riebe et al., 2004) and soil developmental age (Taylor and Blum, 1995; White and Brantley, 2003) are minimized. Numerous studies have demonstrated the dependence of mineral weathering on climate, such as relating runoff rates to river geochemistry (Bluth and Kump, 1994; Godsey et al., 2009; Oliva et al., 2003; West et al., 2005) and soil pedogenesis across climosequences (e.g., Chadwick et al., 2003; Dahlgren et al., 1997; Dere et al., 2016; Dixon et al., 2016; Lybrand and Rasmussen, 2015; Rasmussen et al., 2011). In general, conditions that favor increased water contact time with reactive mineral surfaces promote dissolution reactions

(Anderson et al., 2002; Berner and Berner, 1997; Lasaga et al., 1994; Oliva et al., 2003). However, if weathered products are not flushed away from reaction sites, concentrations approach thermodynamic equilibria with increasing fluid residence time (Benettin et al., 2015; Maher, 2011). Therefore, dissolution reactions rates are also heavily dependent on water flow rates.

It is well established that hillslope topography (e.g., form and structure) is an important control on the spatiotemporal organization of mineral-water interactions by determining water flow paths (e.g., Beven and Germann, 1982; Jencso et al., 2009; Weiler et al., 2006; Western et al., 1999) and by extension, influencing water residence and travel times (e.g., Maher, 2011; McGuire et al., 2005; Tetzlaff et al., 2009; Xiao et al., 2021). In mountainous forested landscapes, hillslopes are often dominated by steep topography and thin, permeable soils which can promote the formation of shallow transient water tables and lateral subsurface flow paths (e.g., storm events, snowmelt) (Freer et al., 2002; Jackson, 1992). Analogous to the horizontal formation of soil horizons within soil pedons, water fluxes in the lateral direction mobilize, translocate, and accumulate solutes downslope from their point of origin (generation), such as those described by the lateral podzolization phenomenon (Bailey et al., 2014; Jankowski, 2014; Sommer et al., 2000, 2001). Subsurface stormflow (also known as "lateral flow", "throughflow", "subsurface runoff", etc.) is often considered a significant runoff generation mechanism in forested headwater catchments (Anderson and Burt 1978; Mosley 1979; Pearce, Stewart, and Sklash 1986; Weiler et al. 2006), and is important for developing hydrologic connectivity between upper and lower areas of the catchment and the rapid transport of solutes to adjacent streams (Bracken and Croke, 2007; Detty and McGuire, 2010; Jencso et al., 2009; McGlynn and McDonnell, 2003; Weiler et al., 2006).

While whole-catchment base cation export during flushing periods is generally well quantified (Inamdar et al., 2009; Knapp et al., 2020; Musolff et al., 2021), less is known about internal catchment variation in lateral solute fluxes in the shallow soil zone (Augustin et al., 2018; Johnson et al., 2000). It might be expected that catchment exports of cations would linearly decrease with increasing discharge due to source limitations, or, as runoff contributions come from increasingly dilute waters. However, studies using concentration discharge (C-Q) relationships have shown that geogenic solutes generally

show “chemostatic” export behavior, meaning changes in concentrations are not proportional to changes in discharge (Godsey et al., 2009). The mechanism behind the relatively invariant export of these solutes across a wide range of catchments and hydrologic conditions is still not fully reconciled although several hypotheses have been proposed, such as the flushing of stored water or cation exchange processes, among others (Clow and Drever, 1996; Kim et al., 2017; Li et al., 2017; Maher, 2011), which would provide additional solutes to stream export and masking a dilution response. It is likely that these mechanisms act non-uniformly within a catchment, especially as catchments wet up and upland soils become more intimately connected with stream networks. Interpretations of C-Q patterns are limited by the aggregated chemical signal of combined hillslope processes at the sampling location or discrete sampling events. Additionally, as Kim et al. (2017) point out, traditional C-Q methods often lack frequent, if any, direct hillslope observations of processes that control the evolution of solute chemistry, which masks the variability of water table dynamics and groundwater chemistry known to exist within catchments (Bailey et al., 2019; Kiewiet et al., 2019; Gannon et al., 2014).

In this study we aim to characterize the spatial arrangement of annual base cation fluxes through the variably saturated shallow soil zone (<1 m) at the hillslope scale. We hypothesize that differences in saturation dynamics, which regulate solute generation and transport, control spatial variations in solute fluxes along hillslopes. To test this hypothesis, we evaluate the explanatory power of shallow groundwater dynamics on base cation mobilization where base cation fluxes were measured. Additionally, we investigate linkages between catchment properties that predict saturation dynamics and observed differences in mineral depletion. We use this data as evidence that solute fluxes within catchments are neither uniform nor random, but rather exist in a systematic spatial arrangement determined by the controls of catchment structure on lateral subsurface flow and chemical weathering processes.

Materials and methods

Site description and experimental design

This study took place at the Hubbard Brook Experimental Forest (HBEF), in watershed 3, a hydrologic reference watershed with no controlled manipulations (Fig. 1). The HBEF, located in the White Mountains of New Hampshire, is classified as a cool temperate, humid-continental climate with an average of 1,400 mm of precipitation annually (Bailey et al., 2003). The watershed is dominated by northern hardwoods, including Sugar Maple (*Acer saccharum*), Yellow Birch (*Betula alleghaniensis*), American Beech (*Fagus grandifolia*), Balsam Fir (*Abies balsamea*), and Mountain White Birch (*Betula papyrifera* var. *cordifolia*).

The bedrock geology of watershed 3 is dominated by Rangeley Snbchist, overlain by glacial till of variable depths. At HBEF, soils are predominantly classified as Spodosols with sandy textures and thick O/A horizons, and local areas of Inceptisols and Histosols (Bailey et al., 2003). Higher elevations of the watershed are dominated by bedrock outcrops and shallow organic soils (Fraser et al., 2020). Intensive soil characterization and mapping led to locally recognized soil map units based on variations in lateral spodic expression that generally occur in a downslope gradient from ridges to lower elevation riparian areas downslope positions (Gillin et al., 2015). Characteristic shallow groundwater regimes (water table occurrence, persistence, and depth) associated with each soil map unit suggests hydrologic behavior is an important soil forming factor in upland positions at HBEF (Bailey et al., 2014; Gannon et al., 2017).

Three areas towards the top of the catchment were chosen as investigative transect sites for this study (Fig. 1). At each of the three transects, wells were installed at three different locations along the hillslope, targeting a range in soil map units along the catena (9 water level logging wells). Wells were constructed using 2-inch diameter PVC with 2 inches of PVC screen (slot size 0.01 inches) and were installed to the top of the C horizon, or if none existed, at the bedrock surface. Previous work at this site suggests that the transient water table, which develops during precipitation and snowmelt events, perches at the top of the C horizon due to differences in saturated hydrologic connectivity (Detty and McGuire, 2010). Therefore, water level measurements were only made in the variably saturated zone (i.e., above the C-horizon) and water levels below this depth was

not measured. Groundwater levels were made using pressure transducer loggers (HOBO Onset U20 & U20L) at 10-minute intervals. Raw pressure data was corrected for atmospheric pressure by using barometric pressure data from a logger installed in a dry well.

Within five meters, adjacent to each of the water level logging wells, narrowly dug pits were carefully excavated to the same depths as the nearby shallow wells. Following soil profile characterization and horizon sampling (described in section 2.2), an additional well was installed to house ion-exchange resins used for making elemental mass flux estimations (Fig. 1).

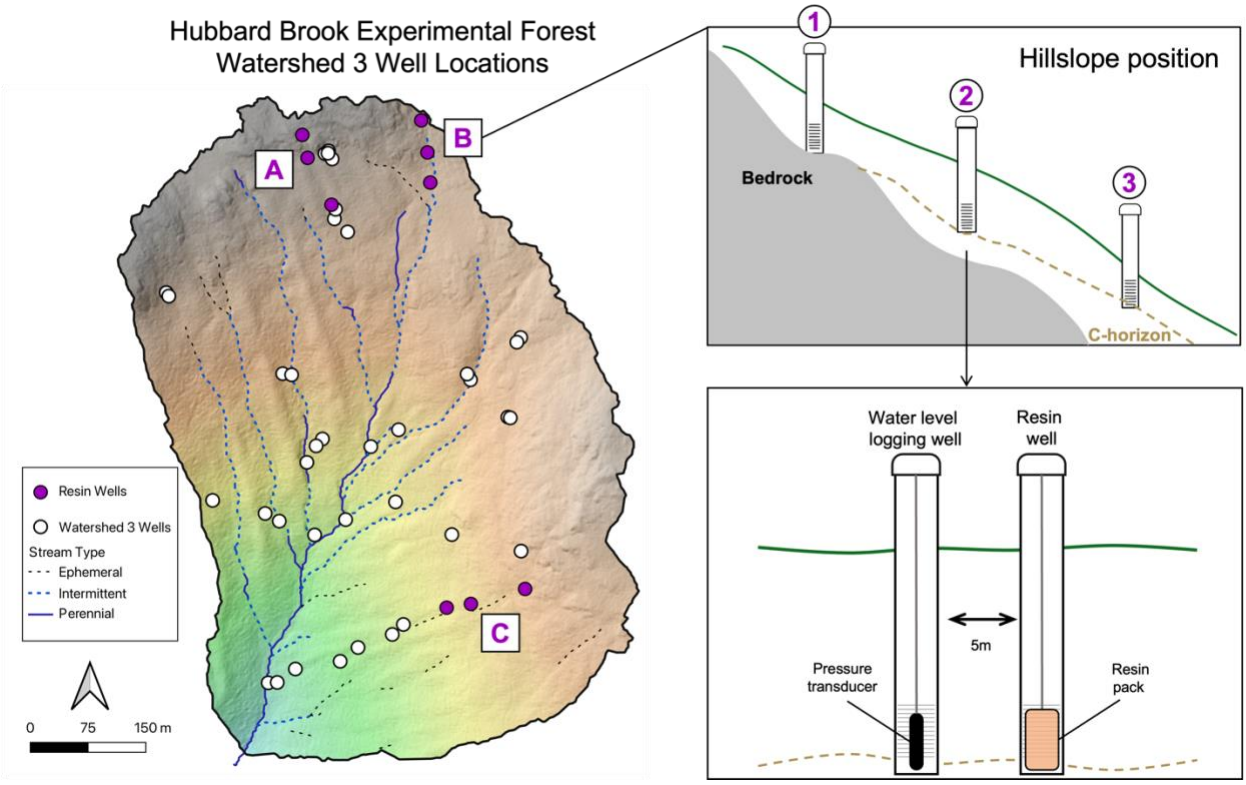

Figure 1. Left: Digital elevation model (DEM) of watershed 3 at Hubbard Brook Experimental Forest, in New Hampshire (USA). Purple circles indicate the locations of three study transects (A-C) and white circles indicate wells that were installed prior to this study that have historical water level data from 2010-2014. Top Right: hillslope cross-section: Along each of the three transects, wells were installed in 2019 along the

hillslope at three different locations (1-3) to the depth of the bedrock or C-horizon interface. Bottom Right: Each location had a well equipped with a pressure transducer to record water levels and within five meters another well was installed where ion exchange resins were placed into for the duration of this study.

Soil characterization and analysis

Soil profiles at all resin-well locations were morphologically characterized and sampled by genetic horizon (Schoeneberger et al., 2012). Samples were air dried for approximately 1 week and then sieved to < 2 mm. For all mineral horizons sampled, 20 grams of each sample were sent to Activation Laboratories (Ancaster, Canada) to be analyzed for minor and trace elemental concentrations by inductively coupled plasma optical emission spectroscopy (ICP-OES) and inductively coupled plasma mass spectrometry (ICP-MS). Elemental data for fourteen samples of deep C-horizon material from (between 1- 6 m) within watershed 3 were also analyzed and average concentrations were used as a proxy for unweathered parent material. Elemental enrichment or depletion factors were determined by calculating tau values for each *i*th element (τ_i; Ca, Na, Mg, and Al) (Brimhall and Dietrich, 1987) using the following equation:

$$\tau_i = \left(\frac{i_w \times \mathrm{Ti}_w}{i_p \times \mathrm{Ti}_p} - 1\right) \quad [1]$$

Values where $\tau > 0$ indicates elemental mass gain (enrichment) and $\tau < 0$ indicates mass loss (depletion) of weathered material (subscript *w*) in mobile element, *i*, in relation to unweathered reference parent material (subscript *p*). Mobile elemental concentrations were indexed to titanium (Ti), which is minimally biogeochemically cycled and resistant against dissolution (Milnes and Fitzpatrick 1989) making it effectively immobile in the environment. Ti was chosen as an index element over Zr, Y, and Rb due to its higher abundance in these soils.

In addition to the nine excavated soil pits (locations of resin wells), a characterization campaign aimed at describing shallow soil horizon distribution (above the C horizon) took place during 2018 and 2019. Auger investigations surrounding the

three study transect locations occurred at a fine-scale gridded resolution (~5-10 m) where soil horizon presence/absence, color, and thickness was described.

Ion-exchange resins and base cation flux estimations

For this study, ion-exchange resins inserted within wells were used for the estimation of elemental mass fluxes through the shallow soil zone. The application of sorbent material enclosed within screened wells to measure solute mass fluxes in groundwater is modeled after the passive flux meter, first described and laboratory evaluated by Hatfield et al. (2004). However, the use of ion exchange resins to measure nutrient load in terrestrial ecosystems and variably saturated soil has been applied widely across soil science to measure nutrient availability and load (e.g., Kjønaas, 1999; Lehmann et al., 2001; Willich and Buerkert, 2016). The use of a wide range of resins in combination with the passive flux meter design has since been adapted for measuring fluxes of organic contaminants (Annable et al. 2005), arsenic (Clark et al., 2005), uranium (Stucker et al., 2011), phosphate (Cho et al. 2007; Padowski et al. 2009), among many others.

Chosen resins were a mixed-bed cation/anion resin combination of Amberlite IRA-400 and IR-120 combined at a 1:1 milliequivalent ratio. Resins were pretreated with 2 *M* KCl by combing the salt solution and resin at a 3:1 solution-to-resin weight ratio and shaken on a fixed-speed reciprocal shaker (Eberback Model E6010) at 180 oscillations min^{-1} (low speed) for two hours. After allowing the resin to settle, the supernatant was decanted, and resins were rinsed with DI water three times to remove excess salts. Approximately 90 g (moist) of resin was assembled into each resin pack, which was encased in nylon wrapped around two rubber washers (OD: 2 inches, ID: 5/8 inches), along a ½ inch CPVC pipe and sealed with electrical tape and kept moist at 4°C until deployment (Fig. 2). Approximately 400 g of pretreated resin was reserved (not deployed) and kept at 4°C to use as blanks to test resins for any background contributions from resin degradation.

Resin packs were attached to a nylon string and pushed down into each assigned resin well across all transects. The resin packs sat at the bottom of each well within screened PVC, allowing for the lateral interception of water flow through the well

without retaining it. Resin packs were exchanged out four times, with deployment periods ranging from 2-4 months each for a total of one year integration from August 2019-2020.

Following each resin deployment, resins were brought back to the lab and each resin pack was opened, weighed for total moist weight, and subsampled to 20g with 3 replicates. Subsamples were extracted with 2 *M* KCl following similar protocols to pretreatment, using a 3:1 solution-to-resin ratio and shaken for 2 hours. Subsamples went through 2 subsequent extractions to ensure the maximum sorbed solutes was retrieved off the resin beads. Both extractant solutions were analyzed for Ca^{2+}, Mg^{2+}, and Na^{+} using ICP-MS for total elemental mass. The chosen KCl extractant limited our ability to measure sorbed potassium (K^{+}) ions on the resins. Any mass extracted from the resin blanks was subtracted from the extractant's value. Calculations and total mass of each solute extracted from these resins for the total year can be found in Pennino et al., 2023. The mass of solute in solution from each resin subsample extractant was then scaled to represent initial resin weight recorded following deployment. On a per-element basis, each deployment mass was then summed for all deployment periods for each resin location. Total elemental mass (scaled to kg) was divided by deployment time (1-year) to calculate annual mass solute flux (kg yr^{-1}) at each location the resins were deployed.

Annual mass fluxes (kg yr^{-1}) were divided by upslope drainage area (ha), which assumes that all water within this area flows down to a central point at the resin location. Upslope drainage area determined for each resin location was derived using the watershed function in WhiteBoxTools in R (Lindsay, 2014). This tool preforms an watershedding operation based on designated outlet pour points (resin locations). The DEM for watershed 3 was prepared for hydrologic analyses by Fill Depressions (Wang and Liu, 2006) and Least Cost Depression Breaching (Lindsay, 2014) prior to preforming the watershedding operation. Pour points were snapped to a flow accumulation grid created from a d8-derived flow direction raster to map areas that drain to each point. Subwatershed boarders (upslope drainage area) were manually adjusted for known surface artifacts and onsite expert knowledge of the landscape to create upslope areas for each resin and logging well location.

Area-normalized solute fluxes (kg ha^{-1} yr^{-1}) were then scaled to represent a 2-D plane of water moving through each resin pack. The height dimension of each plane was

determined by scaling the height of resin intercepting water to the average height of the water table. Mean annual water levels for each resin location were taken from the nearest water level logging well to the resin. The width dimension of the plane was determined by scaled the width of the resin to a 1-m wide point on the landscape. For the terms used in the calculations, refer to Appendix Table A1.

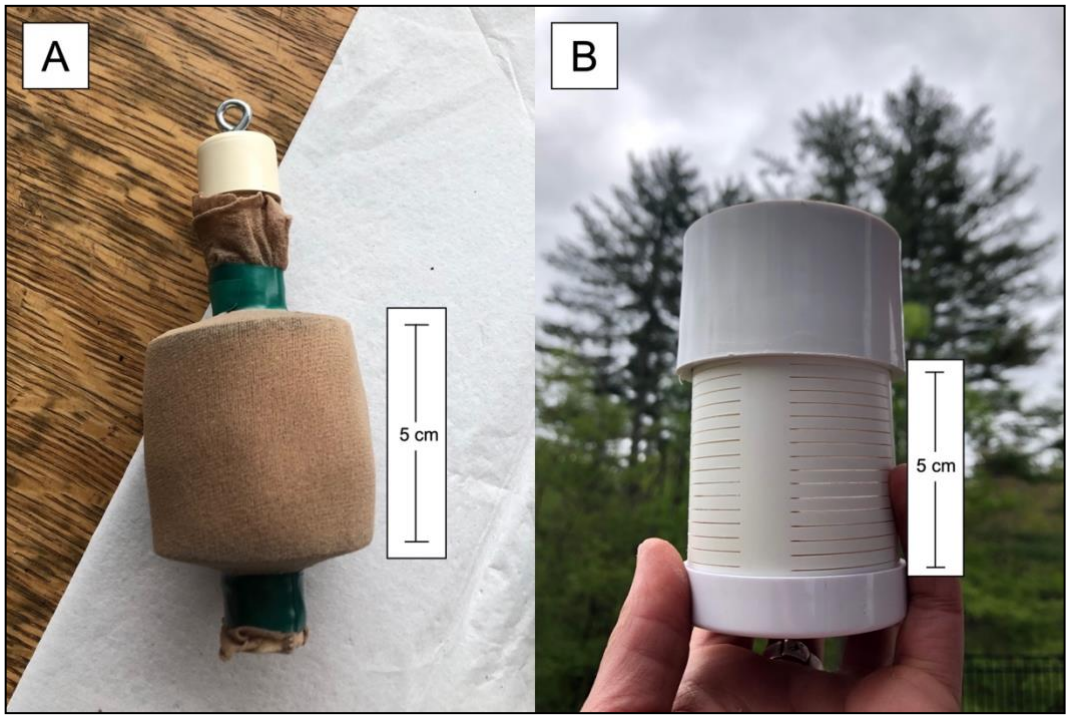

Figure 2. Photographs of resins encased within nylon attached to CVPC piping (A). Resin packs were pushed down into screens attached at the bottom of each well (B) to allow the lateral flow of water through the resin pack.

Saturation metrics and catchment properties

Hydrologic heterogeneity is expected to be a primary control on base cation generation. To test this hypothesis, we calculated saturation dynamics of the transient water table in same nine locations where resins were located during the length of this study. Since topography is a known control on water table dynamics, we also compared calculated hydrologic metrics to topographic information that has been shown to be influential on hillslope hydrologic behavior (e.g., slope, curvature) (Hjerdt et al., 2004) and other

catchment properties that have been useful for predicting spatial patterns in soil development at Hubbard Brook (Gillin et al., 2015).

For this study we focused on two hydrograph metrics: annual saturation frequency and duration at multiple depths. We define saturation frequency as the number of times the water table crossed a threshold depth beneath the surface per year (saturation cycles/yr), where one saturation cycle indicates the water level exceeded and then receded past that depth once. Similarly, saturation duration was calculated as the proportion of time the water table existed at or above a depth during a logging period. Prior to any characterization, water levels were smoothed by aggregating to two-hour timesteps. To test the influence of depth, saturation characteristics were calculated at 5-cm intervals from the soil surface to the depth of the shallowest well (30 cm). If time gaps in the data logging existed, saturation metrics were scaled to a full year.

Upslope attributes were calculated as the mean value of each topographic raster to the spatial extent of the upslope drainage area, determined by watershedding methods outlined in section 2.3. All topographic metrics were calculated generated using R, QGIS (QGIS Development team, 2021), and ArcGIS software and derived from a DEM. All terrain metrics used in this analysis are outlined in Table 1. Additional metrics that were added to the Spearman correlation were depth-weighted means of profile elemental depletion (tau) and the proportion of upslope soil horizon volume for E and B horizons (data used for these metrics are outlined in section 2.2). Values for tau were calculated for all mineral horizons above the C-horizon. Using data collected from extensive auger investigations, total upslope soil volume was determined by finding an average depth to C-horizon, or bedrock if the C did not exist, for each upslope area from the resin location. The average thickness of the B and E horizon within each area was used to determine proportions of the total solum volume. Significance between spearman correlates was evaluated at $p < 0.05$.

To test if relationships between saturation dynamics and catchment attributes at the resin wells (n=9) were applicable at the watershed scale, we analyzed water level data from 34 additional wells installed throughout the catchment, for a total of n=43 wells. Wells were installed between 2008 and 2012 by Detty and McGuire (2010) and Gannon et al. (2014). Chosen wells for this study met the following two qualifications: at least 1

or more years of consecutive water level data and installed into similar shallow depths (at or above the C horizon). A similar timestep aggregation was used to preprocesses all wells prior saturation calculations as the resin wells.

Table 1. Ranges in locally derived and upslope drainage area means of topographic attributes for all wells used in this study. Transect wells are described as those near deployed resins (Figure 1) and are included in the range of values for all watershed 3 (WS3) wells.

Variable	**Metric**	**Topographic characteristic**	**Reference**	**Value range (water level wells) n = 9**	**Value range (WS3 wells) n = 43**
DISTOUT	Linear distance to watershed outlet (m)	Local	QGIS	7 – 172	7 – 267
ELEV	Elevation (m)	Local		602 – 710	529 – 708
TPI100	Topographic position index, 100 m window	Upslope mean	(Guisan et al., 1999)	1.5 – 5.8	-1.3 – 8.4
UAAb	Upslope Accumulated Area, weighted by areas of bedrock and shallow soils	Local	(Gillin et al., 2015)	0.2 – 0.6	0 – 0.6
SLOPE	Downslope gradient (degrees)	Upslope mean	(Hjerdt et al., 2004)	0.17 – 0.36	0.12 – 0.42
PROF	Profile curvature	Upslope mean	QGIS	$-1.7\cdot10^{-3}$ – $7.1\cdot10^{-3}$	$-1.3\cdot10^{3}$ – $8.1\cdot10^{-3}$
PLAN	Planar curvature	Upslope mean	QGIS	$-2.0\cdot10^{-3}$ – $4.3\cdot10^{-2}$	$-2.0\cdot10^{-3}$ – $6.6\cdot10^{-2}$
CONVERGE	Convergence index	Upslope mean	SAGA	-0.4 – 4.3	-0.3 – 4.3
MDFLOW	Multiple direction-infinity flow algorithm	Upslope mean	SAGA; (Seibert and McGlynn, 2007)	57 – 420	57 – 2231
TWI	Topographic Wetness Index ($\ln(m^2)$), using 5m downslope gradient for slope	Upslope mean	SAGA; (Beven and Kirkby, 1979); (Hjerdt et al., 2004)	5.9 – 6.9	5.8 – 7.4

Statistical analyses

Statistical differences between base cation fluxes for each hillslope position and between transects was tested using a one-way analysis of variance test (ANOVA) at a significance level of $p < 0.05$. Simple linear regression models were used to fit relationships between total base cation fluxes (log transformed) and hydrodynamic variables using R software (R Core Team, 2021). The best fit models for frequency and duration were selected based on the highest adjusted r^2 value. The top models chosen for saturation frequency and duration at resin locations were used in a Spearman rank correlation analysis (Spearman, 1904) with local and upslope drainage area properties calculated for the resin well locations, using the 'Hmisc' package in R software Version 4.2.2 (R Core Team, 2021). Local attributes were classified as those extracted at the location of the well. All upslope drainage area properties used in the Spearman correlation were mean values for each upslope drainage area. To investigate the strength of other correlates that may not be represented by the limited number in resin-sites (n = 9), we ran a second Spearman correlation analysis using topographic attributes and hydrodynamic properties including the extended well network of watershed 3 (Fig. 1).

Results

Annual base cation fluxes by hillslope position

Base cations were expected to be greatest in the highest hillslope position (1) in all transects (A, B, C in Fig. 1) and to decrease as a gradient downslope, although no statistical difference in base cation fluxes was found between hillslope positions or by transect. The largest flux estimates for total base cations (sum of Ca^{2+}, Mg^{2+}, and Na^{+}) occurred in hillslope position 1 for transects A and B, at 5.8 and 3.9 kg $ha^{-1}yr^{-1}$, respectively, and generally decreased downslope (Fig. 3). Conversely, total base cations for transect C were greatest in the most downslope position (3) and decreased with increasing elevation, ranging only from 0.54 to 0.21 kg $ha^{-1}yr^{-1}$. Out of all the locations, position C1 had the lowest base cation flux estimations. Elemental fluxes for Ca^{2+} and Na^{+} contributed the greatest toward total base cation flux. Towards the total base cation

flux on average Ca^{2+} contributed 49%, Na^{+} contributed 43%, and Mg^{2+} contributed only 8%.

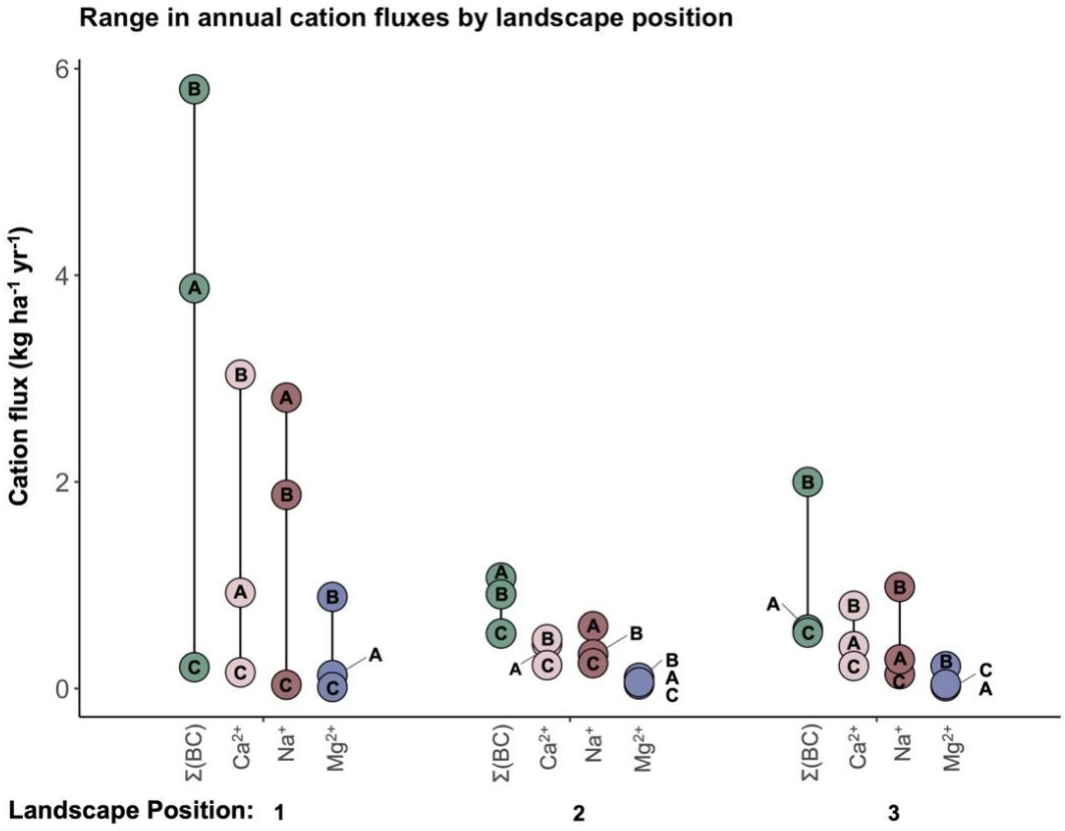

Figure 3. Area-normalized annual solute fluxes (kg ha^{-1} yr^{-1}) for Ca^{2+}, Na^{+}, Mg^{2+}, and sum of base cations measured at three transect locations (A, B, C) at three different hillslopes positions (1, 2, 3).

Hydrodynamic characteristics as predictors of base cation fluxes

During this study period, the presence of the transient water table within the shallow soil zone (<1 m) was responsive to storms and episodic snow melt events (Fig. 4). However, water table depth, persistence, and recession characteristics showed spatial variation between landscape positions.

Water levels associated with resin wells in the upper most hillslope position (1) often exhibited "flashy" behavior, with rapid saturation responses during high flow conditions. On average, water levels rose into and receded completely from the soil

profiles 36 times/yr, with a range of 29-61 saturation cycles/yr. While saturation cycles occurred at a relatively high frequency, duration of saturation through any part of the profile was lower than other landscape positions. The transient water table in any part of the profile only existed in total for 33% of the year. When water did flush through the soil profiles it reached shallow depths (mean response depth 29 cm) near to the soil surface.

Further down the hillslope, the depth to the transient water table tended to exist deeper and for longer periods of time (Fig. 4). A slight exception to this trend was for locations B2 and B3, where the water table was present in the soil profile for a great proportion of the year without receding (83% and 95%, respectively) with an average depth to saturation of ~26 cm (Fig. 4). Nevertheless, the average response depth to the water table for positions 2 and 3 for all transects was 37 cm and 53 cm, respectively. In stark contrast to higher positions on the hillslope, saturation frequency throughout any part of the soil profiles in the two lower positions for all transects was infrequent, with a mean saturation frequency was 16 cycles/yr for position 2, and 8 cycles/yr for position 3.

Overall, saturation duration was a poor predictor of total cation fluxes for all investigated depths ($r^2 \leq 0.22$) compared to saturation frequency (Fig. 5). The number of saturation cycles at or below 15 cm were considered strong predictors ($r^2 \geq 0.54$) whereas shallower depths were not ($r^2 \leq 0.20$). The predictive power of saturation frequency for log transformed total base cations was greatest for 20 cm ($r^2 = 0.86$). Generally, total base cations and individual cation fluxes exponentially increase with an increase frequency in saturation cycles at 20 cm (Fig. 6).

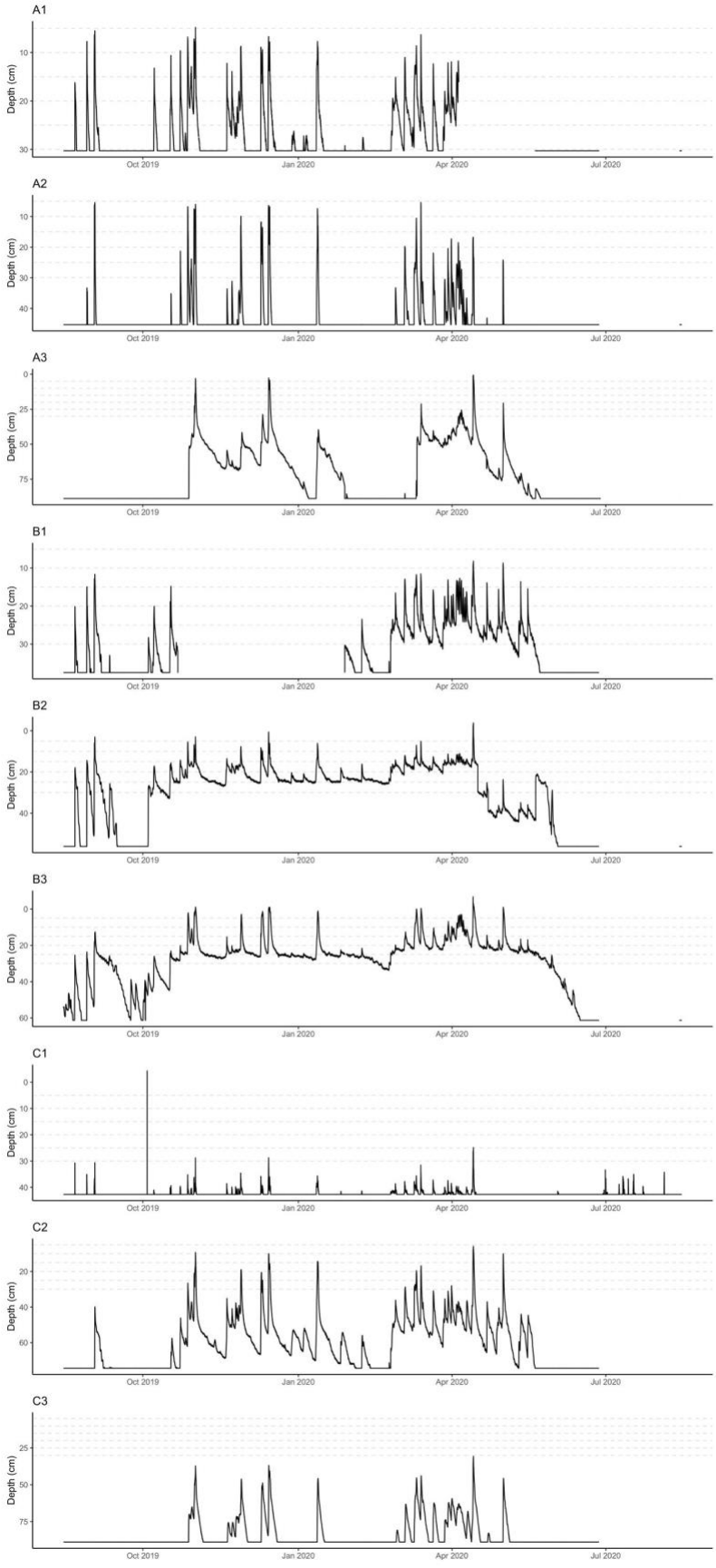
A1
A2
A3
B1
B2
B3
C1
C2
C3
Depth (cm)
Oct 2019
Jan 2020
Apr 2020
Jul 2020

Figure 4. Time series water level recording depths for all wells co-located with wells that held resins (transects A-C, hillslope positions 1-3) during the resin deployment period of one year, from August 2019-2020. All water levels are expressed as depth in centimeters from the soil surface. Steady water levels indicate the absence of the transient water table during that time, whereas no reported recording (blank) indicates missing data from logger errors. Dashed gray lines indicate the depths where saturation frequency and duration were calculated for each well during the study period.

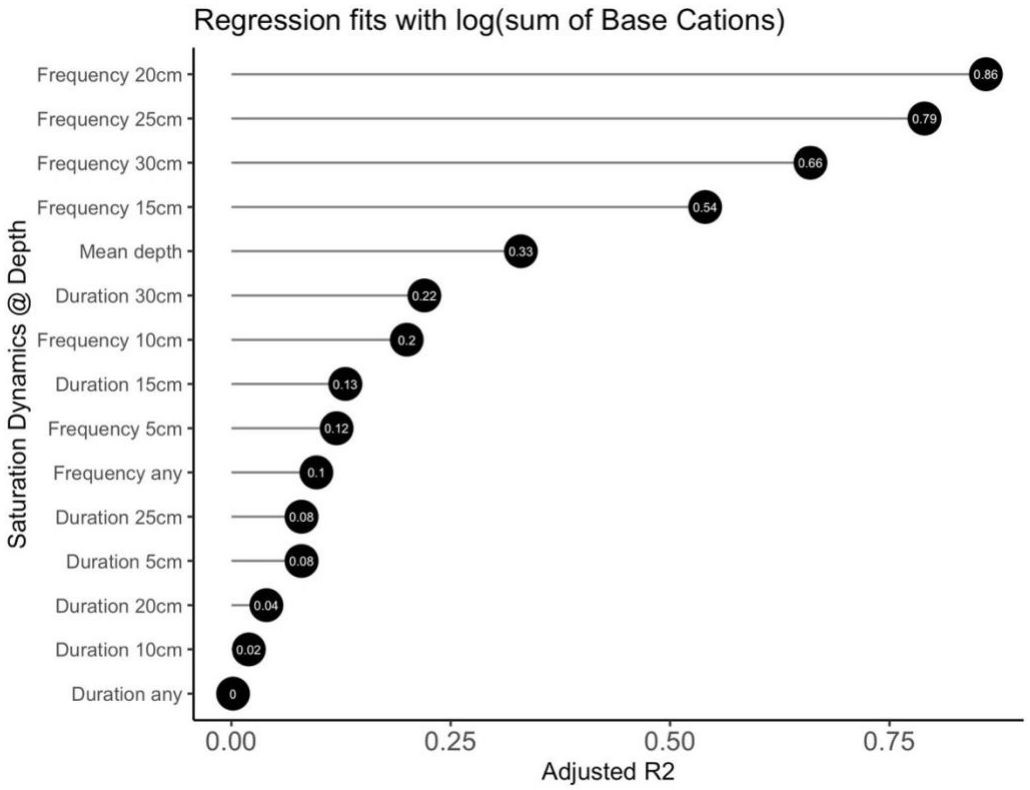

Figure 5. Ranked explanatory variables of sum of base cations used for a simple linear regression model by best fit, determined by highest adjusted r-squared values.

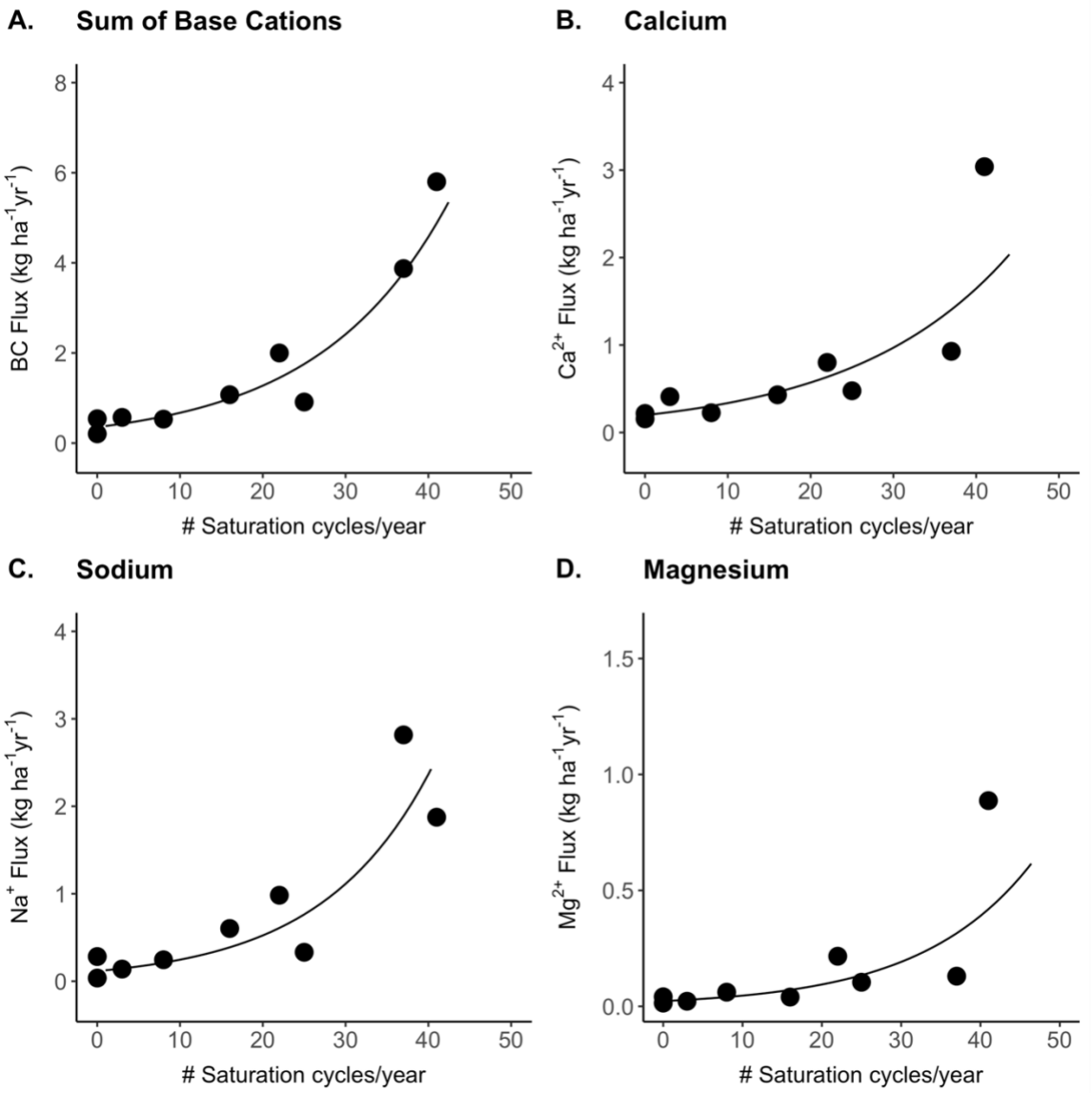

Figure 6. Exponential relationships between measured base cation fluxes (kg ha^{-1} yr^{-1}) and saturation frequency, which is the number of times the water table reached and receded from 20 cm depth from the soil surface (cycles/year) during the resin deployment period.

Correlations between base cation fluxes, hydrodynamics, and topography

Total base cation fluxes and saturation frequency were correlated to similar catchment properties, whereas correlations with saturation duration were weaker. Base cation fluxes were strongly and significantly correlated to the distance from the watershed outlet and saturation frequency (r_s >= 0.83, $p < 0.01$; Fig. 7). In general, the three sites farthest from the watershed outlet in higher elevation portions of the watershed were most cyclically saturated to shallow depths (>25 cycles/yr) and had total base cation fluxes >1 kg ha^{-1} yr^{-1}. Soils draining to these sites typically had a greater upslope volume of E-horizon (as a fraction of the total solum) and the highest proportion of upslope accumulated area weighted by bedrock and shallow-to-bedrock regions (UAAb > 57%).

There were significant negative correlations between the number of soil saturation cycles and the mean upslope topographic wetness index (TWI; r_s = -0.70, $p < 0.05$) and multiple-direction flow accumulation (MD-flow; r_s = -0.61, $p < 0.10$), which are topographic-derived hydrologic attributes used to describe the spatial distribution of soil moisture. Areas on the landscape with high TWI values (predicted as wetter sites) tended to exist in lower elevation sites on the landscape farther away from the watershed divide. These lower positions on the landscape tended to decrease in upslope area that was dominated by bedrock (UAAb <50%) and have a greater proportion of upslope B horizon (>11%) of the entire solum above the C-horizon.

Another pattern to emerge was the spatial distribution of elemental depletion (TAU), which is an index of weathering extent. Tau values for elemental Ca, Na, and Al were most strongly related with saturation frequency ($r_s < -0.71$, $p < 0.01$) (Fig. 7). Tau values for Mg^{2+} were not significantly correlated with any hydrodynamic property measured and was only negatively correlated with upslope drainage properties UAAb, PLAN, and CONVERGE ($r_s > -0.77$, $p < 0.05$).

A second Spearman correlation analysis considered relationships between mean upslope drainage area attributes and hydrologic behavior for the larger well network (n = 43), including logging wells co-located with deployed resins (Fig. 8). Not only did many of these wells have longer consecutive water level data (1-5 yrs), but they were also had a higher spatial distribution across the landscape (Fig. 1) and larger range in topographic properties (Table 1). Similar correlations were observed as those established with resin-

associated logging wells (Fig. 7 and 8). The number of annual saturation cycles increased with increasing elevation ($r_s = 0.46$, $p < 0.01$) and distance to watershed divide ($r_s = -0.52$, $p < 0.01$). Site within 60 m of the watershed divide were higher than 680 m in elevation (range 529 – 710 m). Saturation cycles was negatively correlated with mean upslope drainage area TWI and MD-flow ($r_s = -0.56$ and $r_s = > -0.52$, respectively, $p < 0.01$). A notable contrast between both spearman analyses was the strength and significance of the correlation between saturation duration and topographic attributes. When considering the larger well network, the proportion of time the transient water table existed at or above 30cm correlated with some of the properties as annual saturation cycles (i.e., distance upslope, elevation) although the strength of the correlations was weaker ($r_s < -0.40$; Fig. 8).

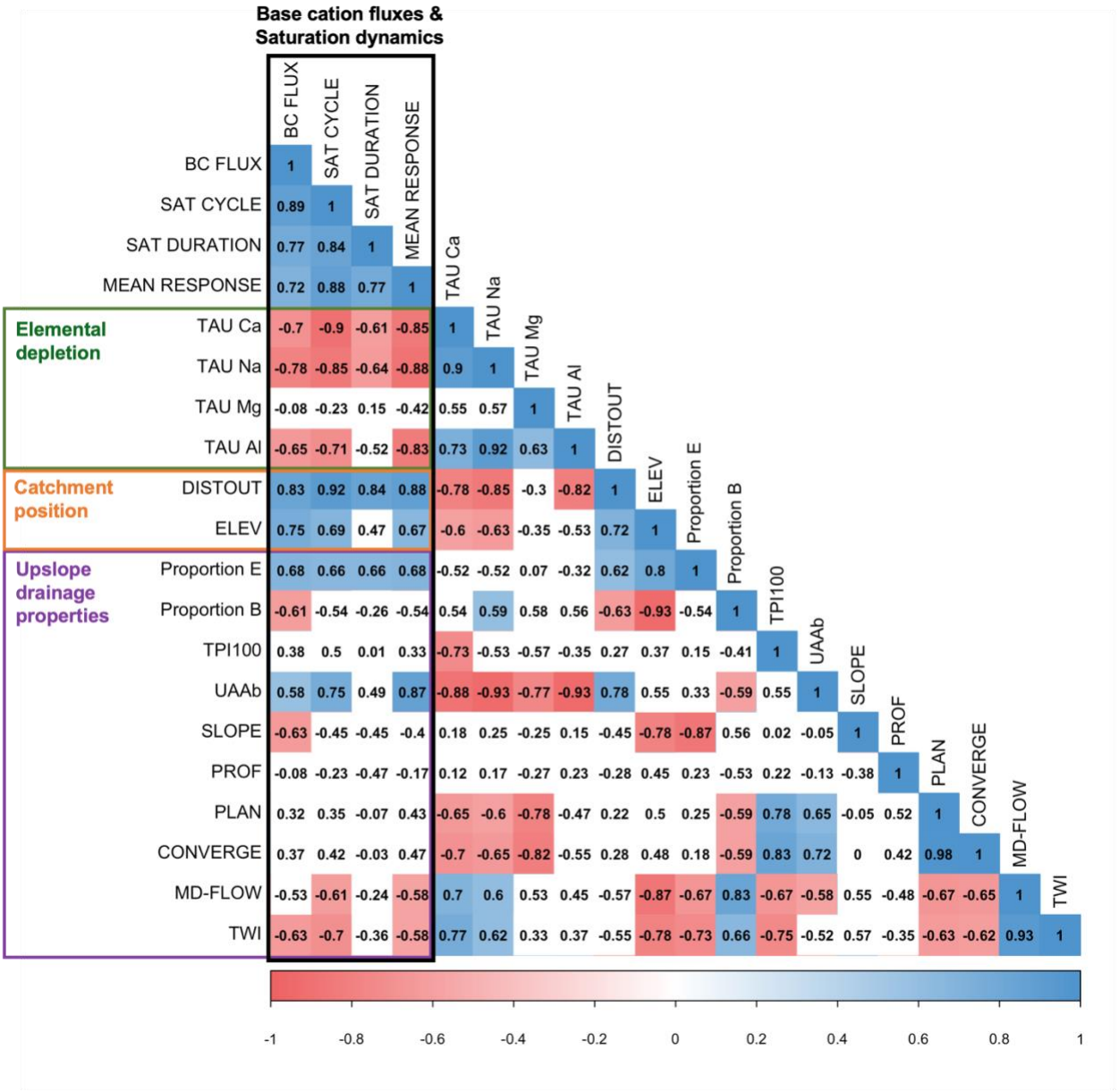

Figure 7. Spearman correlation matrix for base cation fluxes, saturation dynamics, elemental depletion, and catchment attributes for resin wells (see Figure 1, purple boxed region). Colored boxes indicate the significance of the correlation ($p < 0.05$) and the direction of the relationship as negative (red) or positive (blue). Abbreviations are for total base cation flux (BC FLUX), the number of saturation cycles (SAT CYCLES), duration of saturation (SAT DUR), mean water table response depth (MEAN), tau values (TAU), distance to watershed outlet (DISTOUT), local elevation (ELEV), and mean upslope drainage values for gradient (SLOPE), hillslope planar curvature (PLAN), hillslope planar curvature (PROF), convergence (CONVERGE), multiple direction flow

accumulation (MDFLOW), topographic wetness index (TWI), topographic position index, window size 100m (TPI100), terrain ruggedness (RUG), and upslope accumulated area weighted by proportion with bedrock outcrop areas (UAAb).

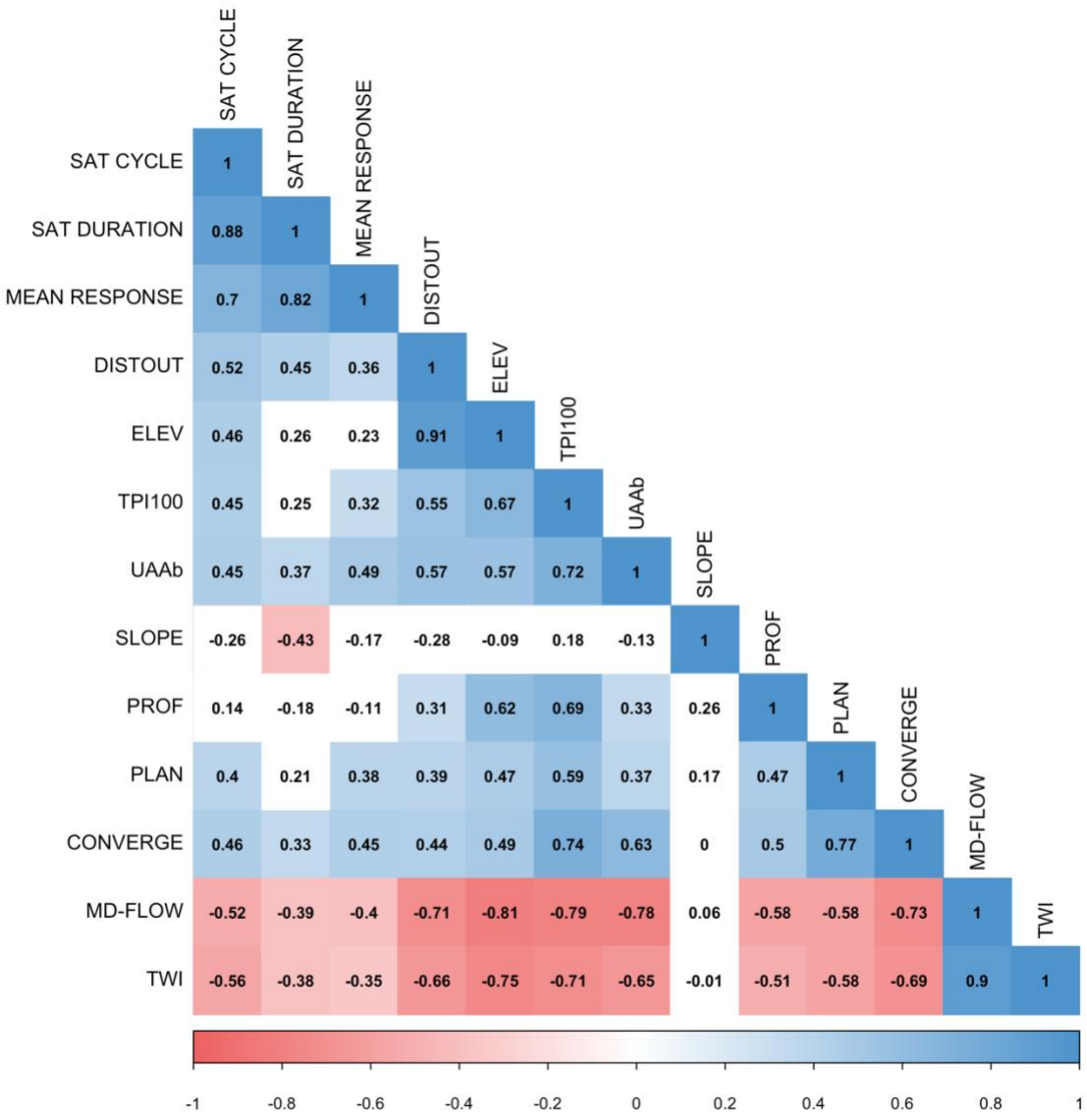

Figure 8. Spearman correlation matrix between saturation dynamics and catchment attributes for the watershed 3 well network of shallow wells (see Figure 1; white points). Colored squares indicate significance of the correlation ($p < 0.05$) and the direction of the relationship as negative (red) or positive (blue). Abbreviations are for total base cation

flux (BC FLUX), the number of saturation cycles (SAT CYCLES), duration of saturation (SAT DUR), mean water table response depth (MEAN), tau values (TAU), distance to watershed outlet (DISTOUT), local elevation (ELEV), and mean upslope drainage values for gradient (SLOPE), hillslope planar curvature (PLAN), hillslope planar curvature (PROF), convergence (CONVERGE), multiple direction flow accumulation (MDFLOW), topographic wetness index (TWI), topographic position index (TPI100), terrain ruggedness (RUG), and upslope accumulated area weighted by proportion of area weighted by bedrock (UAAb).

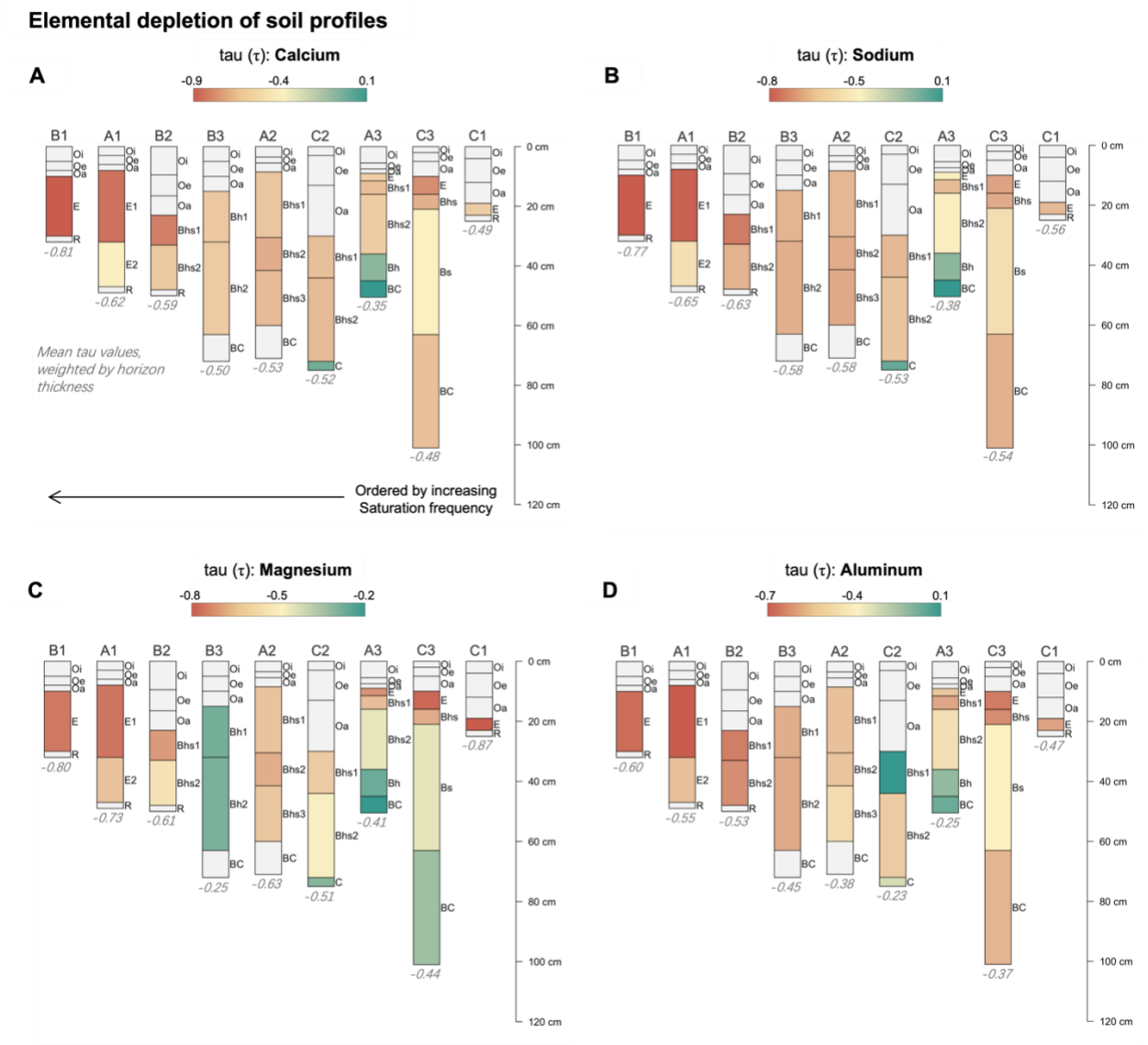

Figure 9. Elemental depletion, expressed by tau values, for soil horizons described in pits within transects A-C that were along hillslope positions 1-3. Soil pits are arranged by how often the transient water table developed (saturation frequency) on an annual basis from left (high soil saturation frequency) to right (low saturation frequency). Tau values that are increasingly negative are more depleted in that element and indicate a weathering loss. Soil profiles are colored by horizon tau values, whereas numbers below each profile are mean, thickness-weighted values for that entire profile for all mineral horizons. Gray boxes indicate where tau values could not be calculated, or where there was missing data.

Discussion

Acidic flushing as a mechanism for base cation generation and translocation

Results from this study show that annual soil saturation frequency, or the number of times in which the transient water table rose to 20 cm or above, was the most important hydrologic variable for predicting total base cation fluxes and individual cation fluxes (Ca^{2+}, Na^{+}, and Mg^{2+}) at a location. It is assumed that 20 cm may be a characteristic depth of variability for saturation frequency for this local setting soils. Below this depth, fluctuations in water table dynamics are too similar and do not capture variation and, above this depth most wells do not have enough data (Fig. 4).

High saturation variability is indicative of the dominance of lateral subsurface flow in those portions of the landscape that expressed frequent and rapid draining of water from the soil profile. Shallow subsurface increases flow rates and decreases fluid residence times, resulting in the physical flushing of solutes from the soil matrix. Furthermore, frequent soil flushing decreases solute concentrations towards thermodynamic disequilibrium, which could increase dissolution reaction rates. The chemical dissolution of plagioclase and would be a primary source for Ca^{2+} and Na^{+} since it weathers quite easily, the Ca-endmember in particular (Blum and Stillings, 1995), which is found in high abundance in this region (Bailey et al., 2003). Our estimated annual fluxes for Ca^{2+} and Na^{+} were on average much higher than Mg^{2+}, which could reflect local mineralogy since Mg^{2+} is common to minor minerals such as biotite, chlorite, and hornblende. Locations where saturation duration at any depth was high and saturation frequency was low, had smaller base cation flux estimations, indicating the presence of longer or isolated flow paths which can result in transport-limited weathering rates if solutions are not often pushed away from chemical equilibrium.

In addition, base cation fluxes were strongly correlated with the proportion of bare bedrock outcrops and associated shallow organic soils in upslope drainage areas (Fig. 7). Bedrock-controlled areas of the landscape, a region with predominately conifers, have been associated with low pH and high concentrations of DOC in shallow groundwater (Bailey et al., 2019) and adjacent streams (Zimmer et al., 2013). The translocation of upslope generated organic acids could be neutralized by the dissolution of silicate minerals in soils draining from bedrock-controlled regions. Experimental

studies have shown that plagioclase weathering accelerates with increasing acidity (e.g., Blum and Stillings, 1995; Welch and Ullman, 1996), and even faster rates for Ca-rich plagioclase (Huang and Kian, 1972), though it is well acknowledged that lab experiments tend to calculate chemical weathering rates at several magnitudes higher compared to field estimations (White and Brantley, 2003). It is likely that shallow subsurface stormflow is an important physical and chemical regulator on soil base cation mobilization and translocation. This explanation compliments a small catchment study by Clow and Drever (1996) who attributed increases in catchment chemical fluxes during high flow events to episodic saturation, subsequent soil flushing from the soil matrix and micropores, and increased chemical weathering rates. Perhaps then, longer water contact time may be a less useful variable for considering controls on base cation fluxes in the shallow soil zone than quantifying conditions that promote disequilibrium (e.g., flushing periods of young water).

Patterns of base cation fluxes could also be attributed to spatial variations in sources such as wet and dry deposition, throughfall and stemflow, organic matter mineralization, and cation exchange. We observed a positive correlation between cation fluxes and elevation, however, bulk precipitation chemistry at Hubbard Brook Experimental Forest (HBEF) has shown no elevational gradient for Ca^{2+}, Na^{+}, or Mg^{2+} deposition, thus we expect this source to contribute minimally toward spatial variation (Likens et al., 1967). Cation desorption off the soil exchange complex could offer another convincing explanation of solute flux patterns when considering rapid flushing periods, since ion exchange processes can occur at a rate of seconds to days and enhanced by decreasing pH (Brantley et al., 2008). At HBEF, the exchangeable cation pools are related to organic matter content, since clay content is low, which is highest in the Oa horizon (Dittman et al., 2007), with exchangeable Ca^{2+} concentrations orders of magnitude higher than Mg^{2+} and K^{+} (Johnson et al., 1991; Likens et al. 1998). Frequent flushing of shallow organic horizons could tap into this labile pool, which would be supported by estimations of Ca^{2+} fluxes in this study being so much greater than Mg^{2+} fluxes. However, Na^{+} on the exchange complex is considered negligible and has been used as a conservative tracer for measuring weathering rates (Bailey et al., 2003), therefore another process would need to be mediating Na^{+} in the same way as Ca^{2+} and

Mg^{2+} (Fig. 6). Additionally, in this region, upper elevations are associated with more coniferous tree species, which have lower Ca^{2+} and Mg^{2+} concentrations in plant tissue than deciduous at lower elevations (Arthur et al., 1999; Likens and Bormann, 1970). As a result, less of these elements are recycled back into the soil, which is reflected by decreased concentrations in exchange complex and organic matter pools with increasing elevation. Therefore, it could not be expected that inputs of base cations from the labile pools to be greater at the top of the watershed where fluxes were found to be greatest.

Soil profiles where saturation frequency was highest (e.g., hillslope position 1 for transects A and B) had the highest estimations of base cation fluxes (Fig. 7) and were also most elementally depleted in calcium, sodium, and aluminum (Fig. 9). This might provide the most compelling argument for base cation fluxes to represent spatial differences in the rates of chemical weathering and translocation. The loss of Ca^{2+}, Na^{+} and Al from the dissolution of plagioclase would agree with the observed higher contribution of Ca^{2+} and Na^{+} to the overall total base cation flux and the extent of depletion of these elements within the soil profiles in this study compared to Mg^{2+} (Fig. 3, Fig. 9). Our findings of high base cation fluxes and mineral depletion in locations where the transient water table often rises and recedes to the shallow portions of the profile compliments the soil morphology observed at each location. Here, soil profiles are dominated by thick E-horizons above shallow bedrock. Eluvial horizons carry a physiochemical memory of long-term elemental weathering loss, and represent past and present hydrologic conditions (Lin, 2011).

A notable exception to our observed trends between elemental loss and estimated base cation fluxes was for soil profile C1, which had only a thin E-horizon (<10 cm; Fig. 9), and the lowest estimations for all base cation fluxes (Fig. 3). Low mineral-water contact area with the sandy E horizon (smaller mineral soil volume) could account for this. It is also likely that saturation frequency here was higher than measured, since the formation of the E-horizon on top bedrock did exist, but since the soil profile was by depth ~85% organic horizon and the water table might have formed and drained quicker than the water logger could record its presence, which for this study was at 10-minute intervals. Organic horizons are known to be extremely porous and rapidly transmit water, which also could have prevented whole profile saturation due to such high saturated

hydraulic conductivity. Water table depths were used in the calculations for flux estimations, and an artificial deeper water table could have underestimated fluxes at this location. Future studies measuring hydrodynamics in shallow mineral soils with flashy water tables could consider smaller time logging intervals to capture this potential variation.

In a nearby watershed at HBEF, Nezat et al. (2004) provides similar evidence of intra-watershed spatial variability of long-term chemical weathering, determining that weathering rates were greater in higher elevations, attributed to increased contributions of biologic activity and organic acidity from conifers in shallow soils. Frequent flushing of acidic waters associated with lateral subsurface flow is the possible driver behind enhanced weathering rates at locations where our observed present-day estimations of annual base cation fluxes are greatest and where more extensive long-term weathering has taken place (high depletion values). Results show that solute fluxes within this catchment are neither uniform nor random, but rather exist in a predictable spatial arrangement that correspond with shallow water dynamics. In addition, this study highlights the importance of bedrock-controlled regions as potential sources of contributing acidity to the lateral subsurface flow component, which could enhance downslope dissolution reactions.

The role of catchment structure on the formation of lateral subsurface flow

Across all sites, the development of the transient water table in the shallow soil zone generally occurred in response to precipitation events (rainfall, snowmelt) (Fig. 4), however, the spatial variability in water table behavior was influenced by topographic attributes calculated for each upslope drainage area (Fig. 8). The ability of DEM-derived topographic indices to predict groundwater responses can often be unclear due to other intervening factors, such as deviations in bedrock topography and permeability contrasts, which can influence flow paths and water table responses not represented by surface topography alone (Tromp-van Meerveld and McDonnell, 2006). However, it was found that the transient water table was most responsive (high saturation frequency, shallower response depths) where upslope topographic convergence and slope planar curvature was greatest (Fig. 8). This could indicate that the formation of a shallow transient water table

is influenced by the degree of flow convergence determined by surface topography or that bedrock topography is parallel to the surface, in the upslope drainage area to a given location.

In steep, forested catchments topographic indices derived from slope and local drainage area can be useful for describing the spatial distribution of soil moisture and groundwater response (e.g., Seibert and McGlynn, 2007; Thompson and Moore, 1996), such as topographic wetness index (TWI), which assumes local slope is a fair representation of the hydraulic gradient (Beven and Kirkby, 1979). Interestingly, for wells in the same watershed, Detty and McGuire (2010) found a positive relationship between local TWI values and the duration of water the shallow water table within any part of the soil profile. Using a similar well network but a larger proportion of upslope locations farther from streams, we found that TWI values were negatively correlated with the persistence of the water table (Fig. 8). Discrepancies in results are likely due to (1) we only considered water table duration for water tables that reached 30 cm or shallower and (2) we used mean TWI for the upslope drainage area instead of local values. Additionally, we found that saturation frequency (i.e., number of soil saturation cycles per year) had an even stronger negative correlation with upslope TWI than saturation duration.

In a catchment with low permeability soils, Rinderer et al. (2014) found the mean TWI (using local slope) of the upslope drainage areas was positively related to the proportion of time the shallow water table rose > 30 cm, whereas our study found TWI (which used slope gradient) to be weakly negatively correlated at this same depth. Besides differences in the slope calculations of TWI, discrepancies in our observations could be attributed to the more conductive soils found at HBEF, which enhances transient and episodic flow conditions and could reduce the strength of the relationship, compared to less conductive soils that slowly drain and a quasi-steady state can be achieved (Rinderer et al., 2014; Seibert et al., 1997). Additionally, surface topography may not be a great indicator of flow path everywhere on the landscape, and the heterogeneity in hydraulic properties may be more influential to local groundwater responses (e.g., topography of a less-permeable layer) that is not being represented by TWI.

In addition to catchment attributes derived from topographic slope, the formation of the transient water table and lateral water movement is also regulated by the conductive properties of the upslope draining soils. Areas on the landscape with higher contributing areas of bedrock outcrops and shallow, organic soils (high UAAb) were positively correlated with an increase in local saturation frequency and mean response depth (Fig. 8). Under high flow conditions, the water storage capacity in thin upslope soils could easily be exceeded, which increases the lateral hydraulic gradient, and water is readily moved downslope by gravitational forces (Anderson and Burt, 1978).

Our results imply that upslope areas with low potential for accumulated wetness, a high degree of flow convergence, and larger proportions of shallow, transmissive soils have a greater tendency for lateral flushing. Rapid water table rise and recessions to shallow depths (high soil saturation frequency, shallow mean response depth) could indicate where lateral subsurface flow may dominate on the landscape. We found these locations tended exist in regions of the catchment near ridges and bedrock outcrops. For deeper soils lower on the hillslope, the transient water table barely reached shallow depths or, for near-stream sites, was perennially saturated. Using soil water potential data for soils in the same watershed, Gannon et al. (2014) found the lateral hydraulic gradient dominated for both wet and dry conditions in soils closer bedrock-controlled areas, where unsaturated lateral fluxes are thought to influence the downslope transport of solutes above the upper extent of the transient water table. It makes sense then why many of the same topographic attributes used in this study that correlated with saturation dynamics (e.g., UAAb, TWI, etc.) were also used to map the distribution of soils in the same watershed (Gillin et al. 2015).

At HBEF, the transport of solutes through lateral flow paths is considered a major process of soil formation (Bailey et al., 2014), where two different modes of podzolization (lateral and vertical) has distinct soil morphology associated with the spatial variation in accumulated organometallic complexes depending of the direction of the dominant water flux (Bourgault et al., 2017; Bourgault et al., 2015). Beyond controlling hillslope redistribution of spodic material, lateral flow paths could also important avenues for base cation transport in the shallow soil zone and mediated by spatial differences in chemical weathering processes. Putting base cation generation into

a hydrological framework is important for understanding not only the "hot spots" on the landscape (bedrock-controlled regions) but also the "hot moments" where lateral subsurface flushing might enhance intrawatershed mineral weathering rates. During larger storm events stream networks are expanded and catchment hydrologic connectivity increases, therefore it could be expected that the transport of solutes from upland soils to streams would be enhanced (Brown et al., 1999; Detty and McGuire, 2010; Hornberger et al., 1994; Jencso et al. 2009), which could alter catchment C-Q relationships.

Conclusions

In this study we used ion-exchange resins collocated with hydrologic measurements within shallow groundwater wells to study the annual integration of chemistry of the transient water table. Fluxes were measured at nine locations at various hillslope positions, for a period of 1-year at a forested headwater catchment in the Hubbard Brook Experimental Forest. It was found that base cation (Ca^{2+}, Na^{+}, Mg^{2+}) fluxes were not uniform throughout the catchment, but in fact ranged from 0.2 – 5.8 kg ha^{-1} yr^{-1} and varied greatly across small spatial scales (10s of meters). To our knowledge, time-integrated *in situ* measurements of annual solute fluxes associated with shallow subsurface stormflow has not yet been presented. More often, direct measurements of groundwater taken during discrete sampling campaigns (e.g., following precipitation events) or catchment outlet chemistry is used to infer upslope sources is extrapolated to an annual scale.

Base cation fluxes were greatest at the top of the watershed and positively and significantly correlated with element depletion of soil profiles in calcium, sodium, and aluminum, which are the major constituents of plagioclase and a dominant parent mineral present in this region. Portions of the watershed that that had the greatest cation loss (annual flux and mineral depletion) were located most upslope, nearest to bedrock outcrops and associated shallow, organic soils. We propose that frequent flushing of organic acids contributed from bedrock-controlled portions of the landscape could enhance the chemical dissolution of primary minerals during flushing periods along lateral subsurface flow paths.

The systematic variation in shallow groundwater dynamics with soil base cation flux estimations underscores the influential role catchment structure has on spatial patterns of solute generation and transport. Upslope drainage properties regulate downslope water table fluctuations, and topographic properties are important for predicting the formation of the transient water table and the enhancement of lateral translocation of geogenic-derived solutes with stormflow. With the continued intensification of the hydrologic cycle, quantifying the connections between catchment structure and groundwater behavior is important for predicting soil base cation replenishment and transport in acid-effected ecosystems, especially as storm frequency and magnitude is expected to increase.

References

Anderson, M.G., and T.P. Burt. 1978. "The Role of Topography in Controlling Throughflow Generation." *Earth Surface Processes* 3 (4): 331–44. https://doi.org/10.1002/esp.3290030402.

Anderson, S.P., W.E. Dietrich, and G.H. Brimhall. 2002. "Weathering Profiles, Mass-Balance Analysis, and Rates of Solute Loss: Linkages between Weathering and Erosion in a Small, Steep Catchment." *GSA Bulletin* 114 (9): 1143–58. https://doi.org/10.1130/0016-7606(2002)1141143:WPMBAA2.0.CO;2.

Annable, M.D., K. Hatfield, J. Cho, H. Klammler, B.L. Parker, J.A. Cherry, and S.C. Rao. 2005. "Field-Scale Evaluation of the Passive Flux Meter for Simultaneous Measurement of Groundwater and Contaminant Fluxes." *Environmental Science & Technology* 39 (18): 7194–7201. https://doi.org/10.1021/es050074g.

Arthur, M.A., T.G. Siccama, and R. D. Yanai. 1999. "Calcium and Magnesium in Wood of Northern Hardwoof Forest Species: Relatons to Site Characteristics." *Canadian Journal of Forest Research* 29: 339–46.

Augustin, F., D. Houle, and F. Courchesne. 2018. "An Approach at Estimating Present Day Base Cation Weathering Rates: A Case Study for the Hermine Watershed, Canada." *Biogeochemistry* 140 (2): 127–44. https://doi.org/10.1007/s10533-018-0479-1.

Bailey, s.W., P.A. Brousseau, K.J. McGuire, and D.S. Ross. 2014. "Influence of Landscape Position and Transient Water Table on Soil Development and Carbon Distribution in a Steep, Headwater Catchment." *Geoderma* 226–227: 279–89. https://doi.org/10.1016/j.geoderma.2014.02.017.

Bailey, S.W., D.C. Buso, and G.E. Likens. 2003. "Implications of Sodium Mass Balance for Interpreting the Calcium Cycle of a Forested Ecosystem." *Ecology* 84 (2): 471–84. https://doi.org/10.1890/0012-9658(2003)084[0471:IOSMBF]2.0.CO;2.

Bailey, S.W., K.J. McGuire, D.S. Ross, M.B. Green, and O.L. Fraser. 2019. "Mineral Weathering and Podzolization Control Acid Neutralization and Streamwater Chemistry Gradients in Upland Glaciated Catchments, Northeastern United States." *Frontiers in Earth Science* 7 (63). https://doi.org/10.3389/feart.2019.00063.

Benettin, Paolo, Scott W. Bailey, John L. Campbell, Mark B. Green, Andrea Rinaldo, Gene E. Likens, Kevin J. McGuire, and Gianluca Botter. 2015. "Linking Water Age and Solute Dynamics in Streamflow at the Hubbard B Rook Experimental Forest, NH , USA." *Water Resources Research* 51 (11): 9256–72. https://doi.org/10.1002/2015WR017552.

Berner, R.A., and E.K. Berner. 1997. “Silicate Weathering and Climate.” In *Tectonic Uplift and Climate Change*, 354–80. Boston, MA: Springer.

Beven, K. J., and M. J. Kirkby. 1979. “A Physically Based, Variable Contributing Area Model of Basin Hydrology.” *Hydrological Sciences Bulletin* 24 (1): 43–69. https://doi.org/10.1080/02626667909491834.

Beven, K., and P. Germann. 1982. “Macropores and Water Flow in Soil.” *Water Resources Research* 18 (5): 1311–25.

Blum, A.E., and L.L. Stillings. 1995. “Chapter 7. FELDSPAR DISSOLUTION KINETICS.” In *Chemical Weathering Rates of Silicate Minerals*, edited by Arthur F. White and Susan L. Brantley, 291–352. De Gruyter. https://doi.org/10.1515/9781501509650-009.

Bluth, G.J.S., and L.R. Kump. 1994. “Lithologic and Climatologic Controls of River Chemistry.” *Geochimica et Cosmochimica Acta* 58 (10): 2341–59. https://doi.org/10.1016/0016-7037(94)90015-9.

Bourgault, R.R., D.S. Ross, and S.W. Bailey. 2015. “Chemical and Morphological Distinctions between Vertical and Lateral Podzolization at Hubbard Brook.” *Soil Science Society of America Journal. 79(2): 428-439.* 79 (2): 428–39. https://doi.org/10.2136/sssaj2014.05.0190.

Bourgault, R.R.., D.S. Ross, S.W. Bailey, T.D. Bullen, K.J. McGuire, and J.P. Gannon. 2017. “Redistribution of Soil Metals and Organic Carbon via Lateral Flowpaths at the Catchment Scale in a Glaciated Upland Setting.” *Geoderma* 307: 238–52. https://doi.org/10.1016/j.geoderma.2017.05.039.

Bracken, L.J., and J. Croke. 2007. “The Concept of Hydrological Connectivity and Its Contribution to Understanding Runoff-Dominated Geomorphic Systems.” *Hydrological Processes* 21 (13): 1749–63. https://doi.org/10.1002/hyp.6313.

Brantley, S.L., J.D. Kubicki, and A.F. White, eds. 2008. *Kinetics of Water-Rock Interaction*. New York: Springer Verlag.

Brimhall, G.H., and W.E. Dietrich. 1987. “Constitutive Mass Balance Relations between Chemical Composition, Volume, Density, Porosity, and Strain in Metasomatic Hydrochemical Systems: Results on Weathering and Pedogenesis.” *Geochimica et Cosmochimica Acta* 51 (3): 567–87.

Brown, V.A., J.J McDonnell, D.A. Burns, and C. Kendall. 1999. “The Role of Event Water, a Rapid Shallow Flow Component, and Catchment Size in Summer Stormflow.” *Journal of Hydrology* 217 (3): 171–90. https://doi.org/10.1016/S0022-1694(98)00247-9.

Chadwick, O.A., R.T. Gavenda, E.F. Kelly, K. Ziegler, C.G. Olson, W.C. Elliott, and D.M. Hendricks. 2003. “The Impact of Climate on the Biogeochemical Functioning of Volcanic Soils.” *Chemical Geology* 202 (3–4): 195–223. https://doi.org/10.1016/j.chemgeo.2002.09.001.

Cho, J., M.D. Annable, J.W. Jawitz, and K. Hatfield. 2007. “Passive Flux Meter Measurement of Water and Nutrient Flux in Saturated Porous Media: Bench-Scale Laboratory Tests.” *Journal of Environmental Quality* 36 (5): 1266–72. https://doi.org/10.2134/jeq2006.0370.

Clow, D.W., and J.I. Drever. 1996. “Weathering Rates as a Function of Flow through an Alpine Soil.” *Chemical Geology* 132 (1–4): 131–41. https://doi.org/10.1016/S0009-2541(96)00048-4.

Cronan, C.S., and C.L. Schofield. 1990. “Relationships between Aqueous Aluminum and Acidic Deposition in Forested Watersheds of North America and Northern Europe.” *Environmental Science & Technology* 24 (7): 1100–1105. https://doi.org/10.1021/es00077a022.

Dahlgren, R.A., J.L. Boettinger, G.L. Huntington, and R.G. Amundson. 1997. “Soil Development along an Elevational Transect in the Western Sierra Nevada, California.” *Geoderma* 78 (3–4): 207–36. https://doi.org/10.1016/S0016-7061(97)00034-7.

Dere, A.L., T.S. White, R.H. April, and S.L. Brantley. 2016. “Mineralogical Transformations and Soil Development in Shale across a Latitudinal Climosequence.” *Soil Science Society of America Journal* 80 (3): 623–36. https://doi.org/10.2136/sssaj2015.05.0202.

Detty, J. M., and K. J. McGuire. 2010. “Topographic Controls on Shallow Groundwater Dynamics: Implications of Hydrologic Connectivity between Hillslopes and Riparian Zones in a till Mantled Catchment.” *Hydrological Processes* 24 (16): 2222–36. https://doi.org/10.1002/hyp.7656.

Dixon, J.L., O.A. Chadwick, and Peter M. Vitousek. 2016. “Climate-driven Thresholds for Chemical Weathering in Postglacial Soils of New Zealand.” *Journal of Geophysical Research: Earth Surface* 121 (9): 1619–34. https://doi.org/10.1002/2016JF003864.

Driscoll, C.T., Gregory B. Lawrence, Arthur J. Bulger, Thomas J. Butler, Christopher S. Cronan, Christopher Eagar, Kathleen F. Lambert, Gene E. Likens, John L. Stoddard, and Kathleen C. Weathers. 2001. “Acidic Deposition in the Northeastern United States: Sources and Inputs, Ecosystem Effects, and Management StrategiesThe Effects of Acidic Deposition in the Northeastern United States Include the Acidification of Soil and Water, Which Stresses Terrestrial and Aquatic Biota.” *BioScience* 51 (3): 180–98. https://doi.org/10.1641/0006-3568(2001)051[0180:ADITNU]2.0.CO;2.

Fraser, O., S.W. Bailey, M.J. Ducey, and K.J. McGuire. 2020. “Predictive Modeling of Bedrock Outcrops and Associated Shallow Soil in Upland Glaciated Landscapes.” *Geoderma* 376.

Freer, J., J.J. McDonnell, K.J. Beven, N.E. Peters, Douglas A. Burns, R. P. Hooper, B. Aulenbach, and C. Kendall. 2002. “The Role of Bedrock Topography on Subsurface Storm Flow.” *Water Resources Research* 38 (12): 5-15–16. https://doi.org/10.1029/2001WR000872.

Gannon, John P., Kevin J. McGuire, Scott W. Bailey, Rebecca R. Bourgault, and Donald S. Ross. 2017. “Lateral Water Flux in the Unsaturated Zone: A Mechanism for the Formation of Spatial Soil Heterogeneity in a Headwater Catchment.” *Hydrological Processes* 31 (20): 3568–79. https://doi.org/10.1002/hyp.11279.

Gannon, J.P., S.W. Bailey, and K.J. McGuire. 2014. “Organizing Groundwater Regimes and Response Thresholds by Soils: A Framework for Understanding Runoff Generation in a Headwater Catchment.” *Water Resources Research* 50 (11): 8403–19. https://doi.org/10.1002/2014WR015498.

Gillin, C.P., S.W. Bailey, K.J. McGuire, and J.P. Gannon. 2015. “Mapping of Hydropedologic Spatial Patterns in a Steep Headwater Catchment.” *Soil Science Society of America Journal* 79 (2): 440–53. https://doi.org/10.2136/sssaj2014.05.0189.

Godsey, S.E., J.W. Kirchner, and D.W. Clow. 2009. “Concentration–Discharge Relationships Reflect Chemostatic Characteristics of US Catchments.” *Hydrological Processes* 23 (13): 1844–64. https://doi.org/10.1002/hyp.7315.

Guisan, A., S.B. Weiss, and A.D. Weiss. 1999. “GLM versus CCA Spatial Modeling of Plant Species Distribution.” *Plant Ecology* 143 (1): 107–22. https://doi.org/10.1023/A:1009841519580.

Hatfield, Kirk, Michael Annable, Jaehyun Cho, P.S.C. Rao, and Harald Klammler. 2004. “A Direct Passive Method for Measuring Water and Contaminant Fluxes in Porous Media.” *Journal of Contaminant Hydrology* 75 (3–4): 155–81. https://doi.org/10.1016/j.jconhyd.2004.06.005.

Hjerdt, K.N., J.J. McDonnell, J. Seibert, and A. Rodhe. 2004. “A New Topographic Index to Quantify Downslope Controls on Local Drainage: TECHNICAL NOTE.” *Water Resources Research* 40 (5). https://doi.org/10.1029/2004WR003130.

Hornberger, G.M., K.E. Bencala, and D.M. McKnight. 1994. “Hydrological Controls on Dissolved Organic Carbon during Snowmelt in the Snake River near Montezuma, Colorado.” *Biogeochemistry* 25 (3): 147–65. https://doi.org/10.1007/BF00024390.

Huang, W.H., and W.C. Kian. 1972. “Laboratory Dissolution of Plagioclase Feldspars in Water and Organic Acids at Room Temperature.” *American Mineralogist* 57: 1849–59.

Inamdar, S., J. Rupp, and M. Mitchell. 2009. “Groundwater Flushing of Solutes at Wetland and Hillslope Positions during Storm Events in a Small Glaciated Catchment in Western New York, USA.” *Hydrological Processes* 23 (13): 1912–26. https://doi.org/10.1002/hyp.7322.

Jackson, C.R. 1992. “Hillslope Infiltration and Lateral Downslope Unsaturated Flow.” *Water Resources Research* 28 (9): 2533–39.

Jankowski, M. 2014. “The Evidence of Lateral Podzolization in Sandy Soils of Northern Poland.” *Catena*, Landscapes and Soils through Time, 112 (January): 139–47. https://doi.org/10.1016/j.catena.2013.03.013.

Jencso, K., B.L. McGlynn, M.N. Gooseff, S.M. Wondzell, K.E. Bencala, and L.A. Marshall. 2009. “Hydrologic Connectivity between Landscapes and Streams: Transferring Reach- and Plot-Scale Understanding to the Catchment Scale.” *Water Resources Research* 45 (4). https://doi.org/10.1029/2008WR007225.

Johnson, C.E., C.T. Driscoll, T.G. Siccama, and G.E. Likens. 2000. “Element Fluxes and Landscape Position in a Northern Hardwood Forest Watershed Ecosystem.” *Ecosystems* 3 (2): 159–84. https://doi.org/10.1007/s100210000017.

Johnson, C.E., A. Johnson, and T. Siccama. 1991. “Whole-Tree Clear-Cutting Effects on Exchangeable Cations and Soil Acidity.” *Soil Science Society of America Journal* 55: 502–8.

Johnson, J., E.G. Pannatier, S. Carnicelli, G. Cecchini, N. Clarke, Nathalie Cools, Karin Hansen, et al. 2018. “The Response of Soil Solution Chemistry in European Forests to Decreasing Acid Deposition.” *Global Change Biology* 24 (8): 3603–19. https://doi.org/10.1111/gcb.14156.

Johnson, N. M., C.T. Driscoll, J.S. Eaton, G.E. Likens, and W.H. McDowell. 1981. “‘Acid Rain’, Dissolved Aluminum and Chemical Weathering at the Hubbard Brook Experimental Forest, New Hampshire.” *Geochimica et Cosmochimica Acta* 45 (9): 1421–37.

Kiewiet, L., J. Freyberg, and H.J. van Meerveld. 2019. “Spatiotemporal Variability in Hydrochemistry of Shallow Groundwater in a Small Pre-Alpine Catchment: The Importance of Landscape Elements.” *Hydrological Processes* 33 (19): 2502–22. https://doi.org/10.1002/hyp.13517.

Kim, H., W.E. Dietrich, B.M. Thurnhoffer, J.K.B. Bishop, and I.Y. Fung. 2017. "Controls on Solute Concentration-discharge Relationships Revealed by Simultaneous Hydrochemistry Observations of Hillslope Runoff and Stream Flow: The Importance of Critical Zone Structure." *Water Resources Research* 53 (2): 1424–43. https://doi.org/10.1002/2016WR019722.

Kjønaas, O.J. 1999. "In Situ Efficiency of Ion Exchange Resins in Studies of Nitrogen Transformation." *Soil Science Society of America Journal* 63 (2): 399–409. https://doi.org/10.2136/sssaj1999.03615995006300020019x.

Knapp, J.L.A., J. von Freyberg, B Studer, L. Kiewiet, and J.W. Kirchner. 2020. "Concentration–Discharge Relationships Vary among Hydrological Events, Reflecting Differences in Event Characteristics." *Hydrology and Earth System Sciences* 24 (5): 2561–76. https://doi.org/10.5194/hess-24-2561-2020.

Lasaga, A.C., J.M. Soler, J. Ganor, T.E. Burch, and K.L. Nagy. 2994. "Chemical Weathering Rate Laws and Global Geochemical Cycles." *Geochimica et Cosmochimica Acta* 58 (10): 2361–86. https://doi.org/10.1016/0016-7037(94)90016-7.

Lawrence, G.B., D.A. Burns, and K. Riva-Murray. 2016. "A New Look at Liming as an Approach to Accelerate Recovery from Acidic Deposition Effects." *Science of The Total Environment* 562: 35–46. https://doi.org/10.1016/j.scitotenv.2016.03.176.

Lawrence, G.B., P.W. Hazlett, I.J. Fernandez, R. Ouimet, S.W. Bailey, W.C. Shortle, K.T. Smith, and M.R. Antidormi. 2015. "Declining Acidic Deposition Begins Reversal of Forest-Soil Acidification in the Northeastern U.S. and Eastern Canada." *Environmental Science & Technology* 49 (22): 13103–11. https://doi.org/10.1021/acs.est.5b02904.

Lehmann, J., K. Kaiser, and I. Peter. 2001. "Exchange Resin Cores for the Estimation of Nutrient Fluxes in Highly Permeable Tropical Soil." *Journal of Plant Nutrition and Soil Science* 164 (1): 57–64.

Li, L., Chen Bao, Pamela L. Sullivan, Susan Brantley, Yuning Shi, and Christopher Duffy. 2017. "Understanding Watershed Hydrogeochemistry: 2. Synchronized Hydrological and Geochemical Processes Drive Stream Chemostatic Behavior." *Water Resources Research* 53 (3): 2346–67. https://doi.org/10.1002/2016WR018935.

Likens, G. E., F. H. Bormann, N. M. Johnson, and R. S. Pierce. 1967. "The Calcium, Magnesium, Potassium, and Sodium Budgets for a Small Forested Ecosystem." *Ecology* 48 (5): 772–85. https://doi.org/10.2307/1933735.

Likens, G.E., and F. H. Bormann. 1970. “Chemical Analyses of Plant Tissues from the Hubbard Brook Ecosystem in New Hampshire.” *Yale School of Forestry & Environmental Studies Bulletin Series* 58: 1–24.

Likens, G.E., C.T. Driscoll, and D.C. Buso. 1996. “Long-Term Effects of Acid Rain: Response and Recovery of a Forest Ecosystem.” *Science* 272 (5259): 244–46.

Likens, G.E., C.T. Driscoll, D.C. Buso, T.G. Siccama, C.E. Johnson, G.M. Lovett, T.J. Fahey, et al. 1998. “The Biogeochemistry of Calcium at Hubbard Brook.” *Biogeochemistry* 41 (2): 89–173. https://doi.org/10.1023/A:1005984620681.

Lindsay, J.B. 2014. “The Whitebox Geospatial Analysis Tools Project and Open-Access GIS.” Proceedings of the GIS Research UK 22nd Annual Conference.

Lybrand, R.A., and C. Rasmussen. 2015. “Quantifying Climate and Landscape Position Controls on Soil Development in Semiarid Ecosystems.” *Soil Science Society of America Journal* 79 (1): 104–16. https://doi.org/10.2136/sssaj2014.06.0242.

Maher, K. 2011. “The Role of Fluid Residence Time and Topographic Scales in Determining Chemical Fluxes from Landscapes.” *Earth and Planetary Science Letters* 312 (1): 48–58. https://doi.org/10.1016/j.epsl.2011.09.040.

McGlynn, Brian L., and Jeffrey J. McDonnell. 2003. “Role of Discrete Landscape Units in Controlling Catchment Dissolved Organic Carbon Dynamics.” *Water Resources Research* 39 (4). https://doi.org/10.1029/2002WR001525.

McGuire, K. J., J. J. McDonnell, M. Weiler, C. Kendall, B. L. McGlynn, J. M. Welker, and J. Seibert. 2005. “The Role of Topography on Catchment-scale Water Residence Time.” *Water Resources Research* 41 (5). https://doi.org/10.1029/2004WR003657.

Millot, Romain, Jérôme Gaillardet, Bernard Dupré, and Claude Jean Allègre. 2002. “The Global Control of Silicate Weathering Rates and the Coupling with Physical Erosion: New Insights from Rivers of the Canadian Shield.” *Earth and Planetary Science Letters* 196 (1): 83–98. https://doi.org/10.1016/S0012-821X(01)00599-4.

Milnes, A.R., and R.W. Fitzpatrick. 1989. “Titanium and Zirconium Minerals.” In *Minerals in the Environment*, 1:1131–1205.

Mosley, M.P. 1979. “Streamflow Generation in a Forested Watershed, New Zealan.” *Water Resources Research* 15 (4): 795–806.

Musolff, A., Q. Zhan, R. Dupas, C. Minaudo, J. H. Fleckenstein, M. Rode, J. Dehaspe, and K. Rinke. 2021. “Spatial and Temporal Variability in Concentration-Discharge Relationships at the Event Scale.” *Water Resources Research* 57 (10). https://doi.org/10.1029/2020WR029442.

Nezat, C.A., J.D. Blum, A. Klaue, C.E. Johnson, and TG. Siccama. 2004. “Influence of Landscape Position and Vegetation on Long-Term Weathering Rates at the Hubbard Brook Experimental Forest, New Hampshire, USA.” *Geochimica et Cosmochimica Acta* 68 (14): 3065–78. https://doi.org/10.1016/j.gca.2004.01.021.

Oliva, P., J. Viers, and Bernard Dupré. 2003. “Chemical Weathering in Granitic Environments.” *Chemical Geology*, Controls on Chemical Weathering, 202 (3): 225–56. https://doi.org/10.1016/j.chemgeo.2002.08.001.

Padowski, J.C., E.A. Rothfus, J.W. Jawitz, H. Klammler, K. Hatfield, and M.D. Annable. 2009. “Effect of Passive Surface Water Flux Meter Design on Water and Solute Mass Flux Estimates.” *Journal of Hydrologic Engineering* 14 (12): 1334–42. https://doi.org/10.1061/(ASCE)HE.1943-5584.0000127.

Pearce, A., M.K. Stewart, and M.G. Sklash. 1986. “Storm Runoff Generation in Humid Headwater Catchments. 1. Where Does the Water Come From?” *Water Resources Research* 22 (8): 1263–72.

Pennino, A.M., K.J. McGuire, B.D. Strahm, and S.W. Bailey. 2023. Hubbard Brook Experimental Forest: Watershed 3 – One year of resin-extracted solutes from variably saturated soils ver 2. Environmental Data Initiative. https://doi.org/10.6073/pasta/60f964ffa4e180eb19ee9249219cfa4e (Accessed 2023-05-14).

Rasmussen, C., S. Brantley, D. deB. Richter, A. Blum, J. Dixon, and A.F. White. 2011. “Strong Climate and Tectonic Control on Plagioclase Weathering in Granitic Terrain.” *Earth and Planetary Science Letters* 301 (3–4): 521–30. https://doi.org/10.1016/j.epsl.2010.11.037.

Riebe, Clifford S., James W. Kirchner, and Robert C. Finkel. 2004. “Erosional and Climatic Effects on Long-Term Chemical Weathering Rates in Granitic Landscapes Spanning Diverse Climate Regimes.” *Earth and Planetary Science Letters* 224 (3): 547–62. https://doi.org/10.1016/j.epsl.2004.05.019.

Rinderer, M., H. J. van Meerveld, and J. Seibert. 2014. “Topographic Controls on Shallow Groundwater Levels in a Steep, Prealpine Catchment: When Are the TWI Assumptions Valid?” *Water Resources Research* 50 (7): 6067–80. https://doi.org/10.1002/2013WR015009.

Schoeneberger, Philip J., D.A. Wysocki, and E.C. Benham. 2012. *Field Book for Describing and Sampling Soils*. Government Printing Office.

Seibert, J., K. Bishop, and L. Nyberg. 1997. “A Test of Topmopdel’s Ability to Predict Spatially Distributed Groundwater Levels.” *Hydrologic Processes* 11: 1131–44.

Seibert, Jan, and Brian L. McGlynn. 2007. “A New Triangular Multiple Flow Direction Algorithm for Computing Upslope Areas from Gridded Digital Elevation Models: A NEW TRIANGULAR MULTIPLE-FLOW DIRECTION.” *Water Resources Research* 43 (4). https://doi.org/10.1029/2006WR005128.

Siemion, J., M.R. McHale, G.B. Lawrence, D.A. Burns, and M.R. Antidormi. 2018. “Long-term Changes in Soil and Stream Chemistry across an Acid Deposition Gradient in the Northeastern United States.” *Journal of Environmental Quality* 47 (3): 410–18.

Sommer, M., D. Halm, C. Geisinger, I. Andruschkewitsch, M. Zarei, and K. Stahr. 2001. “Lateral Podzolization in a Sandstone Catchment.” *Geoderma* 103 (3): 231–47. https://doi.org/10.1016/S0016-7061(01)00018-0.

Sommer, M, D Halm, U Weller, M Zarei, and K Stahr. 2000. “Lateral Podzolization in a Granite Landscape.” *SOIL SCI. SOC. AM. J.* 64: 9.

Spearman, C. 1904. “The Proof and Measurement of Association between Two Things.” *American Journal of Psychology* 15: 72–101.

Stucker, V., J. Ranville, M. Newman, A. Peacock, J. Cho, and K. Hatfield. 2011. “Evaluation and Application of Anion Exchange Resins to Measure Groundwater Uranium Flux at a Former Uranium Mill Site.” *Water Research* 45 (16): 4866–76. https://doi.org/10.1016/j.watres.2011.06.030.

Taylor, A., and J.D. Blum. 1995. “Relation between Soil Age and Silicate Wearhering Rates Determined from the Chemical Evolution of a Glacial Chronosequence.” *Geology* 23 (11): 979–82.

Tetzlaff, D., J. Seibert, K. J. McGuire, H. Laudon, D. A. Burns, S. M. Dunn, and C. Soulsby. 2009. “How Does Landscape Structure Influence Catchment Transit Time across Different Geomorphic Provinces?” *Hydrological Processes* 23 (6): 945–53. https://doi.org/10.1002/hyp.7240.

Thompson, J.C., and R.D. Moore. 1996. “Relations between Topography and Water Table Depth in a Shallow Forest Soil.” *Hydrologic Processes* 10: 1513–25.

Tromp-van Meerveld, H. J., and J. J. McDonnell. 2006. “Threshold Relations in Subsurface Stormflow: 2. The Fill and Spill Hypothesis.” *Water Resources Research* 42 (2). https://doi.org/10.1029/2004WR003800.

Wang, L, and H. Liu. 2006. “An Efficient Method for Identifying and Filling Surface Depressions in Digital Elevation Models for Hydrologic Analysis and Modelling.” *International Journal of Geographical Information Science* 20 (2): 193–213.

Weiler, M., J.J. McDonnell, H.J. van Meerveld, and T Uchida. 2006. “Subsurface Stormflow.” In *Encyclopedia of Hydrological Sciences*. https://doi.org/10.1002/0470848944.hsa119.

Welch, S.A., and W.J. Ullman. 1996. “Feldspar Dissolution in Acidic and Organic Solutions: Compositional and PH Dependence of Dissolution Rate.” *Geochimica et Cosmochimica Acta* 60 (16): 2939–48. https://doi.org/10.1016/0016-7037(96)00134-2.

West, A.J., A. Galy, and M. Bickle. 2005. “Tectonic and Climatic Controls on Silicate Weathering.” *Earth and Planetary Science Letters* 235 (1): 211–28. https://doi.org/10.1016/j.epsl.2005.03.020.

Western, A.W., R.B. Grayson, G. Blöschl, G.R. Willgoose, and T.A. McMahon. 1999. “Observed Spatial Organization of Soil Moisture and Its Relation to Terrain Indices.” *Water Resources Research* 35 (3): 797–810. https://doi.org/10.1029/1998WR900065.

White, A.F., and A.E. Blum. 1995. “Effects of Climate on Chemical Weathering in Watersheds.” *Geochimica et Cosmochimica Acta* 59 (9): 1729–47. https://doi.org/10.1016/0016-7037(95)00078-E.

White, A.F., and S.L. Brantley. 2003. “The Effect of Time on the Weathering of Silicate Minerals: Why Do Weathering Rates Differ in the Laboratory and Field?” *Chemical Geology* 202 (3–4): 479–506. https://doi.org/10.1016/j.chemgeo.2003.03.001.

Willich, M., and A. Buerkert. 2016. “Leaching of Carbon and Nitrogen from a Sandy Soil Substrate: A Comparison between Suction Plates and Ion Exchange Resins.” *Journal of Plant Nutrition and Soil Science* 179 (5): 609–14. https://doi.org/10.1002/jpln.201600036.

Xiao, D., S.L. Brantley, and Li Li. 2021. “Vertical Connectivity Regulates Water Transit Time and Chemical Weathering at the Hillslope Scale.” *Water Resources Research* 57 (8). https://doi.org/10.1029/2020WR029207.

Zimmer, M.A., S.W. Bailey, K.J. McGuire, and T.D. Bullen. 2013. “Fine Scale Variations of Surface Water Chemistry in an Ephemeral to Perennial Drainage Network.” *Hydrological Processes* 27 (24): 3438–51. https://doi.org/10.1002/hyp.9449.

Appendix A

Table A1. Table of terms used for annual cation flux calculations. Resin locations are labeled by transect (A-C) and hillslope position (1-3) (Figure 1). Total mass of cations extracted from resins was measured over four time periods for a total deployment time over one continuous year (365 days). Average water table height was calculated from wells with water level loggers that were closest to resin location with continuous data and was only calculated for 281 days (August-May 2020) due to availability of water level data. Additional information regarding the calculation and use of these terms can be found in Materials and Methods: *Ion-exchange resins and base cation flux estimations*.

Location	Annual mass extracted (mg)			Average water table height	Upslope area (ha)	Days deployed	Resin height (cm)	Resin width (cm)	DEM width (cm)
	Ca^{2+}	Mg^{2+}	Na^{+}						
A1	88.54	12.35	206.79	9.1	0.0448	365	0.381	5.08	100
A2	64.52	6.05	69.39	13.2	0.1021	365	0.381	5.08	100
A3	67.35	3.69	17.54	32.9	0.2791	365	0.381	5.08	100
B1	326.17	95.18	154.87	12.0	0.0664	365	0.381	5.08	100
B2	80.18	17.43	42.91	33.8	0.2937	365	0.381	5.08	100
B3	244.36	65.85	230.79	35.3	0.5563	365	0.381	5.08	100
C1	88.28	7.83	15.14	2.5	0.0843	365	0.381	5.08	100
C2	150.13	40.51	125.62	21.1	0.7262	365	0.381	5.08	100
C3	186.82	35.18	186.43	18.2	0.8056	365	0.381	5.08	100

Table A2. Table of annual base cation fluxes (kg ha^{-1} yr^{-1}) for each resin location. Resin locations are labeled by transect (A-C) and hillslope position (1-3) (Figure 1). Total base cation fluxes are calculated as the sum of each cation flux.

	Fluxes (kg ha^{-1} yr^{-1})			
Location	**Ca^{2+}**	**Mg^{2+}**	**Na^{+}**	**Total (Ca+Mg+Na)**
A1	0.9	0.1	2.8	3.9
A2	0.4	0.0	0.6	1.1
A3	0.4	0.0	0.1	0.6
B1	3.0	0.9	1.9	5.8
B2	0.5	0.1	0.3	0.9
B3	0.8	0.2	1.0	2.0
C1	0.2	0.0	0.0	0.2
C2	0.2	0.1	0.2	0.5
C3	0.2	0.0	0.3	0.5

Chapter 2

Hydrodynamic Drivers of Shallow Groundwater DOC Concentrations

Abstract

It is well recognized that the contribution of dissolved organic carbon (DOC) flushing from shallow soils to streams increases during storm events. However, the characterization of groundwater chemistry is often focused on near-stream soils or inferred from watershed export rather than intensive hillslope sampling. Increasingly, studies have shown that shallow groundwater dynamics and chemistry exhibits more intra-watershed variability than previously thought. Yet, spatiotemporal relationships between groundwater behavior and DOC concentrations are not well established. Across 46 storm events, shallow groundwater chemistry and water table responses were examined for a well network (n=56 wells) within a steep forested headwater catchment. Terrain-based metrics were used to group wells and characterize groundwater behavior by catchment position, which were generally classified as "upslope," "mid-slope," and "near-stream." During an event, the peak water level reached (maximum watertable height) in soil profile during a storm event was the best predictor of DOC concentrations. Results show that in this catchment upslope positions, which are nearest to areas of shallow organic soils, frequently saturated to shallow depths and had higher DOC concentrations than downslope counterparts. In contrast, mid-slope and near-stream sites had significantly lower DOC concentrations, especially when storm events did not facilitate a rise in the water table to shallow depths. These findings suggest that in some catchments, DOC export during storm events could be highly influenced by hillslope soils that are closest to areas of organic acid generation and most responsive to precipitation inputs, rather than near-stream riparian zones. This study highlights the importance of spatially and temporally intensive shallow groundwater characterization across forested catchments for the interpretation of DOC mobilization events.

Introduction

In forested ecosystems, the leaching of dissolved organic carbon (DOC) from the decomposing forest floor provides a significant carbon input to mineral soils (Froberg et al., 2006; Guggenberger et al., 1994; Kalbitz and Kaiser, 2008; McDowell and Likens, 1998; Neff and Asner, 2001; Qualls and Haines, 1991). Fluxes of DOC from organic horizons to mineral soils are regulated by organic matter availability and quality, dynamics of biotic consumption and production of DOC, and the movement of DOC with soil water flow. Increased inputs of organic acids (e.g., DOC) are known to enhance metal transport (Huber et al., 2002; Lundstom et al., 2000; Ugolini and Dahlgren, 1989; van Hees and Lundstom, 2000) and mineral weathering reactions (Drever and Vance, 1994; Drever and Stillings, 1997; Lawrence et al., 2014; Raulund-Rasmussen et al., 1998). Therefore, the spatial distribution of DOC across landscapes has large impacts on the cycling, movement, and retention of nutrients and elements within and between ecosystems. Because of the crucial role DOC has in mediating ecological function and pedogenic processes, further exploration of the mechanisms controlling soil solution DOC variability during leaching events in forested catchments is warranted.

Soil moisture conditions exhibit significant control on the transport of DOC within a soil profile. Concentrations of DOC in soils are often highest near the litter layer and decrease with soil depth due to the degradation of DOC in solution through microbial consumption, complexation with primary and secondary minerals, and the reprecipitation with cations (Kalbitz et al., 2000). In coarse-textured soils in humid climates, these physiochemical processes of mobilization and translocation of elements enhanced by organic acids lead to the self-aggregation of soil horizons through podzolization (Lunstom, 2000; Sauer et al., 2007). Some studies suggest that podzolization can be largely episodic, enhanced by increases in water fluxes during storm events and snowmelt (e.g., Schaetzl et al., 2015).

At the catchment scale, podzolization processes can be driven by the covariation of topography and hydrology (Martinez et al., 2018; Musielok et al., 2021; Sommer et al., 2001). For example, hillslope patterns of soil morphology and chemistry have shown podzol soils in higher portions of landscapes with thick eluviated horizons and thin spodic horizon development, with more developed spodic horizons formed downslope

(Bailey et al., 2014; Bourgault et al., 2015; Sommer et al., 2000; 2001). Hillslope gradients of podzolization are attributed to spatial drivers of upslope mobilization of organic acids with weathered materials and lateral transport and immobilization downslope with shallow groundwater. This is assumed to be due to topographically-controlled shallow groundwater occurrence, persistence, and direction of flow within distinct podzol units affecting distribution of water and solutes (Detty and McGuire, 2010; Gannon et al., 2014; Gannon et al., 2017). Therefore, the formation of shallow water tables provides insight to how soils are hydrologically connected across hillslopes and potentially act as sources of DOC to streams (Bracken and Croke, 2007; Gannon et al., 2015; Jensco et al., 2009; Stutter et al., 2012; Zimmer and McGlynn, 2018).

When catchments are drier, groundwater stays deeper in the soil profile, which is dilute in DOC, and streams may only be connected to near-stream riparian soils. During storm events, water levels rise higher into soil profiles and interact with soil solutions richer in DOC. Additionally, as catchments wet up, the contributing source area of soil water to streams also expands laterally as upslope soils become saturated. In upslope regions where soil depths are shallow, storage is limited and saturation may occur frequently. Furthermore, in shallow forest soils, organic horizons represent a larger proportion of the soil profile. The flushing of DOC from hillslope soils during storm events increases as they become hydrologically connected to downslope streams with the movement of shallow groundwater (Boyer et al., 1997; Brown et al., 1999; Hood et al., 2006; McGlynn and McDonnell, 2003), either through soil matrix or through macropores and other preferential water flow paths (Beven and Germann, 1982; McDonnell et al., 1991). However, determining when, where, and by what mechanism DOC flushing occurs within a catchment is spatiotemporally dynamic, and is a continued point of research (Laudon et al., 2011; van Verseveld et al., 2008) and conversation (Burns, 2005).

This study aims to examine relationships between groundwater behavior and DOC concentrations in the shallow soil zone. To do this, groundwater hydrologic responses and water chemistry was analyzed for discrete storm events in a spatially-distributed shallow well network at Hubbard Brook Experimental Forest, NH, for when the transient water table is best predicted to form in shallow soils throughout the

catchment. To identify distinct landscape units that may act hydrologically similar, terrain-based wetness metrics were used as an organizing principle to group wells, which have also been shown to be useful in predicting podzol types in this region (Gillin et al., 2015). Given that the magnitude and timing of DOC export to streams is dependent on spatial patterns in carbon sources and transport processes across landscapes, a better understanding of hydrologic controls on DOC within a catchment is needed.

Methods and Materials

Site Description and Field Sampling

This study took place at Hubbard Brook Experimental Forest (HBEF) in New Hampshire, which is a long-term ecosystem research (LTER) site. Samples were collected within watershed 3, which is a 42.4 ha gauged hydrological reference watershed (Fig. 1). The HBEF is a cool-temperate and humid forest, with annual precipitation of 1,400 mm. The landscape is forested by northern hardwood species, including balsam fir (*Abies balsamea*), mountain white birch (*Betula papyrifera* var. *cordifolia*), and red spruce (*Picea rubens*) towards ridgetops, and transitioning predominately to sugar maple (*Acer saccharum*), yellow birch (*Betula alleghaniensis*), and American beech (*Fagus grandifolia*) at lower elevations. The elevation within this watershed ranges from 527-732 m.

Soils in this region are primarily well-drained Spodosols with sandy textures and thick O/A horizons, and smaller areas of Inceptisols and Histosols. Soil depth across this catchment generally increases as a downslope gradient from shallow ridgetops dominated by bedrock outcrops to downslope riparian areas that can be many meters deep. The bedrock geology of Watershed 3 is Rangeley Schist, overlain by glacial till depositions (~14 kya) of variable depths (Bailey et al., 2003).

A total of 42 instrumented shallow wells across Watershed 3 were used for this study (Fig. 1). The distribution of wells across the catchment covers a wide range in catchment properties (e.g., soil depth, soil type, landform, elevation). All wells were constructed of PVC pipe (3.18 or 5.08 cm OD) and screening (lateral slot size 0.025 cm). Wells for this study include those installed by Detty and McGuire (2010), Gannon et al., (2014), Benton et al., (2022), among others. The maximum depth of measured water

levels of each well varied from 30 cm - 125 cm. Well screens were either placed at or into the upper C horizon, or if no C horizon existed, to the depth of bedrock. All wells were instrumented with water level loggers that recorded at 10-minute intervals.

Groundwater samples used for this study (n = 261) were collected over 46 sampling dates across nearly 10 years (August 2011 to October 2020), although not every well was sampled during each sampling event. The number of wells sampled on a sampling date varied between 1 - 20 wells. The formation and persistence of the shallow, transient water table at Hubbard Brook is responsive to rain and snowmelt, therefore many of the sampling dates coincided with storm events. Using a peristaltic pump, wells were purged and allowed to recharge prior to the collection of a water sample. All samples were stored in 0.5 L bottles and brought back to the HBEF laboratory for processing within the same day. For the analysis of DOC, samples were filtered through an ashed 0.45 um glass microfiber filter and frozen until analysis. Sample analysis was performed by the United State Department of Agriculture Forest Service, Forestry Sciences Laboratory in Durham, NH. Concentrations of DOC were measured on a Shimadzu TOC-5000A (Shimadzu Corp., Kyoto, Japan).

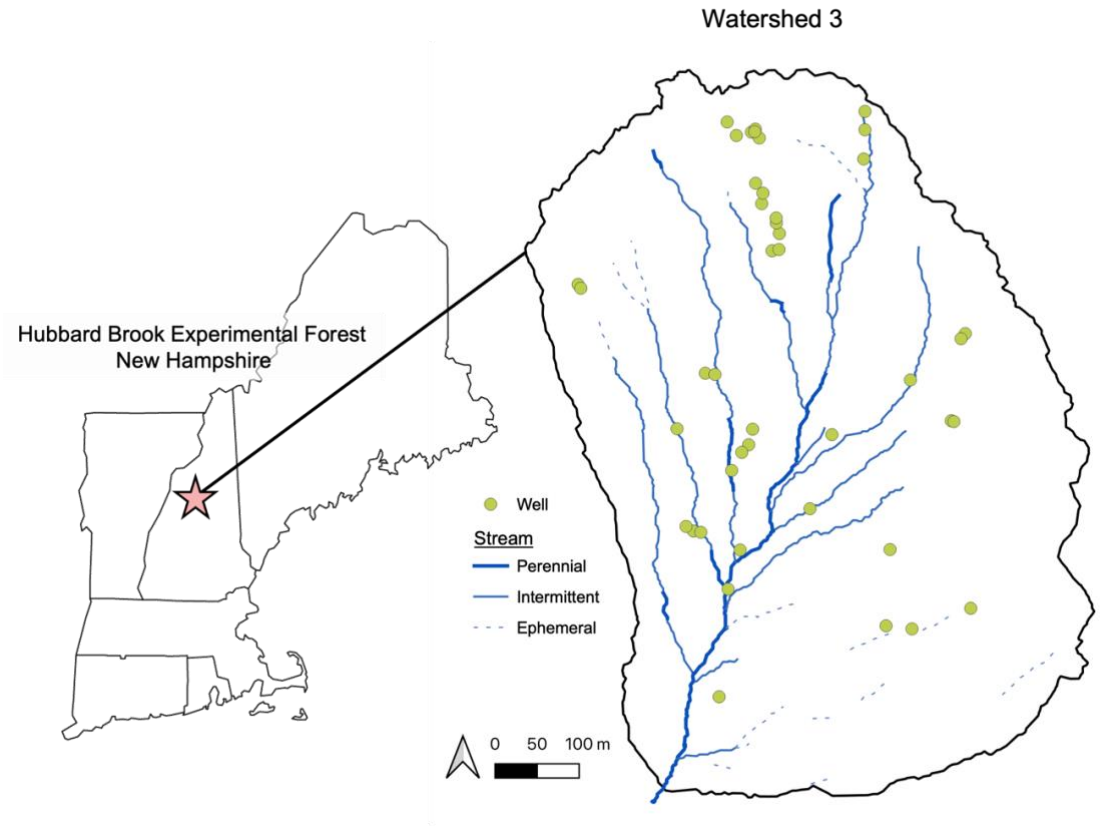

Figure 1. Regional map of New England and the location of Watershed 3 at the Hubbard Brook Experimental Forest, in New Hampshire, USA. All wells shown throughout the catchment (green circles) are those where groundwater grab samples were taken for this study from 2011-2020 and where water level measurements were made.

Characterization of Precipitation Events

To determine the time interval over which hydrologic responses were measured, storm events during the snow-free portion of the year were identified using aggregated hourly precipitation data gathered from rain gauge 19 (June-August 2011), gauge 1 (2011-2016) and gauge 4 (2016-2020) at HBEF (USFS Northern Research Station, 2022). Delineations of single events were extracted from time series data using the “HydRun" toolbox (Tang and Carey, 2017) adapted for R (Albertross, 2021) (Fig. 2). Any event was identified as rainfall exceeding 1.3 mm (0.5 inches) with a maximum time gap between any rainfall of 24 hours.

Total event rainfall (mm) was calculated by taking the sum of rainfall for the entire precipitation event. Maximum rainfall intensity (mm/hr) was measured at the maximum total rainfall that occurred during a 1-hour period. Storm intensity (mm/hr) was determined by dividing the total event rainfall by the event duration. A total of 9 sampling events were identified as 'non-events,' and these samples were not excluded from this study so that a wide range in environmental conditions could be represented. If no storm was identified using HydRun that corresponded with a sampling date, rainfall characteristics were calculated for only the sample day and the two days before.

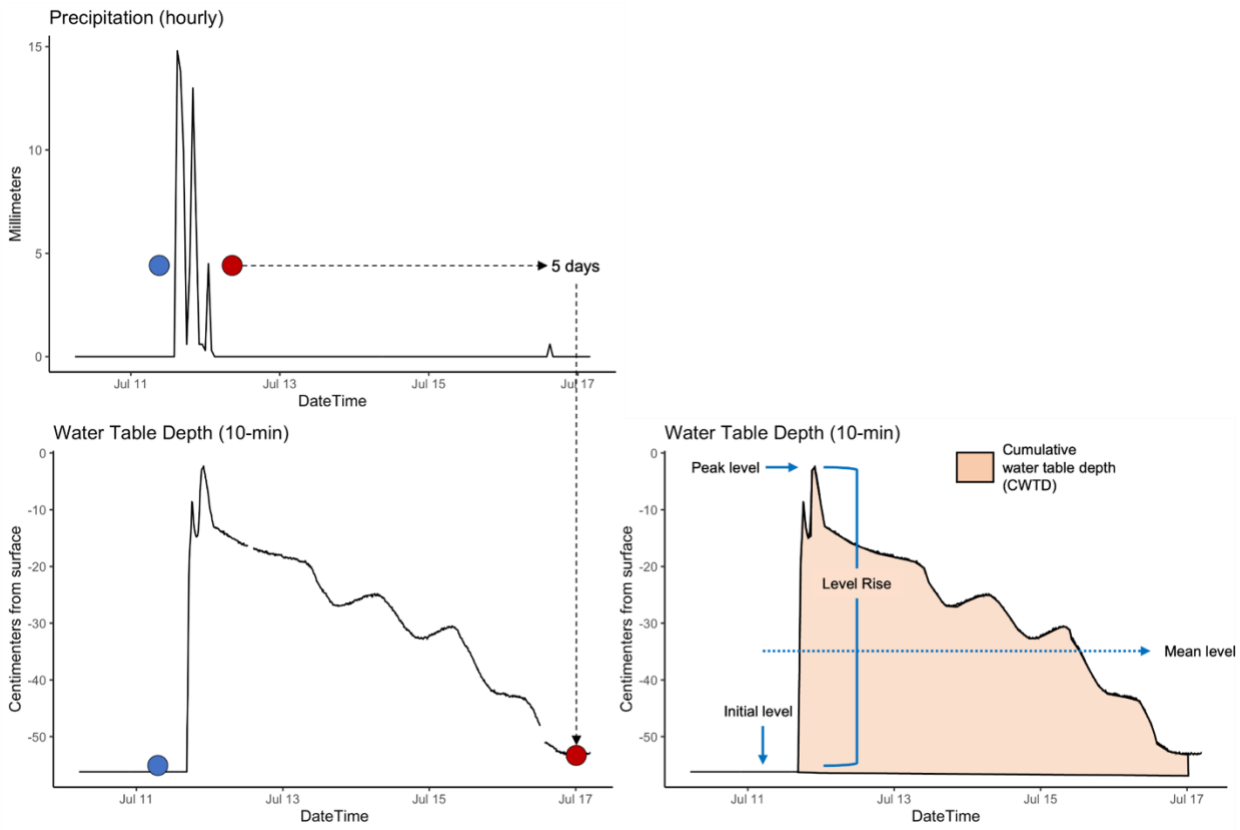

Figure 2. Top: Delineation of a precipitation event for which storm characteristics were calculated across, which is calculated from the start of the storm (blue dot) to the end (red dot). Bottom: Water table metrics were calculated starting from the start of the precipitation and ending 5 days after the precipitation event ended.

Water table dynamics

To assess water table fluctuations in response to precipitation events, several response metrics were calculated from 10-minute water level time series data. All water level data was analyzed as depth from the soil surface, in centimeters. All water table metrics were calculated for when the precipitation event started until five days after the event ended (Fig. 2).

Initial water levels were extracted as the first water level recording at the start of the precipitation event. Peak water table levels were determined as the shallowest depth the water table reached during the duration of the event. The total water table rise was calculated by subtracting the initial water level from the peak level. Mean water levels were the average water table level during the duration of the event. Cumulative water table depth (CWTD) during each event was calculated using the "trapz" function in R, which calculates the area under the curve (Borchers, 2019). Larger values of CWTD typically indicate a more persistently lower water table depth (deeper in the profile = high depth values), whereas smaller CWTD indicates a quick and/or consistently shallow water level response.

Terrain attributes

All topographic metrics were computed from a 5-m digital elevation model (DEM) of watershed 3 at HBEF. Hillslope contributing areas (i.e., sub-catchments) were determined for each well location using the watershed function in WhiteBoxTools in R (Lindsay, 2014). This tool performs a watershedding operation based on designated outlet pour points (well locations). The DEM was preprocessed by first filling sinks (Wang and Liu, 2006) and least cost depression breaching (Lindsay, 2014), prior to any watershed delineation. Pour points were snapped to a flow accumulation grid created from a d8-derived flow direction raster to map areas that drain to each point. Sub-watershed borders were manually adjusted for known surface artifacts and onsite expert knowledge of the landscape for well location.

Topographic attributes for each contributing area were calculated at the mean value for each topographic raster. Topographic wetness index (TWI) was calculated using the downslope gradient in a 5 m direction (Hjerdt, 2004) instead of local slope (Beven

and Kirkby, 1979). The TWI is a metric used to quantify topographic controls on hydrology by describing the tendency for water flow to accumulate in some area. Topographic position index (TPI) was calculated by taking the difference between the elevation of a pixel and the mean elevation of the surrounding pixels in a 100-m radius (Guisan et al., 1999). Larger TPI values represent higher elevation locations, like ridges, whereas smaller values represent landforms such as toe- and footslopes.

Bedrock-weighted upslope accumulated area (UAAb) was calculated with a multiple flow direction algorithm (Seibert and McGlynn, 2007). This metric is expressed as the normalized ratio between UAA and UAA weighted by bedrock outcrop cells, where bedrock outcrops were assigned large weighting values (Gillin et al., 2015). UAAb values vary between 0-1, where a value of 1 indicates an entire upslope area is comprised of bedrock and shallow soils. Local elevation of each well and the linear distance to the nearest perennial stream was extracted at the well point location (stream network outlined in Fig 1).

Statistical Analyses

All statistical analyses and figure creation were performed in R software Version 4.2.2 (R Core Team, 2021). To examine how certain wells grouped together based on common contributing area topographic metrics (TWI, TPI, UAAb), a k-means clustering analysis was performed in R. A k-means analysis groups data points as clusters so that similar points group together by reducing the within-cluster sum of squares (MacQueen, 1967). The optimal number of clusters (minimum *k* number of centroids) was determined by the elbow, or inflection point, where the rate of decline in the within-sum of squares is reduced for *k* number of groups. Significant differences in topographic metrics and DOC concentrations between k-means well groups were identified with a Kruskal-Wallis test (Kruskal & Wallis, 1952) followed by a post-hoc Dunn's test, which is appropriate for comparing groups with uneven sample sizes.

To identify top hydrodynamic predictors of DOC concentrations, a regression tree analysis was performed using the "rpart" package (Therneau & Atkinson, 2019). Prior to the creation of the regression tree, water table response metrics were assessed in a correlation plot, and anything correlated at r = 0.85 or greater was determined to be

collinear and removed from the analysis. The predictor variables used in the model were peak water level, initial water level, net water table rise, and cumulative water table depth (CWTD). The regression tree was fit using a minimum split of 2, a minimum bucket size that was 10% of the sample size, and complexity parameter of 0.01. Post-pruning of the tree was determined by the minimum classification error. The tree was fitted using a training data set (80% of the sample size) and the remaining testing set (20%) was used to evaluate the model's performance and calculate the root mean square error (RMSE).

Relationships between DOC concentrations and important water table response metrics variables revealed from the regression tree analysis were analyzed first with a simple linear regression model, without an interaction term. Interactions between this relationship by the well group (k-means group) were then tested in a separate model, to test for the influence of topographic structure on increasing predictive power. If the interaction term was significantly significant, the interaction term was determined to be important. A Shapiro-Wilk test was used to evaluate the normality assumptions of the data.

Results

Characteristics of k-means Groundwater Groups

The number of k-means clustering groups identified three groups of wells as most appropriate for this dataset. Clusters were based on characteristics of contributing area topographic wetness (TWI) and topographic position (TPI), and the proportion of bedrock-weighted upslope accumulation area (UAAb) for each well location (Fig. 3). There were 14 wells assigned to group one, 20 in group two, and 22 in group three.

Wells in group one existed higher in the watershed (612 - 710m) and farthest away from perennial streams (mean 300 m away) (Fig. 4). Wells in group three were lowest in elevation (529 - 699 m) and closest to a perennial stream (mean 50 m away), the closest well was within 3 meters of a stream. Those classified in well group two fell in the middle of groups one and three for elevation and distance to the stream. For this reason, this study will refer to well groups 1, 2, and 3 as "upslope," "midslope," and "near-stream," respectively.

Upslope wells had significantly higher values of UAAb (> 0.5, $p < 0.05$), compared with wells in the midslope and near-stream groups (Fig. 3). Contributing areas to upslope wells had higher relative mean elevations (high TPI values) compared to the other two groups, which reflects their proximity to bedrock outcrops and shallow soils at the ridgetops. In comparison, midslope and near-stream wells had significantly lower UAAb and TPI values, in lower hillslope positions further away from bedrock-dominated areas of the catchment. Some values for TPI were negative for near-stream wells, indicating areas that some contributing areas were mostly flat or have nearly no slope. Near-stream and midslope wells had significantly higher mean upslope TWI values compared to upslope wells and were not significantly different from each other.

DOC concentrations were not significantly different between all well groups, and only upslope wells had significantly higher concentrations compared to downslope wells (Fig. 4). A total of 261 samples were analyzed, with 95 samples classifying as upslope, 82 midslope, and 84 near-stream samples. The spread in DOC concentrations was greatest in upslope wells (1.0 - 31.2 mg/L; sd = 6.6), with a mean concentration of 10.0 mg/L. Samples in midslope positions had a mean of 3.4 mg/L (sd = 3.3) and near-stream positions had a mean of 2.1 mg/L (sd = 2.0).

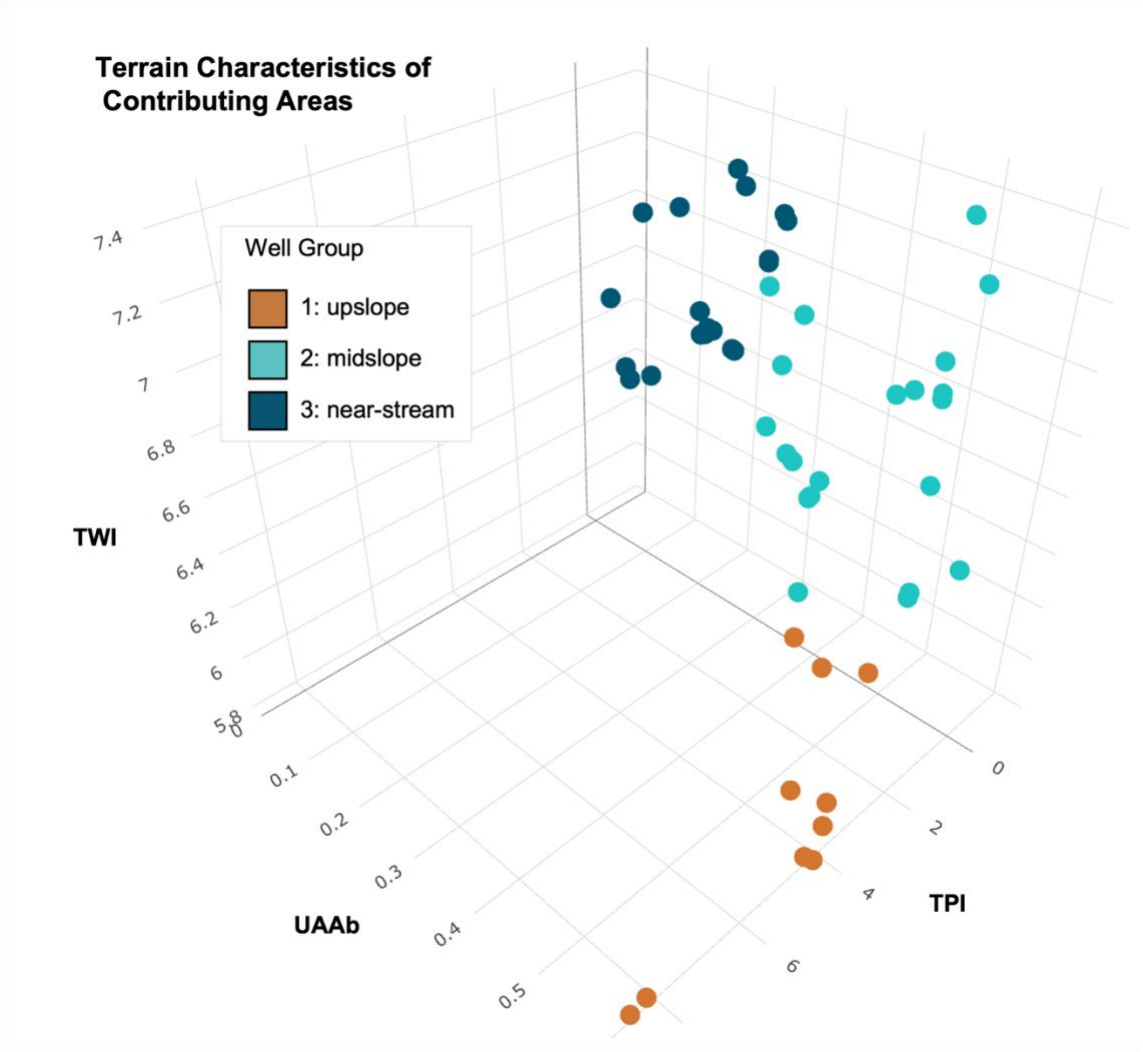

Figure 3. Three-dimensional plot of the terrain metrics within contributing areas for each well used in the k-means clustering analysis: topographic wetness index (TWI), topographic position index (TPI), and bedrock-weighted upslope accumulation areas (UAAb). Each well is colored by the k-means cluster (well group) it was assigned to. Some wells existed within the same DEM pixel or directly adjacent, therefore some points might be slightly or completely overlapping.

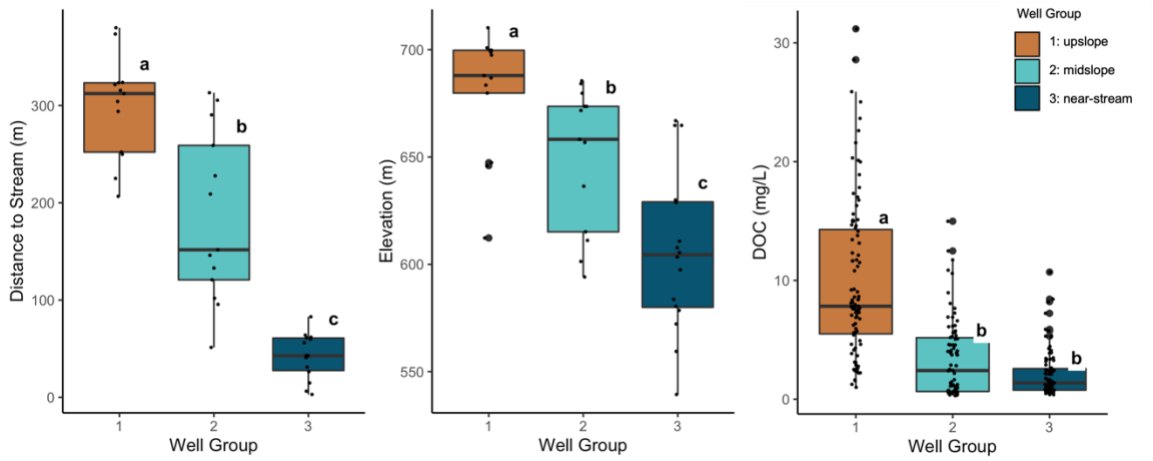

Figure 4. Box plots showing the difference between wells in landscape position as linear distance to nearest perennial stream (A) and local elevation (B). A map of the watershed 3 stream network can be found in Figure 1. Plot C shows the distribution of groundwater dissolved organic carbon (DOC) concentrations taken from wells (n = 261), which have been classified into three well groups 1-3. Different lowercase letters above each box denote significant differences between well groups ($p < 0.05$).

Storm event groundwater responses

Total precipitation across all sampled events varied between 0-152 mm, with a mean of 35 mm. The largest of these sampled events occurred directly after Hurricane Irene in 2011. The average duration of a given event spanned 69 hours, which is approximately across 3 days. The maximum hourly intensity of precipitation was 39 mm/hr, with a mean of 7.2 mm/hr. Additional summary statistics for all 46 sampled events are provided in Table 1. Characteristics for each storm event can be found in Appendix Table B1.

Near-stream wells were generally wet for the largest proportion of the year. Two wells in this group had persistently high-water tables, and during sampled events reached the soil surface (<5 cm). The remaining wells had deeper water tables that would rise higher into soil profiles during precipitation events (high water level rise). Across all characterized storms, only 15 samples (out of 84) were taken from a well in this group where the water table did not reach within 50 cm of the soil surface, calculated as peak water level.

In contrast, the shallow water table in wells classified as upslope (higher in elevation, furthest from perennial streams) only formed during precipitation events (e.g., rainfall, snowmelt). Soils here were quick to wet up and drain following events, and during the storms had characteristically smaller CWTD and shallow peak water levels that reached near-surface (Table 2).

Groundwater behavior in wells that were classified as midslope were less generalizable than near-stream or upslope well groups. Two wells in this group acted like those near-stream that stayed consistently wet near the soil surface, and during sampled storm events would reach the soil surface. The remaining wells acted similar to upslope wells in that they were responsive to storm events (high peak water levels, large water table rise) albeit with longer recession times or had deep water tables that never reached above 50cm. The large proportion of wells in the midslope group that had deeper groundwater storm responses likely reflects why this group had the highest mean CWTD, lowest mean water level, and lowest peak water level during a characterized sample event.

Table 1. Summary statistics for the storm events (n=46) for when groundwater samples for DOC chemistry were taken in this study.

Metrics	Total Precipitation (mm)	Event duration (hr)	Max Hourly Intensity (mm/hr)	Whole storm Intensity (mm/hr)
Minimum	0.0	25.0	0.0	0.0
Maximum	151.5	192.0	38.9	2.8
Mean	35.4	69.0	6.6	0.6

Table 2. Summary statistics for hydrologic response metrics calculated for each precipitation event for each well group (upslope, midslope, and near-stream). All metrics were rounded to the nearest whole centimeter, except for cumulative water table depth (CWTD) which was rounded to the nearest tens.

Water table storm response:		Upslope	Midslope	Near-stream
Peak level (cm)	mean	15	39	28
	range	0 - 84	0 - 109	0 - 90
	sd	14	30	24
Mean level (cm)	mean	43	54	43
	range	16 – 95	3 – 102	6 – 99
	sd	17	30	27
Rise (cm)	mean	37	28	24
	range	0 – 92	0 – 79	0 – 78
	sd	28	21	21
CWTD (cm)	mean	1,670	2,280	2,250
	range	80 – 8,800	10 – 11,930	50 – 10, 240
	sd	1,580	2,420	2,420

Hydrodynamic predictors of DOC concentrations

The regression tree model created had a total of three splits with four leaf nodes. Comparisons between observed and predicted DOC values for the resulting regression tree model had a root mean square error (RMSE) of 2.4. The peak water table level was shown to be the most important explanatory hydrologic response metric for predicting DOC concentrations in shallow groundwater during storm events (Fig. 5). The root split of the regression tree was identified as whether the water table reached 13 cm or shallower during a storm event (Fig. 6).

In this model, the mean concentration in groundwater samples where the water table surpassed 13 cm towards the soil surface was 6.0 mg/L, which is approximately three times higher than when the water table did not (mean concentration 1.9 mg/L). When the water table did reach shallow depths ($\leq$ 13 cm from the surface), 45 samples were taken from wells that were classified as upslope whereas only 15 and 11 samples were classified as midslope and near-stream wells, respectively.

Concentrations of groundwater DOC were even higher when the total water table rise during an event was greater than 14 cm (mean DOC 7.4 mg/L, max DOC concentration of 31.2 mg/L), which was calculated as the jump in initial water table level to the peak. Total water table rise during an event was considered the second most important variable in this regression model (Fig. 5). This tree node had the greatest proportion of samples that came from upslope wells (76%). The proportion of samples that derived from upslope wells compared to the other two landscape positions decreased when the water level rise was less than 41cm (30%). In terms of average hydrologic behavior, the upslope wells generally responded with the greatest rise in water table during a storm event from the beginning of the storm to peak (mean 37 cm).

The tree node with the lowest DOC concentrations consisted of groundwater samples taken from wells where the peak water level never exceeded into the top 46 cm of the soil profile, with a mean concentration of only 1.1 mg/L and max DOC = 8.1 mg/L. Most of these samples (70%) were taken from midslope wells, whereas upslope wells contributed the least (5%).

Linear regression models were used to examine the relationship between peak water table height on DOC concentrations with and without accounting for well groups as

an interaction term. The first model with no interaction term had an r^2 of 0.29 ($p < 0.001$), where DOC concentrations increased in a log-linear relationship with a rise in peak water table reached during an event (shallower; Fig. 7). In the second model, the interaction of k-means well groups increased the total variance explained by 25% (r^2 of 0.54, $p < 0.001$). Across all well groups, DOC concentrations had similar relationships with peak water table height, where higher concentrations were related to smaller (shallower) water table heights (Fig. 7). Grouping variables together were considered significant ($p < 0.05$) in predicting relationships between peak height and DOC concentrations. This model suggests that accounting for the presence of upslope and near-stream wells has a larger effect on DOC concentrations, than accounting for midslope wells, which were not statistically significantly different from either of the other two well groups ($p > 0.05$).

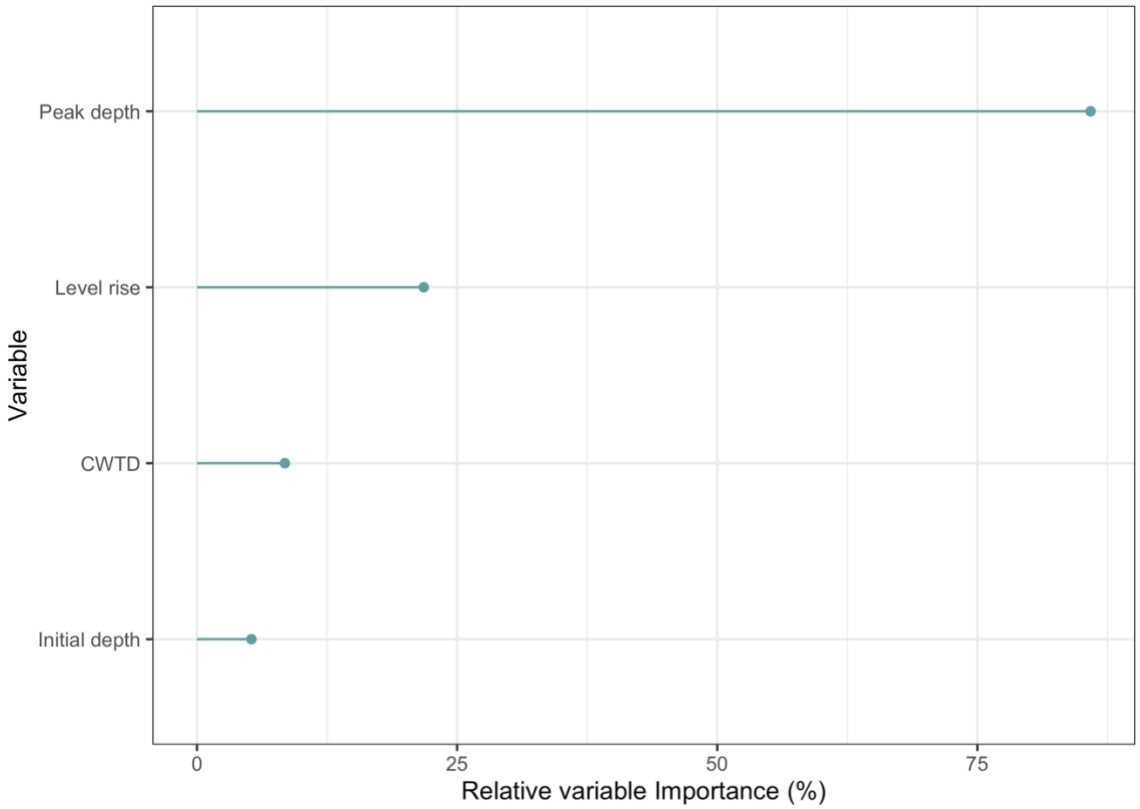

Figure 5. Lollipop graph of the variables (water table response metrics) used in the regression tree analysis, ranked by variable importance for the model. The mean depth throughout a storm event was excluded from this analysis due to being significantly correlated with the other variables.

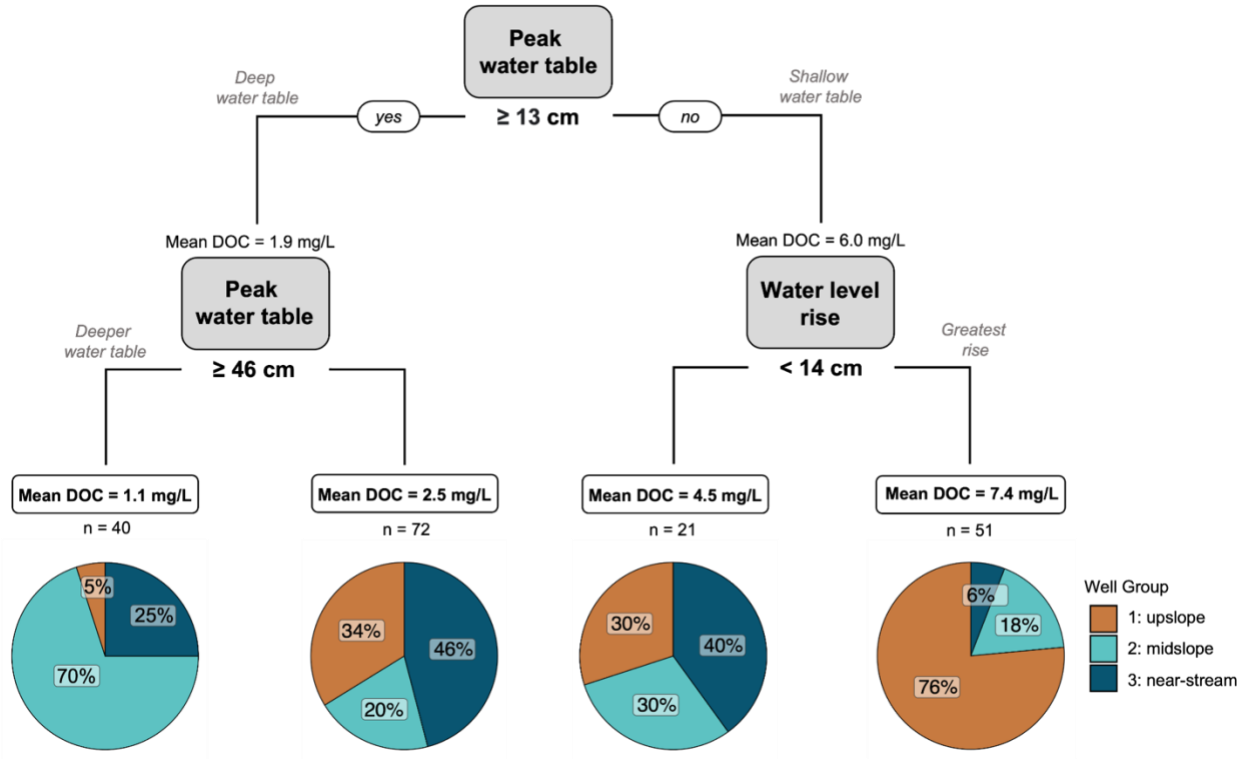

Figure 6. Regression tree for groundwater DOC concentrations with water table response metrics during a sampled event as predictors. Predictor variables used for this analysis were peak water level reached, initial water level, water level rise, and cumulative water level depth. Mean DOC concentrations are reported for all that fall into each leaf node. Pie charts represent the proportion of each well group represented in the number of samples (n=sample size) at each node. The ranking of importance of each predictor variable is shown in Figure 5.

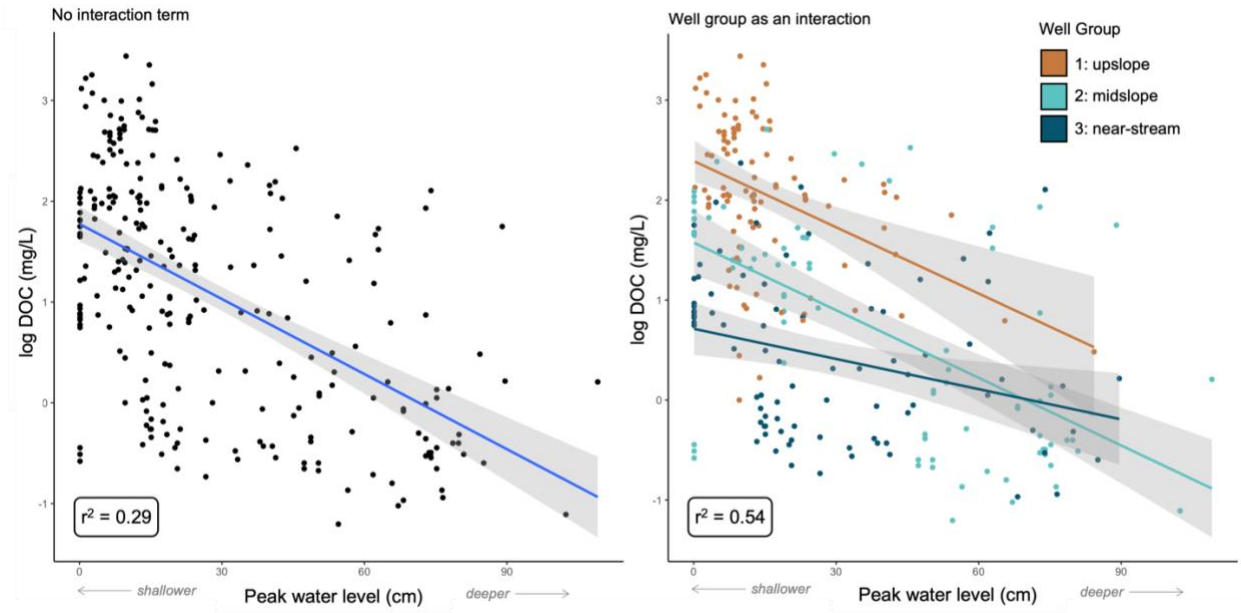

Figure 7. Changes in dissolved organic carbon (DOC) concentrations with peak water level reached during an event. The best-fitting regression models (lines) with standard error (shaded areas) are given for models that did not (A) and did (B) account for well groups as an interaction term in the model.

Discussion

The influence of contributing area topography on groundwater responses

By using terrain-based wetness metrics as organizing principles, this study categorized the well network into three groups. Common shallow groundwater responses within well groups, suggest that water table dynamics during storms are, at least in part, topographically mediated by contributing catchment morphology. For example, the well group with the highest topographic wetness (TWI) and lowest topographic position (TPI) within the contributing area, named in this study as 'near-stream,' were mostly found in areas of topographic depression, lower in elevation, and/or closest to perennial streams. The proportion of time that the water table existed during an event in these wells was often the greatest in the well network, and hydrologic behavior in these locations acted functionally like those described as riparian areas by others (e.g., Burt et al., 2002; McGlynn and McDonnell, 2003). Relationships between the persistence of shallow water tables, indicating wetter landscape positions, in locations with larger contributing areas

and high TWI values are consistent with those found other forested watersheds (Detty and McGuire, 2010; Jencso et al., 2009; Pacific et al., 2011).

In contrast, the well group that was classified as upslope had statistically higher subcatchment TPI values and low TWI values. Higher bedrock-weighted upslope accumulated area (UAAb) indicates they exist higher in the watershed near ridges or bedrock outrops, where mineral soils in these portions of watershed 3 have been described as shallow-to-bedrock (Bailey et al., 2014). Limited water storage capacity coupled with steeper slope gradients enhances the rapid transmission of water, which could explain observed flashy water table behavior during precipitation events. This would indicate upslope wells representing areas on the landscape have a high potential for topographically-forced lateral hydrologic flushing rather than storage (Hornberger et al., 1994; Kuras et al., 2008). Drainage area characteristics that enhance hydrologic flushing support observations made by Gannon et al. (2017), where occurrence of lateral unsaturated flow was dominant in shallow soils nearest to bedrock outcrops within the same watershed.

In steep headwater catchments, topographic indices that describe the tendency for lateral redistribution of soil moisture (e.g., topographic wetness, upslope accumulated area, hillslope convergence) have been useful in identifying the distribution and behavior of water tables (Jensco et al., 2009; Detty and McGuire, 2010; Pacific et al., 2011; Rinderer et al., 2014; Singh et al., 2018). Relationships between surface topography and groundwater responses are based on the general understanding that in shallow well-drained soils, hydrologic fluxes and flow paths are strongly driven by topographic gradients. However, the assumption that all lateral subsurface flow from an upslope area arrives uniformly to a downslope point in a catchment cannot be expected when local attributes of the soil override hydrologic connectivity, such as soil depth or preferential flow and macropores (Beven and Germann, 1982; Jones, 2010).

Less generalizable and highly variable water table responses during storm events in the midslope well group could indicate portions of the landscape where groundwater behavior is poorly predicted by surface topography. For example, several studies have shown that the relationship between surface topography and hillslope hydrologic responses is flow-dependent, and often more related to subsurface topography (e.g.,

bedrock microtopography, restrictive layer) (Freer et al., 2002; Tromp-van Meerveld and McDonnell, 2006). Additionally, the transient water table in many of the wells in the midslope group typically stayed deep during storm events, which could indicate they are often hydrologically disconnected from upslope sources as water is laterally redistributed across hillslopes. By building on existing work by Detty and McGuire (2010), future studies could examine the temporal dynamics of surface topography influences on water table response at HBEF, such as Singh et al. (2018).

Shallow groundwater flushing as a mechanism for DOC transport

Regardless of landscape position, there was a positive relationship between how high the water table reached within the soil profile and DOC concentrations measured at the same location during storm events across the well network (Fig. 4a; Fig. 7). This could reflect the movement of groundwater rising higher into soil profiles, accessing soil solutions richer in organic acidity. At HBEF it is well documented that soil solution DOC is highest in the O-horizon and decreases with depth (e.g., Dittman et al., 2007; LoRusso et al., 2022; Palmer et al., 2004, 2005). However, water tables in all well groups reached shallow depths during storm events, and yet groundwater samples from upslope wells consistently had higher DOC concentrations while also having a short interaction time during an event (quick rise and recession).

Prediction power of water table height on DOC concentrations increased when accounting for differences by well group, which were categorized on characteristics of their contributing area. Because of this, it could be assumed there is a spatially dominant, upslope control on the DOC variability besides just water table dynamics within the soil profile itself. Wells described in the upslope group had characteristically high accumulated areas that comprised of bedrock outcrops (UAAb). Bedrock outcrops, intermixed with shallow organic soils, have been extensively mapped at HBEF (Fraser et al., 2020). Bedrock-dominated areas on the landscape are typically in higher elevation ridge zones with coniferous vegetation (e.g., spruce, fir, birch) and waters draining from these parts of the landscape have markedly high DOC concentrations and low pH values (Bailey et al., 2019; Dittman et al., 2007).

The prevailing hypothesis for soil development near bedrock outcrops is that frequent flushing of organic acids contributed by decomposing upslope organic soils contributes to downslope enhancement of mineral weathering rates (Bailey et al., 2014). Spatial differences in groundwater DOC concentrations observed in this study supports the idea that the transport of weatherable acidity is enhanced in these portions of the landscape, especially during larger storm events. Mineral soils formed directly downslope from bedrock-dominated regions have been described with profiles dominated by thick eluvial horizons (e.g., E horizons) down to bedrock, largely depleted in weatherable elements. Under acidic conditions, dissolved organic acids form Fe-Al complexes (spodic material) and are moved in solution until, under more pH neutral conditions, they become immobilized. Translocated spodic material is thought to re-precipitate directly downslope of strongly eluviated soils, as seen by soil profiles that have extremely thick Bhs horizons, a designation for accumulated illuvial Fe-Al-OM. This fundamentally follows the traditional view of podzolization processes (e.g., Lundstrom et al., 2000), except that in bedrock-controlled portions of the landscape the redistribution of spodic materials occurs in the downslope direction along flow paths, rather than vertically through a single soil profile with percolating water (Sommer et al., 2000; 2001; Bailey et al., 2014; Bourgault et al., 2017; Gannon et al., 2017).

The spatial patterns of water table behavior and DOC chemistry within the catchment underscores the impact upslope soil solution chemistry has on downslope soil development. Flashy water table responses (shallow peak water levels, high absolute rise, quick recession) in soils draining from bedrock outcrops provides a mechanistic basis for the flushing of organic acidity during storm events. Additionally, this suggests that flushing events may be a rate-limiting process for hillslope mobilization of spodic material (Krettek & Rennert, 2021; Schaetzl et al., 2015) and for DOC to streams (Boyer et al., 1997; Hood et al., 2006; Inamdar & Mitchell, 2006; Lambert et al., 2014) in headwater catchments.

Often riparian areas (i.e., near-stream) are described as the dominant and quickest contributors of catchment DOC export, located at the interface of hillslopes and streams (Jencso et al., 2009). However, significantly lower DOC concentrations in soils near-stream observed in this study, and others, suggest that DOC sources may be from discrete

portions of hillslope where DOC concentrations are highest (Bailey et al., 2019; Gannon et al., 2017; Zimmer et al., 2019) or from different flow pathways that are not riparian sourced (Radke et al., 2019). Gannon et al., 2017 proposed two ways upper hillslope soils could act as dominant DOC sources: (1) the rapid transport of DOC with preferential flow through macropores directly downslope to streams or (2) improved connection of hillslope soils to ephemeral streams with the expansion of the stream network higher into the landscape. Regardless, both processes would be enhanced with projected increases in storm frequency and intensity throughout the northeastern US (Hicke et al., 2022).

Conclusions

Shallow groundwater dynamics and DOC chemistry within this watershed was shown to be extremely variable across the catchment. Terrain-based wetness metrics were used to group wells and characterize groundwater behavior by landscape position. During a storm event, the peak water table height best explained DOC concentrations. Therefore, DOC mobilization and transport could be enhanced during conditions when shallow groundwater is higher in the profile and when soils are hydrologically connected. This relationship was strongest in wells nearest to bedrock outcrops and associated shallow soils, which are likely significant sources of DOC input to soils directly downslope. At HBEF this region is higher up in the catchment, and while being a distant source that takes up a relatively small proportion of the landscape, could be extremely important to whole catchment DOC export. Because of the unique ties between shallow groundwater dynamics and DOC mobilization, future work should assess the impacts of increased flushing in regards the transport of DOC to streams and the alteration of soil C pools in a changing climate.

Additionally, this study highlights the importance of spatially and temporally intensive shallow groundwater characterization across forested catchments, which is still lacking. Only few studies have shown variability in groundwater dynamics and/or solute chemistry along hillslopes and even less that explicitly test event-specific dynamics. Most often, experimental studies focus on measurements within riparian zones since they can represent a primary and rapid source of DOC to streams. Results presented in this study

could suggest otherwise, and shallow groundwater dynamics and chemistry in hillslope soils farther away from streams may warrant further investigations. The resources required for installing and maintaining a high-frequency well monitoring network across catchments with repeated chemistry sampling campaigns are limiting factors. These hurdles highlight the benefits of long-term experimental sites, with multiple research goals and mutual needs.

References

Albertross, C. 2021. HydRun. https://github.com/codyalbertross/HydRun.git.

Bailey, S.W., Buso, D.C. and Likens, G.E., 2003. Implications of sodium mass balance for interpreting the calcium cycle of a forested ecosystem. *Ecology*, *84*(2), pp.471-484.

Bailey, S.W., Brousseau, P.A., McGuire, K.J. and Ross, D.S., 2014. Influence of landscape position and transient water table on soil development and carbon distribution in a steep, headwater catchment. *Geoderma*, *226*, pp.279-289.

Bailey, S.W., McGuire, K.J., Ross, D.S., Green, M.B. and Fraser, O.L., 2019. Mineral weathering and podzolization control acid neutralization and streamwater chemistry gradients in upland glaciated catchments, northeastern United States. *Frontiers in Earth Science*, *7*, p.63.

Benton, J.R., McGuire, K.J. and Schreiber, M.E., 2022. Subsurface permeability contrasts control shallow groundwater flow dynamics in the critical zone of a glaciated, headwater catchment. *Hydrological Processes*, *36*(9), p.e14672.

Beven, K. and Germann, P., 1982. Macropores and water flow in soils. *Water Resources Research*, *18*(5), pp.1311-1325.

Borchers HW (2019) pracma: practical numerical math functions. R package version 2.2.9. https://CRAN.R-project.org/package=pracma

Bourgault, R.R., Ross, D.S. and Bailey, S.W., 2015. Chemical and morphological distinctions between vertical and lateral podzolization at Hubbard Brook. *Soil Science Society of America Journal*, *79*(2), pp.428-439.

Bourgault, R.R., Ross, D.S., Bailey, S.W., Bullen, T.D., McGuire, K.J. and Gannon, J.P., 2017. Redistribution of soil metals and organic carbon via lateral flowpaths at the catchment scale in a glaciated upland setting. *Geoderma*, *307*, pp.238-252.

Bower, J.A., Bailey, S.W., Pennino, A.M., and Duston, S.A. 2022. Hubbard Brook Experimental Forest: Watershed 3 Lateral Weathering Pedon Description. Environmental Data Initiative.

Bower, J.A., Ross, D.S., Bailey, S.W., Pennino, A.M., Jercinovic, M.J., McGuire, K.J., Strahm, B.D., Schreiber, M.E. 2023. Development of a lateral topographic weathering gradient in forested podzols. Geoderma. ***In review.***

Boyer, E.W., Hornberger, G.M., Bencala, K.E. and McKnight, D.M., 1997. Response characteristics of DOC flushing in an alpine catchment. *Hydrological Processes*, *11*(12), pp.1635-1647.

Bracken, L.J. and Croke, J., 2007. The concept of hydrological connectivity and its contribution to understanding runoff-dominated geomorphic systems. *Hydrological Processes: An International Journal*, *21*(13), pp.1749-1763.

Brown, V.A., McDonnell, J.J., Burns, D.A. and Kendall, C., 1999. The role of event water, a rapid shallow flow component, and catchment size in summer stormflow. *Journal of Hydrology*, *217*(3-4), pp.171-190.

Burns, D., 2005. What do hydrologists mean when they use the term flushing?. *Hydrological Processes: An International Journal*, *19*(6), pp.1325-1327.

Burt, T.P., Pinay, G., Matheson, F.E., Haycock, N.E., Butturini, A., Clement, J.C., Danielescu, S., Dowrick, D.J., Hefting, M.M., Hillbricht-Ilkowska, A. and Maitre, V., 2002. Water table fluctuations in the riparian zone: comparative results from a pan-European experiment. *Journal of Hydrology*, *265*(1-4), pp.129-148.

Detty, J.M. and McGuire, K.J., 2010a. Threshold changes in storm runoff generation at a till-mantled headwater catchment. *Water Resources Research*, *46*(7).

Detty, J.M. and McGuire, K.J., 2010b. Topographic controls on shallow groundwater dynamics: implications of hydrologic connectivity between hillslopes and riparian zones in a till mantled catchment. *Hydrological Processes*, *24*(16), pp.2222-2236.

Dittman, J.A., Driscoll, C.T., Groffman, P.M. and Fahey, T.J., 2007. Dynamics of nitrogen and dissolved organic carbon at the Hubbard Brook Experimental Forest. *Ecology*, *88*(5), pp.1153-1166.

Drever, J. I., and Stillings, L.L. "The role of organic acids in mineral weathering." *Colloids and Surfaces A: physicochemical and engineering aspects* 120, no. 1-3 (1997): 167-181.

Drever, J.I. and Vance, G.F., 1994. Role of soil organic acids in mineral weathering processes. *Organic acids in geological processes*, pp.138-161.

Fraser, O.L., Bailey, S.W., Ducey, M.J. and McGuire, K.J., 2020. Predictive modeling of bedrock outcrops and associated shallow soil in upland glaciated landscapes. *Geoderma*, *376*, p.114495.

Freer, J., McDonnell, J.J., Beven, K.J., Peters, N.E., Burns, D.A., Hooper, R.P., Aulenbach, B. and Kendall, C., 2002. The role of bedrock topography on subsurface storm flow. *Water Resources Research*, *38*(12), pp.5-1.

Fröberg, M., Berggren, D., Bergkvist, B., Bryant, C. and Mulder, J., 2006. Concentration and fluxes of dissolved organic carbon (DOC) in three Norway spruce stands along a climatic gradient in Sweden. *Biogeochemistry*, *77*, pp.1-23.

Gannon, J.P., Bailey, S.W. and McGuire, K.J., 2014. Organizing groundwater regimes and response thresholds by soils: A framework for understanding runoff generation in a headwater catchment. *Water Resources Research*, *50*(11), pp.8403-8419.

Gannon, J.P., McGuire, K.J., Bailey, S.W., Bourgault, R.R. and Ross, D.S., 2017. Lateral water flux in the unsaturated zone: A mechanism for the formation of spatial soil heterogeneity in a headwater catchment. *Hydrological Processes*, *31*(20), pp.3568-3579.

Gillin, C.P., Bailey, S.W., McGuire, K.J. and Gannon, J.P., 2015. Mapping of hydropedologic spatial patterns in a steep headwater catchment. *Soil Science Society of America Journal*, *79*(2), pp.440-453.

Guggenberger, G., Zech, W. and Schulten, H.R., 1994. Formation and mobilization pathways of dissolved organic matter: evidence from chemical structural studies of organic matter fractions in acid forest floor solutions. *Organic Geochemistry*, *21*(1), pp.51-66.

Guisan, A., Weiss, S.B. and Weiss, A.D., 1999. GLM versus CCA spatial modeling of plant species distribution. *Plant Ecology*, *143*, pp.107-122.

Hicke, J.A., S. Lucatello, L.D., Mortsch, J. Dawson, M. Domínguez Aguilar, C.A.F. Enquist, E.A. Gilmore, D.S. Gutzler, S. Harper, K. Holsman, E.B. Jewett, T.A. Kohler, and KA. Miller, 2022: North America. In: *Climate Change 2022: Impacts, Adaptation and Vulnerability.* Contribution of Working Group II to the Sixth Assessment Report of the Intergovernmental Panel on Climate Change [H.-O. Pörtner, D.C. Roberts, M. Tignor, E.S. Poloczanska, K. Mintenbeck, A. Alegría, M. Craig, S. Langsdorf, S. Löschke, V. Möller, A. Okem, B. Rama (eds.)]. Cambridge University Press, Cambridge, UK and New York, NY, USA, pp. 1929–2042, doi:10.1017/9781009325844.016.

Hjerdt, K.N., McDonnell, J.J., Seibert, J. and Rodhe, A., 2004. A new topographic index to quantify downslope controls on local drainage. *Water Resources Research*, *40*(5).

Hood, E., Gooseff, M.N. and Johnson, S.L., 2006. Changes in the character of stream water dissolved organic carbon during flushing in three small watersheds, Oregon. *Journal of Geophysical Research: Biogeosciences*, *111*(G1).

Hornberger, G.M., Bencala, K.E. and McKnight, D.M., 1994. Hydrological controls on dissolved organic carbon during snowmelt in the Snake River near Montezuma, Colorado. *Biogeochemistry*, *25*, pp.147-165.

Huber, C., Filella, M. and Town, R.M., 2002. Computer modelling of trace metal ion speciation: practical implementation of a linear continuous function for

complexation by natural organic matter. *Computers & Geosciences*, *28*(5), pp.587-596.

Inamdar, S.P. and Mitchell, M.J., 2006. Hydrologic and topographic controls on storm-event exports of dissolved organic carbon (DOC) and nitrate across catchment scales. *Water Resources Research*, *42*(3).

Inamdar, S.P., O'leary, N., Mitchell, M.J. and Riley, J.T., 2006. The impact of storm events on solute exports from a glaciated forested watershed in western New York, USA. *Hydrological Processes: An International Journal*, *20*(16), pp.3423-3439.

Jencso, K.G., McGlynn, B.L., Gooseff, M.N., Wondzell, S.M., Bencala, K.E. and Marshall, L.A., 2009. Hydrologic connectivity between landscapes and streams: Transferring reach-and plot-scale understanding to the catchment scale. *Water Resources Research*, *45*(4).

Jones, J.A.A., 2010. Soil piping and catchment response. *Hydrological processes*, *24*(12), pp.1548-1566.

Kalbitz, K., Solinger, S., Park, J.H., Michalzik, B. and Matzner, E., 2000. Controls on the dynamics of dissolved organic matter in soils: a review. *Soil Science*, *165*(4), pp.277-304.

Kalbitz, K. and Kaiser, K., 2008. Contribution of dissolved organic matter to carbon storage in forest mineral soils. *Journal of Plant Nutrition and Soil Science*, *171*(1), pp.52-60.

Krettek, A. and Rennert, T., 2021. Mobilisation of Al, Fe, and DOM from topsoil during simulated early Podzol development and subsequent DOM adsorption on model minerals. *Scientific Reports*, *11*(1), p.19741.

Koehler, M.A. and Linsley, R.K., 1951. Predicting the Runoff from Storm Rainfall, Research Paper n. 34. *Weather Bureau, US Dept of Commerce: Washington, DC, USA.*

Kruskal, W.H. and Wallis, W.A., 1952. Use of ranks in one-criterion variance analysis. *Journal of the American Statistical Association*, *47*(260), pp.583-621.

Kuraś, P.K., Weiler, M. and Alila, Y., 2008. The spatiotemporal variability of runoff generation and groundwater dynamics in a snow-dominated catchment. *Journal of Hydrology*, *352*(1-2), pp.50-66.

Lambert, T., Pierson-Wickmann, A.C., Gruau, G., Jaffrézic, A., Petitjean, P., Thibault, J.N. and Jeanneau, L., 2014. DOC sources and DOC transport pathways in a small

headwater catchment as revealed by carbon isotope fluctuation during storm events. *Biogeosciences*, *11*(11), pp.3043-3056.

Laudon, H., Berggren, M., Ågren, A., Buffam, I., Bishop, K., Grabs, T., Jansson, M. and Köhler, S., 2011. Patterns and dynamics of dissolved organic carbon (DOC) in boreal streams: the role of processes, connectivity, and scaling. *Ecosystems*, *14*, pp.880-893.

Lawrence, C., Harden, J. and Maher, K., 2014. Modeling the influence of organic acids on soil weathering. *Geochimica et Cosmochimica Acta*, *139*, pp.487-507.

Lindsay, J.B., 2014, April. The whitebox geospatial analysis tools project and open-access GIS. In *Proceedings of the GIS Research UK 22nd Annual Conference, The University of Glasgow* (pp. 16-18).

Lundström, U.S., van Breemen, N. and Bain, D., 2000. The podzolization process. A review. *Geoderma*, *94*(2-4), pp.91-107.

MacQueen, J., 1967, June. Classification and analysis of multivariate observations. In *5th Berkeley Symp. Math. Statist. Probability* (pp. 281-297). Los Angeles LA USA: University of California.

Martinez, P., Buurman, P., Lopes-Mazzetto, J.M., Giannini, P.C.F., Schellekens, J. and Vidal-Torrado, P., 2018. Geomorphological control on podzolisation–an example from a tropical barrier island. *Geomorphology*, *309*, pp.86-97.

McDonnell, J.J., Owens, I.F. and Stewart, M.K., 1991. A CASE STUDY OF SHALLOW FLOW PATHS IN A STEEP ZERO-ORDER BASIN 1. *JAWRA Journal of the American Water Resources Association*, *27*(4), pp.679-685.

McDowell, W.H. and Likens, G.E., 1988. Origin, composition, and flux of dissolved organic carbon in the Hubbard Brook Valley. *Ecological Monographs*, *58*(3), pp.177-195.

McGlynn, B.L. and McDonnell, J.J., 2003. Quantifying the relative contributions of riparian and hillslope zones to catchment runoff. *Water Resources Research*, *39*(11).

Musielok, Ł., Drewnik, M., Szymański, W., Stolarczyk, M., Gus-Stolarczyk, M. and Skiba, M., 2021. Conditions favoring local podzolization in soils developed from flysch regolith–A case study from the Bieszczady Mountains in southeastern Poland. *Geoderma*, *381*, p.114667.

Neff, J.C. and Asner, G.P., 2001. Dissolved organic carbon in terrestrial ecosystems: synthesis and a model. *Ecosystems*, *4*, pp.29-48.

Pacific, V.J., McGlynn, B.L., Riveros-Iregui, D.A., Welsch, D.L. and Epstein, H.E., 2011. Landscape structure, groundwater dynamics, and soil water content influence soil respiration across riparian–hillslope transitions in the Tenderfoot Creek Experimental Forest, Montana. *Hydrological Processes*, *25*(5), pp.811-827.

Palmer, S.M., Driscoll, C.T. and Johnson, C.E., 2004. Long-term trends in soil solution and stream water chemistry at the Hubbard Brook Experimental Forest: relationship with landscape position. *Biogeochemistry*, *68*(1), pp.51-70.

Palmer, S.M., Wellington, B.I., Johnson, C.E. and Driscoll, C.T., 2005. Landscape influences on aluminium and dissolved organic carbon in streams draining the Hubbard Brook valley, New Hampshire, USA. *Hydrological Processes: An International Journal*, *19*(9), pp.1751-1769.

Qualls, R.G., Haines, B.L. and Swank, W.T., 1991. Fluxes of dissolved organic nutrients and humic substances in a deciduous forest. *Ecology*, *72*(1), pp.254-266.

Radke, A.G., Godsey, S.E., Lohse, K.A., McCorkle, E.P., Perdrial, J., Seyfried, M.S. and Holbrook, W.S., 2019. Spatiotemporal heterogeneity of water flowpaths controls dissolved organic carbon sourcing in a snow-dominated, headwater catchment. Frontiers in Ecology and Evolution, 7, p.46.

Raulund-Rasmussen, K., Borggaard, O.K., Hansen, H.C.B. and Olsson, M., 1998. Effect of natural organic soil solutes on weathering rates of soil minerals. *European Journal of Soil Science*, *49*(3), pp.397-406.

Rinderer, M., Van Meerveld, H.J. and Seibert, J., 2014. Topographic controls on shallow groundwater levels in a steep, prealpine catchment: When are the TWI assumptions valid?. *Water Resources Research*, *50*(7), pp.6067-6080.

Sauer, D., Sponagel, H., Sommer, M., Giani, L., Jahn, R. and Stahr, K., 2007. Podzol: Soil of the year 2007. A review on its genesis, occurrence, and functions. *Journal of Plant Nutrition and Soil Science*, *170*(5), pp.581-597.

Schaetzl, R.J., Luehmann, M.D. and Rothstein, D., 2015. Pulses of podzolization: The relative importance of spring snowmelt, summer storms, and fall rains on Spodosol development. *Soil Science Society of America Journal*, *79*(1), pp.117-131.

Seibert, J. and McGlynn, B.L., 2007. A new triangular multiple flow direction algorithm for computing upslope areas from gridded digital elevation models. *Water resources research*, *43*(4).

Singh, N.K., Emanuel, R.E., Nippgen, F., McGlynn, B.L. and Miniat, C.F., 2018. The relative influence of storm and landscape characteristics on shallow groundwater

responses in forested headwater catchments. *Water Resources Research*, *54*(12), pp.9883-9900.

Sommer, M., Halm, D., Weller, U., Zarei, M. and Stahr, K., 2000. Lateral podzolization in a granite landscape. *Soil Science Society of America Journal*, *64*(4), pp.1434-1442

Sommer, M., Halm, D., Geisinger, C., Andruschkewitsch, I., Zarei, M. and Stahr, K., 2001. Lateral podzolization in a sandstone catchment. *Geoderma*, *103*(3-4), pp.231-247.

Sommer, M., Halm, D., Geisinger, C., Andruschkewitsch, I., Zarei, M. and Stahr, K., 2001. Lateral podzolization in a sandstone catchment. *Geoderma*, *103*(3-4), pp.231-247.

Stutter, M.I., Dunn, S.M. and Lumsdon, D.G., 2012. Dissolved organic carbon dynamics in a UK podzolic moorland catchment: linking storm hydrochemistry, flow path analysis and sorption experiments. *Biogeosciences*, *9*(6), pp.2159-2175.

Tang, W. and Carey, S.K., 2017. Hyd R un: a MATLAB toolbox for rainfall–runoff analysis. *Hydrological Processes*, *31*(15), pp.2670-2682.

Therneau, T.M. and Atkinson, E.J., 2018. An introduction to recursive partitioning using the RPART routines. 2019. *URL: https://cran. r-project. org/web/packages/rpart/vignettes/longintro. Pdf.*

Tromp-van Meerveld, H.J. and McDonnell, J.J., 2006. Threshold relations in subsurface stormflow: 2. The fill and spill hypothesis. *Water Resources Research*, *42*(2).

USDA Forest Service, Northern Research Station. 2022. Hubbard Brook Experimental Forest: Daily Precipitation Rain Gage Measurements, 1956 - present ver 18. Environmental Data Initiative. https://doi.org/10.6073/pasta/aed7e68772106753f3c7deef4f75e09c (Accessed 2022-11-08).

van Hees, P.A.W. and Lundström, U.S., 2000. Equilibrium models of aluminum and iron complexation with different organic acids in soil solution. *Geoderma*, *94*(2-4), pp.201-221.

Zimmer, M.A. and McGlynn, B.L., 2018. Lateral, vertical, and longitudinal source area connectivity drive runoff and carbon export across watershed scales. *Water Resources Research*, *54*(3), pp.1576-1598.

Appendix B

Table B1. Precipitation information for each storm calculated for when a groundwater sample was taken.

Sampled Date	Precipitation Start Date	Precipitation End Date	Total Precipitation (mm)	Event Duration (hr)	Max Hourly Intensity (mm)	Whole storm Intensity (mm/hr)
8/16/11	8/13/11 17:00	8/17/11 1:00	95.4	80	9.9	1.2
8/29/11	8/27/11 7:00	8/29/11 13:00	151.5	54	18.8	2.8
11/3/11	11/1/11 12:00	11/6/11 17:00	2.1	125	0.3	0.0
11/4/11	11/1/11 12:00	11/6/11 17:00	2.1	125	0.3	0.0
11/7/11	11/1/11 12:00	11/6/11 17:00	2.1	125	0.3	0.0
2/1/12	1/30/12 16:00	2/2/12 15:00	7.5	71	0.9	0.1
2/2/12	1/30/12 16:00	2/2/12 15:00	7.5	71	0.9	0.1
2/8/12	2/6/12 0:00	2/8/12 0:00	0.0	72	0.0	0.0
3/22/12	3/20/12 0:00	3/22/12 0:00	0.0	72	0.0	0.0
4/24/12	4/21/12 6:00	4/24/12 19:00	73.5	85	8.6	0.9
7/31/12	7/28/12 4:00	7/30/12 3:00	22.2	47	6.9	0.5
8/10/12	8/9/12 8:00	8/13/12 4:00	146.3	92	38.9	1.6
10/9/12	10/7/12 9:00	10/8/12 13:00	6.6	28	2.2	0.2
10/22/12	10/18/12 21:00	10/20/12 16:00	39.8	43	6.4	0.9
10/29/12	10/29/12 5:00	10/31/12 22:00	68.8	65	21.6	1.1
10/30/12	10/29/12 5:00	10/31/12 22:00	68.8	65	21.6	1.1
11/6/12	11/4/12 0:00	11/6/12 0:00	0.3	72	0.3	0.0
11/21/12	11/19/12 0:00	11/21/12 0:00	0.0	72	0.0	0.0
12/3/12	11/30/12 19:00	12/3/12 11:00	24.1	64	4.9	0.4
12/18/12	12/16/12 1:00	12/20/12 0:00	48.0	95	2.1	0.5
1/2/13	12/29/12 0:00	12/30/12 22:00	12.4	46	1.6	0.3
1/14/13	1/13/13 16:00	1/14/13 17:00	1.4	25	1.1	0.1
1/28/13	1/28/13 0:00	2/1/13 0:00	59.6	96	11.4	0.6
1/31/13	1/28/13 0:00	2/1/13 0:00	59.6	96	11.4	0.6
2/13/13	2/10/13 22:00	2/12/13 12:00	9.3	38	1.8	0.2
2/26/13	2/23/13 1:00	2/25/13 10:00	26.8	57	3.2	0.5
3/11/13	3/11/13 17:00	3/13/13 10:00	52.9	41	6.1	1.3
3/12/13	3/11/13 17:00	3/13/13 10:00	52.9	41	6.1	1.3
3/13/13	3/11/13 17:00	3/13/13 10:00	52.9	41	6.1	1.3
3/27/13	3/25/13 0:00	3/27/13 0:00	0.9	72	0.3	0.0
4/1/13	3/31/13 10:00	4/2/13 4:00	20.3	42	4.5	0.5
4/11/13	4/8/13 12:00	4/11/13 10:00	23.3	70	4.1	0.3
6/27/13	6/22/13 5:00	6/30/13 5:00	77.0	192	14.3	0.4
6/28/13	6/22/13 5:00	6/30/13 5:00	77.0	192	14.3	0.4
6/6/19	6/3/19 13:00	6/6/19 18:00	41.1	77	4.4	0.5
6/11/19	6/10/19 11:00	6/11/19 22:00	39.8	35	8.6	1.1
6/18/19	6/15/19 12:00	6/17/19 6:00	4.4	42	0.8	0.1

6/25/19	6/24/19 23:00	6/27/19 10:00	27.3	59	7.9	0.5
7/2/19	6/28/19 12:00	7/1/19 5:00	17.1	65	3.8	0.3
7/8/19	7/6/19 2:00	7/7/19 4:00	10.7	26	6.6	0.4
7/12/19	7/11/19 3:00	7/12/19 14:00	69.6	35	14.8	2.0
7/16/19	7/16/19 3:00	7/18/19 8:00	4.3	53	1.2	0.1
7/23/19	7/21/19 6:00	7/23/19 20:00	15.8	62	1.6	0.3
1/28/20	1/25/20 8:00	1/28/20 23:00	12.3	87	3.1	0.1
10/14/20	10/12/20 19:00	10/14/20 6:00	56.8	35	14.5	1.6
10/17/20	10/15/20 19:00	10/17/20 19:00	35.9	48	4.6	0.7

Chapter 3

Spatiotemporal Patterns of Organic Horizon Saturation During Storm Events

Abstract

Dissolved organic carbon (DOC) is transported to streams with subsurface flow as draining water intercepts soils with accumulated organic matter. It is well known that within the soil profile, organic horizons contain the largest amounts of stored DOC. However, determining where and how often groundwater intercepts organic horizons across landscape that are well drained is not well quantified. At Hubbard Brook Experimental Forest (HBEF), shallow groundwater behavior is extremely variable, due to differences in upslope drainage area and soil depth. In this landscape, soil depth generally decreases closer to bedrock outcrops, which exists in higher elevations. This study measured shallow groundwater responses and organic horizon saturation dynamics in 56 wells across 136 storm events during snow-free months within a small headwater catchment at HBEF. Wells were grouped by bedrock-weighted upslope accumulated area (UAAb) values, which is a topographic metric derived from UAA that represents the proportion of bedrock outcrops in a particular drainage area. Bedrock outcrops in this region are often surrounded by thin organic soils and typically exist higher in the landscape. Water levels in locations with the highest UAAb values most frequently reached organic horizons during storm events, especially during the spring and fall months. In addition, groundwater from these wells on average had the highest DOC concentrations. The spatial patterns in the frequency and duration of organic horizon saturation were important for recognizing landscape components that act as source areas of organic acidity, which in this study was furthest from the stream network. Additionally, temporal dynamics of organic horizon saturation identify crucial moments of DOC mobilization, which happened during seasons of high catchment wetness. This research highlights the need for incorporating intra-watershed hydrologic variability as a driver in ecosystem C-fluxes.

Introduction

During periods of increased catchment wetness (e.g., snowmelt, storm events), groundwater movement through the shallow soil zone plays a critical role in regulating stormflow generation (Anderson and Burt, 1990; Sidle et al., 2000; Shanley et al., 2015), nutrient export and stream chemistry (Hornberger et al., 1994; Inamdar et al., 2009; Godsey et al., 2009; McGlynn and McDonnell, 2003; Welsch et al., 2001;), and soil biogeochemical processes (Lin, 2003; Ma et al., 2017; McClain et al, 2003). Catchment structure (i.e., the arrangement of topography, geology, soil properties, and vegetation cover) can affect water storage and movement through soil profiles and along flow paths across landscapes, both spatially and temporally. Therefore, predicting relationships among precipitation events, shallow groundwater behavior, and associated ecosystem fluxes can be complex.

In steep mountainous catchments, where water movement strongly follows the predominant slope gradient, it is largely understood there are strong relationships between topography and the spatial variability of groundwater levels (Anderson and Burt, 1978), even though the strength of these relationships is timescale dependent. For example, several studies have found that portions of the landscape with higher upslope accumulated areas (UAA) (bigger contributing drainage area), such as riparian soils, tend to have the largest groundwater response magnitude and water level persistence in soil profiles, thereby often acting as primary source areas to streams (Detty and McGuire, 2010; Jencso et al., 2009). However, in upland areas where soils are generally thin on top of bedrock, or a less permeable soil layer exists, vertical water movement is restricted and water levels have been shown to reach closest to the soil surface, especially during the beginning portions of a storm hydrograph (Benton et al., 2022; Gannon et al., 2014). By only accounting for the tendency for subsurface water accumulation, the dynamics of soil saturation within the soil profile farther from streams can be overlooked. In shallow soil regions of the catchment, such as where bedrock is close to the surface, subsurface stormflow parallel to the soil surface has substantial influence on groundwater dynamics. Therefore, spatiotemporally extensive studies to examine controls on groundwater

responses during storm events within the soil profile are still needed for understanding hydrologically-dependent biogeochemical processes across catchments.

Generally, there are strong and positive correlations between the formation and rise of water tables within the shallow soil zone with increasing rainfall inputs and intensities (Tromp-van Meerveld and McDonnell, 2006; Rinderer et al., 2016, Penna et al., 2015; Singh et al., 2018). The magnitude of groundwater response is often seasonally dependent, due to differences in antecedent catchment wetness and uptake demands by vegetation (Swank and Douglass, 1974; Doble and Cosbie, 2016, Shanley et al., 2016).

Under conditions where water tables reach higher in the soil profile, flow paths intercept surface organic soil horizons rich in organic acidity that are extremely porous. The rapid mobilization of dissolved organic carbon (DOC) from the forest floor during these wetting and subsequent leaching events is considered one of the most significant inputs of C to mineral soils (Guggenberger et al., 1994; Froberg et al., 2006; Kalbitz and Kaiser, 2008; McDowell and Likens, 1998; Neff and Asner, 2001; Qualls and Haines, 1991;). Increases in soil solution acidity are known to enhance chemical dissolution rates (Drever and Stillings, 1997; Drever and Vance, 1994; Raulund-Rasmussen et al., 1998; Lawrence et al., 2014) and the formation of soluble metal-organic complexes (Huber et al., 2002; Lundström et al., 2000). While the presence of the water table near the soil surface is a critical driver of DOC transport and associated biogeochemical processes, the frequency and duration of surface soil saturation events is currently underrecognized in the context of ecosystem-scale C fluxes.

In addition to the implications of organic soil horizon saturation for DOC transport, the formation, transport, and accumulation of organically-complexed forms of iron and aluminum (i.e., spodic materials) in the shallow soil zone are dominant processes of podzolization, which often occurs in coarse-textured acidic soils in cool and humid climates. In the northeastern US forest ecosystem at Hubbard Brook Experimental Forest (HBEF; New Hampshire, USA), it is thought that the magnitude and direction of the dominant hydrologic flux has led to the formation of distinct podzol types (regionally known as hydropedological units) which vary in podzolization expression by the presence and dominance of eluviated and illuviated soil horizons within profiles (Bailey et al., 2014; Gannon et al., 2014). Whole-solum saturation dynamics have been described

by others at Hubbard Brook (e.g., Detty and McGuire, 2010), and have shown that temporal patterns in water table occurrence, depth, and persistence vary by landscape positions. Differences in water table exceedance probabilities, which describe the likelihood of the shallow groundwater to exceed certain depths, display distinct variations by soil horizon (Bailey et al., 2014) and whole-profile morphology (Gannon et al., 2014). Despite these known relationships between hydrologic behavior, solution chemistry, and soil development along hillslopes, determining where and when groundwater explicitly intercepts the organic horizon and the implications for surface saturation for DOC mobilization are not well quantified. Furthermore, the prediction of soil morphology and processes linked to hydrologic variation are often limited to using metrics of surface topography (e.g., UAA, slope, elevation) without the integration of subsurface variation in soil properties that also influence groundwater table dynamics.

The objective of this study was to evaluate spatiotemporal controls on organic horizon saturation, in a small headwater catchment at HBEF. This research uses bedrock-weighted upslope accumulated area (UAAb) as a representative topographic metric to account for known differences in drainage area size and soil depth characteristics across the catchment. In general, areas on the landscape with higher proportions of bedrock outcrops in drainage areas (high UAAb values) tend to exist at higher elevations, are shallower to bedrock, and have limited water storage capacity. Conversely, lower UAAb values are found in parts of the landscape closer to streams where soils are thickest. By examining groundwater dynamics during discrete storm events across a four-year period, the following research questions were addressed:

1. How do groundwater responses vary throughout the catchment during storm events?
2. Are there observable spatial and temporal patterns of organic horizon saturation dynamics (i.e., frequency, duration)?
3. What are the implications of organic horizon saturation for DOC mobility across the catchment?

Methods & Materials

Site Description and Soil Description

This study takes place at Hubbard Brook Experimental Forest (HBEF), located in the White Mountains of New Hampshire, USA (Fig. 1). The climate of this region is considered cool-temperate with annual precipitation of 1,400 mm on average, with a large portion falling as snow during the winter. The research site is throughout Watershed 3, which has been historically instrumented and used as a hydrologic reference watershed for long-term ecological research (Fig. 1). Watershed 3 is a relatively small, forested headwater catchment which drains approximately 42.4 ha. Because of its size, precipitation does not differ greatly across the catchment. The watershed is south-facing and the elevation ranges from 572 to 732 m. The landscape is forested by northern hardwood species, including balsam fir (*Abies balsamea*), mountain white birch (*Betula papyrifera* var. *cordifolia*), and red spruce (*Picea rubens*) towards ridgetops at higher elevations, and transitions to predominately sugar maple (*Acer saccharum*), yellow birch (*Betula alleghaniensis*), and American beech (*Fagus grandifolia*) at lower elevations.

The dominant geology of Watershed 3 is the Rangeley schist formation, overlain by soils that have formed from glacial till of variable depths deposited ~14 kya. Solum thickness and depth to bedrock generally increases downslope towards streams. Soils within Watershed 3 have been described largely as Spodosols and are generally well-drained, coarse-textured with thick organic horizons at the surface. Soils within this watershed have been further classified into distinct podzol types, regionally known as hydropedological units, to describe the range in podzol development that covaries with shallow water table behavior (Bailey et al., 2014; Gannon et al., 2014; Gillin et al., 2014).

In 2019, a field campaign hand excavated and described 36 soil pits within three sub-catchments with Watershed 3 (Fig. 1) (Bower et al., 2023). Soils were morphologically described by genetic horizon, including depths of organic horizons (Oi, Oe, Oa). Organic horizons were classified by texture and color. The lower depth of the most bottom organic horizon (Oa) was found to vary between 8 to 30 cm, with a median depth of 14 cm.

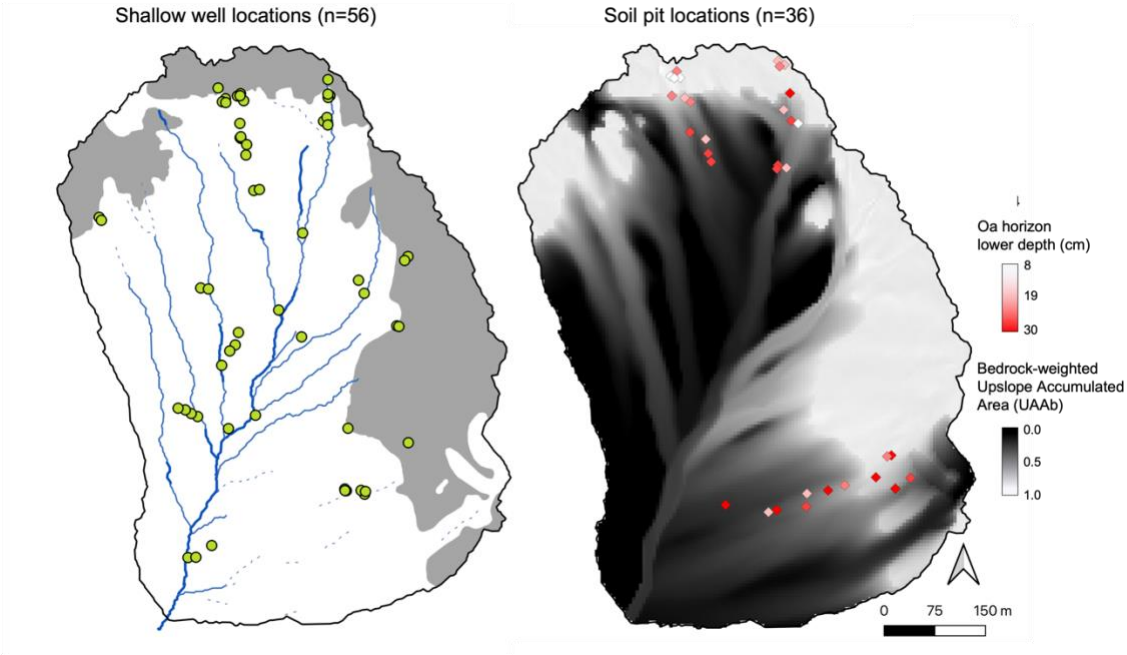

Figure 1. Map of Watershed 3 at Hubbard Brook Experimental Forest, in the White Mountains of New Hampshire. Left: Green dots represent the shallow groundwater wells with logged data used in this study (n=56), blue lines represent the stream network (darkest blue is perennial streams), grey portions of the map are areas of the landscape dominated by bedrock outcrops and shallow organic soils on top of bedrock. Right: Map of bedrock-weighted upslope accumulated area (UAAb) and locations of excavated soil pits colored by the bottom depth of the Oa horizon.

Well monitoring network

Instrumented wells throughout Watershed 3 include those installed by Detty and McGuire (2010), Gannon et al. (2014), and Benton et al. (2022), among others. This study specifically focuses on shallow groundwater levels, therefore well selection was refined to those that were within <150 cm of the soil surface and were not installed deeper than the upper 10 cm of the C horizon. The C horizon at this site is often recognized as a confining layer that percolating water often perches on (Detty and McGuire, 2010; Benton et al., 2022). Wells located within a known stagnant seep were also excluded from this analysis (Bourgault et al., 2022). Water levels analyzed for this

study came from a total of 56 wells distributed throughout the catchment (Fig. 1), recorded at 10-minute intervals, although not all wells were actively recording simultaneously. Water levels analyzed for this study spanned four continuous years from 2011-2012 and 2019-2020 during the snow-free months (May-November).

Hydroclimatic Data

A precipitation dataset was created from data recorded at 15-minute intervals from three different rain gauges (RG1, RG4, and RG23), all located within < 3.5 km from the Watershed 3 outlet with data spanning from 2011-2020 (USDA Forest Service, Northern Research Station, 2022). The use of multiple rain gauges was to cover the largest possible time extent with 15-minute precipitation data recorded at HBEF, which started in July of 2011. All other available rainfall data was recorded at 1-day sum intervals. Discrete storms were classified by total rainfall >6.35 mm (0.25 inches) with a maximum time gap of no rainfall of 12 hours. The identification of each storm based on these parameters was determined by using the 'HydRun' toolbox (Tang and Carey, 2017) adapted for R. Total storm precipitation was calculated as the total rainfall from the beginning to the end of the storm event.

For every identified storm event, water levels from any active logging well were extracted from the start of the storm event to 24 hours past the end of the storm event (Fig. 2). The use of 24 hours post-storm, rather than the end of the storm event, was used to account for potential lag times in groundwater responses. If water levels did not rise above 2-cm of the maximum logging depth, the logged levels were considered a "non-response" to a storm event. Groundwater response metrics were only calculated for those that were considered to have a storm response. Peak water levels were determined as the shallowest depth the water level reached during the event. Smaller peak values correspond with more shallow depths, closer to the soil surface. The amount of time the water table sat above 14 cm and 30 cm during a storm event was calculated to represent organic horizon saturation duration (in hours) for the median and maximum catchment O horizon depth, respectively.

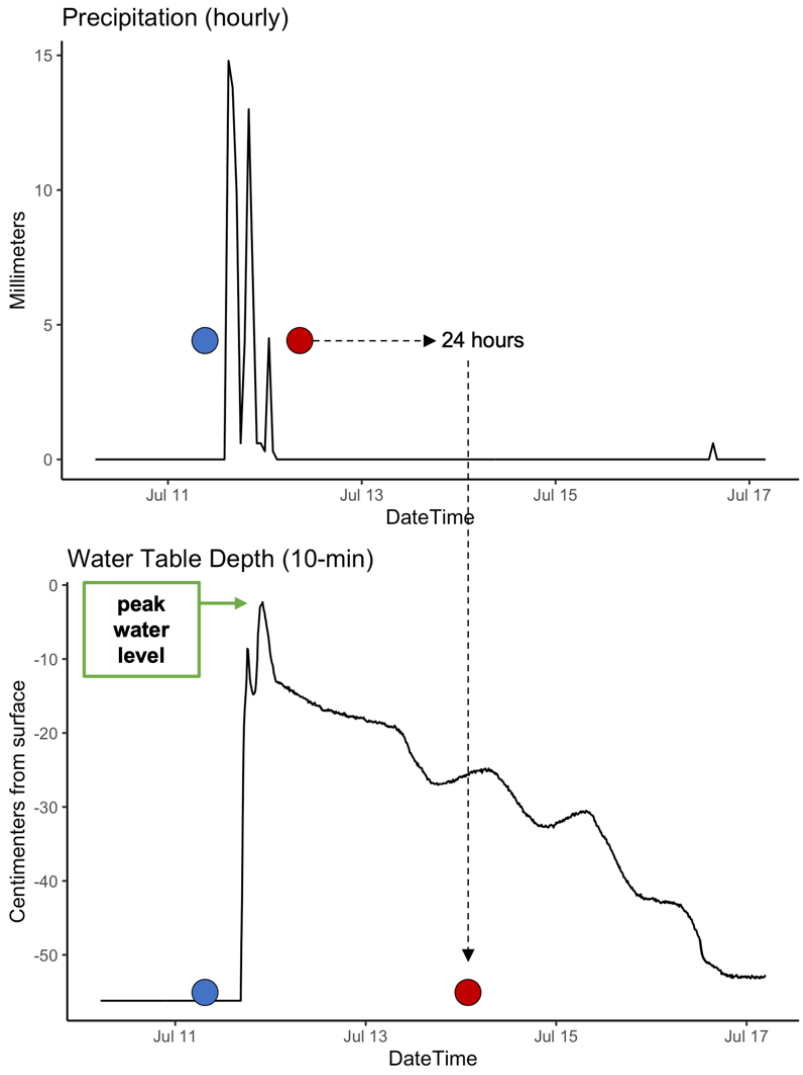

Figure 1. Top: Delineation of storm event time periods for which total precipitation was calculated across, which is calculated from the start of the storm (blue dot) to the end of the storm (red dot). Bottom: Water table response metrics were calculated from the start of the storm event (blue dot) to 24-hours post end of the storm (red dot).

Shallow groundwater DOC concentrations

Groundwater chemistry used for this study were collected over multiple sampling campaigns ranging from July 2009 to October 2020 (Bailey et al., 2023). For this analysis, DOC chemistry is only provided for groundwater taken from wells used in this study, during snow-free months (n=261). During sample collection, wells were fully purged of water and samples were collected using a peristaltic pump in a 0.5 L bottle,

after water levels were recharged. For the analysis of DOC, samples were filtered through an ashed 0.45 µm glass microfiber filter and frozen until analysis. Sample analysis was performed by the United State Department of Agriculture Forest Service, Forestry Sciences Laboratory in Durham, NH. Concentrations of DOC were measured on a Shimadzu TOC-5000A (Shimadzu Corp., Kyoto, Japan).

Terrain and Statistical Analyses

Bedrock-weighted upslope accumulated area (UAAb) was calculated with a multiple flow direction algorithm (Seibert and McGlynn, 2007). This metric is expressed as the normalized ratio between UAA and UAA weighted by bedrock outcrop cells, where bedrock outcrops were assigned large weighting values (Gillin et al., 2015). UAAb values vary between 0-1, where a value of 1 indicates an entire upslope area is comprised of bedrock and shallow soils. Values of UAAb were extracted at the well location. Shallow wells were categorized into groups based on UAAb value at the well location. Based on the distribution of UAAb values for the wells, groups were split into four equal quantiles (Q1-Q4).

Seasonal differences in groundwater responses were analyzed between spring (May-June), summer (July-Aug), and fall (Sept-Nov). Statistical differences between groundwater groups and groundwater response metrics were tested using a Kruskall Wallace test. To determine which groups were significantly different from each other a Pairwise Wilcox Test was performed. Significance levels for all analyses was determined at $p < 0.05$ and $p < 0.001$. All statistical analyses and figure creation were performed in R software Version 4.2.2 (R Core Team, 2021).

Results

Storm events and topographic metrics

During time periods of recorded water levels for all snow-free months, a total of 136 storms were classified. The amount of precipitation that fell for these events varied widely between 6.6 to 151.5 mm (~0.25-6 inches) (Table 1). The largest of the characterized events occurred directly after Hurricane Irene in August of 2011. Most of the rainfall events (75^{th} percentile) were below 35 mm (1.3 inches). The distributions of

total storm rainfall were heavily skewed right, with a higher proportion of storms with smaller values across the range of characterized storms. No significant differences in total precipitation between seasons was observed.

Upslope accumulated area weighted by bedrock (UAAb) at each well location varied between 0-0.63. In general, UAAb was positively related with elevation (r_s= 0.59, $p < 0.001$) and the highest values of UAAb were for well locations nearest ridges among bedrock outcrops and associated shallow soils (Fig. 4). In contrast, the lowest values of UAAb were located nearest to the perennial stream network. Correspondingly, UAAb at a location was negatively related to mean values of upslope topographic wetness (TWI) (r_s= -0.41, $p < 0.001$). Wells were grouped within quantiles of UAAb, and ranges of UAAb values for each category can be found in Figure 3.

Table 1. Total number and summary statistics for characterized storms used in this study for each snow-free season. No statistical differences in storm metrics were found between seasons.

Season	Storms (n=)	minimum	maximum	median	sd
Spring (May-Jun)	46	6.8	81.0	18.1	17.8
Summer (Jul-Aug)	41	6.7	151.5	16.1	32.4
Fall (Sept- Nov)	49	6.6	89.2	16.9	19.5

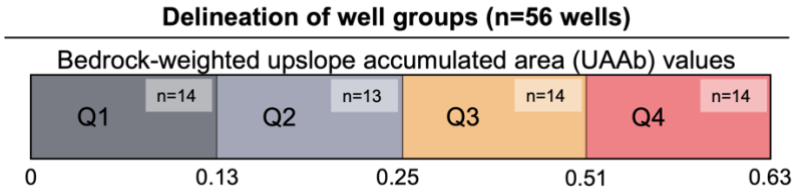

Figure 3. Quartile ranges for bedrock-weighted upslope accumulated area (UAAb) for well locations in this study. Wells were categorized into four equal groups based on the quartile ranges of UAAb (Q1-Q4), which varied between 0 and 0.63.

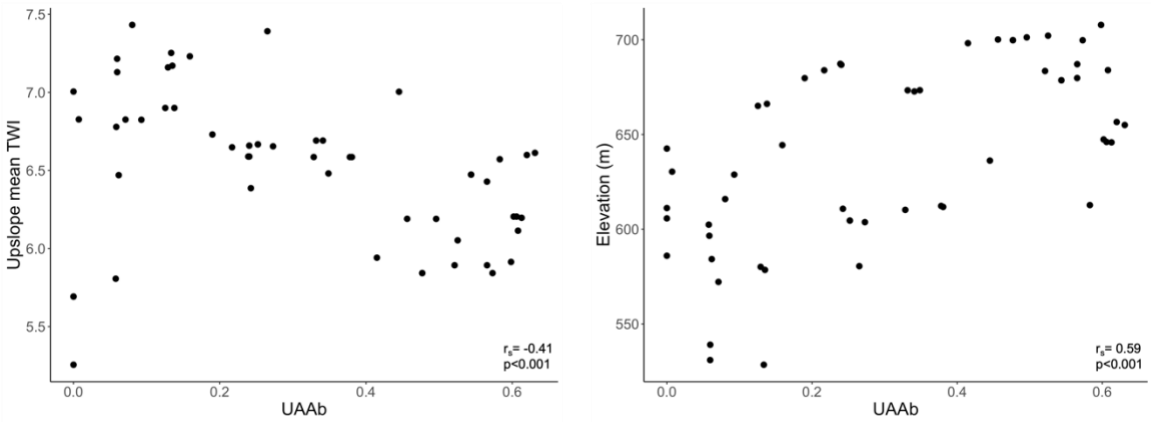

Figure 4. Relationship between bedrock-weighted Upslope Accumulated Area (UAAb) and Topographic Wetness Index (TWI) and elevation at the location of each well.

Groundwater response magnitude

The total number of logged records where groundwater levels were actively collecting data during a characterized storm event was 3,496. Of these, wells were responsive 2,831 times (81%). Overall response rates by season for spring, summer, and fall were 91%, 64%, and 84%, respectively (Fig. 5a). The formation of transient shallow groundwater during a storm event was highest in Q1 and Q4 wells, especially during the spring, followed by the fall (> 87%) (Fig. 5b). Response rates for all well groups were lowest during the summer months, but especially in Q3 wells, where responses only occurred in this group for half of the characterized storm events (50%).

There were significant differences between peak water levels reached during an event between each UAAb well group ($p < 0.001$) (Fig. 6). The highest peak water levels were found in the Q4 well group, with a median value at 18 cm from the soil surface. Peak water levels in this group were most tightly clustered around the mean (sd = 14.5 cm). The lowest median value for any well group was for Q2 at 56.5 cm. However, one

well (named D1) in Q2 had the shallowest median peak water level response out of any well across all events, at 3.8 cm from the surface. Peak water levels generally increased (deeper in the profile) with decreasing UAAb values from 0.63 – 0.13 (Q4 to Q2), with a slight increase in wells in Q1 (median = 39.7 cm; UAAb values 0.0 – 0.13).

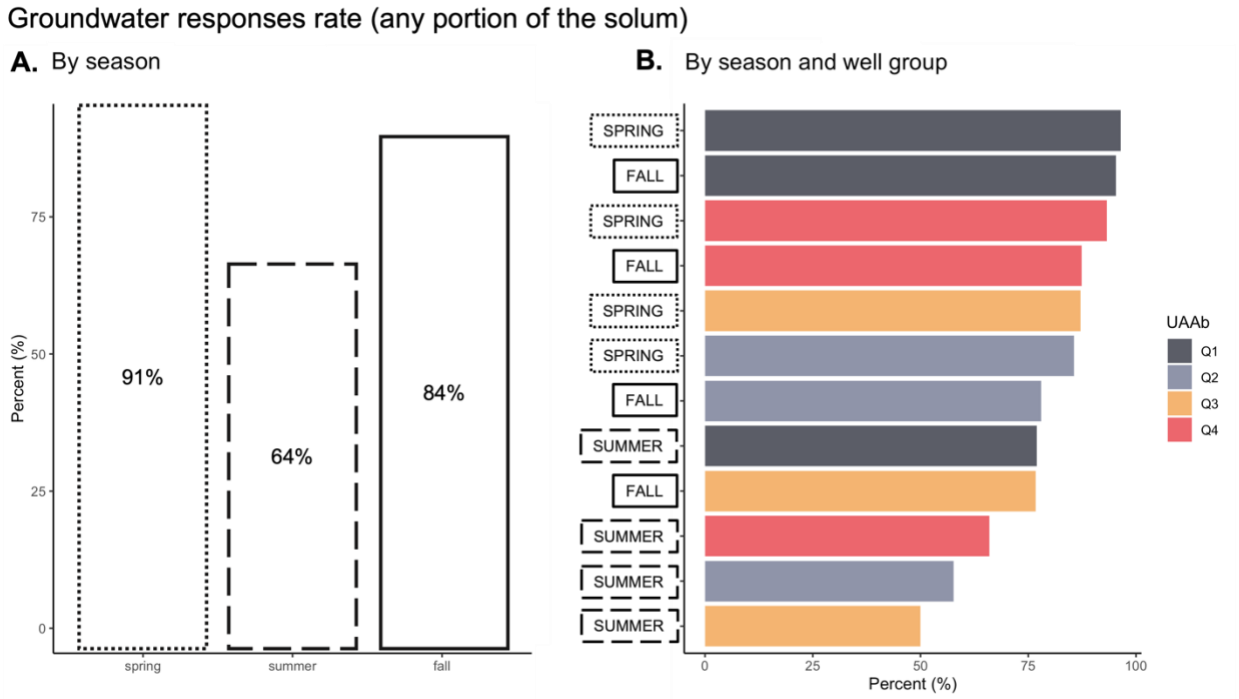

Figure 5. Groundwater response rates by A) season and B) season by well group (Q1-Q4). A groundwater response was determined by a rise in the water level at least 2 cm above the maximum recording depth. The number of responses were divided by total responses + non-responses to arrive a response rate percentage (%).

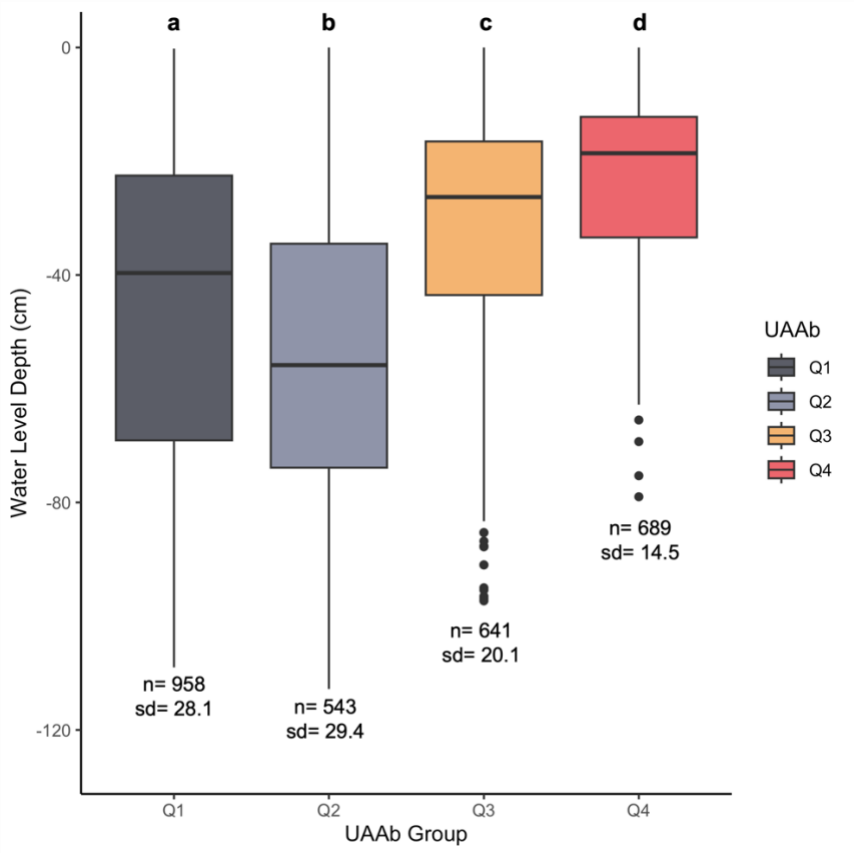

Figure 6. Boxplots of peak water level for all storm event groundwater responses between groundwater groups. Lower case letters above each box denote significant differences between well groups ($p < 0.001$). Boxplot lines display the range of minimums and maximum values, boxes represent the interquartile range, and dots show outliers.

Organic horizon saturation dynamics and DOC concentrations

The distribution in water levels for a given event reached shallower into the soil profile with increasing total storm precipitation (Fig. 7). Trend lines for each well group show that, in general, the amount of rain needed for water levels to reach into the organic horizons was smallest for soils in well group Q3 and Q4 wells, and largest for Q1 and Q2.

Peak water levels within group Q4 almost always crossed into the maximum observed depth of the Oa horizon (30 cm) (Fig. 7; Fig. 9). The number of times the water table reached the organic horizon in this group was highest for any logged event with a response reaching at or above mean and deepest Oa horizons depth 32% and 69%,

respectively (Table 2). This happened most often during the spring and fall months (Fig. 8). A total of 8 out of the 14 wells within Q4 sat for at least 2 hours above the median O horizon depth during an event (14 cm) (Fig. 9), for wells in group Q3 this was 5 out of 14 wells. Water levels in soils within the well group Q3 generally reached the deepest O horizon threshold in storms with greater than ~25 mm of precipitation, which is within the 75th percentile of the storm event distribution, but only reached the median Oa depth for storms greater than ~ 60 mm.

Water levels in group Q1 would often only cross into the organic horizons for storms greater than ~85 mm. This amount of rain was only observed to happen four times (during snow-free months) over the course of 4 years of the water level dataset, which was greater than 75th percentile of storm precipitation amounts of all characterized storms (n=136). While there were instances of water levels reaching the Oa horizon depths in Q1 wells during a storm event (11% for median Oa depth, 36% for deepest Oa depth), the general tendency lines show a large majority of the responses did not (Table 2, Fig. 7).

In contrast to the other well groups, water levels in well group Q3 reached the organic horizon the least number of times throughout this study (Fig. 7), especially during the summer (Fig. 8). One well in Q2 ("D1") sat for the longest period out of any well in the organic horizon depths 14 cm and 30 cm, at 28 and 44 hours respectively (Fig. 9). Often, water levels in this specific well would sit within the organic horizon depth range for the entirety of a storm event, regardless of storm magnitude. However, this well could be considered an outlier for this well group, since it was the only well with a median water level peak that reached into the organic horizons (Fig. 9), and Q2 group overall had the lowest median peak water level response (Fig. 6) and saturated the O horizon the least number of times for all events (Table 2).

Average groundwater DOC concentrations were highest in well group Q4 (Table 2; mean = 13.5 mg/L), particularly for those wells that often reached into the organic horizon (Fig. 9). In contrast, wells in group Q1 and Q2 that often reached organic horizon depths had much lower DOC concentrations, with an average of < 6.3 mg/L. No statistical differences between Q1 and Q2 were observed, even though six wells in Q1 frequently rose above 30cm, compared to just one in Q2.

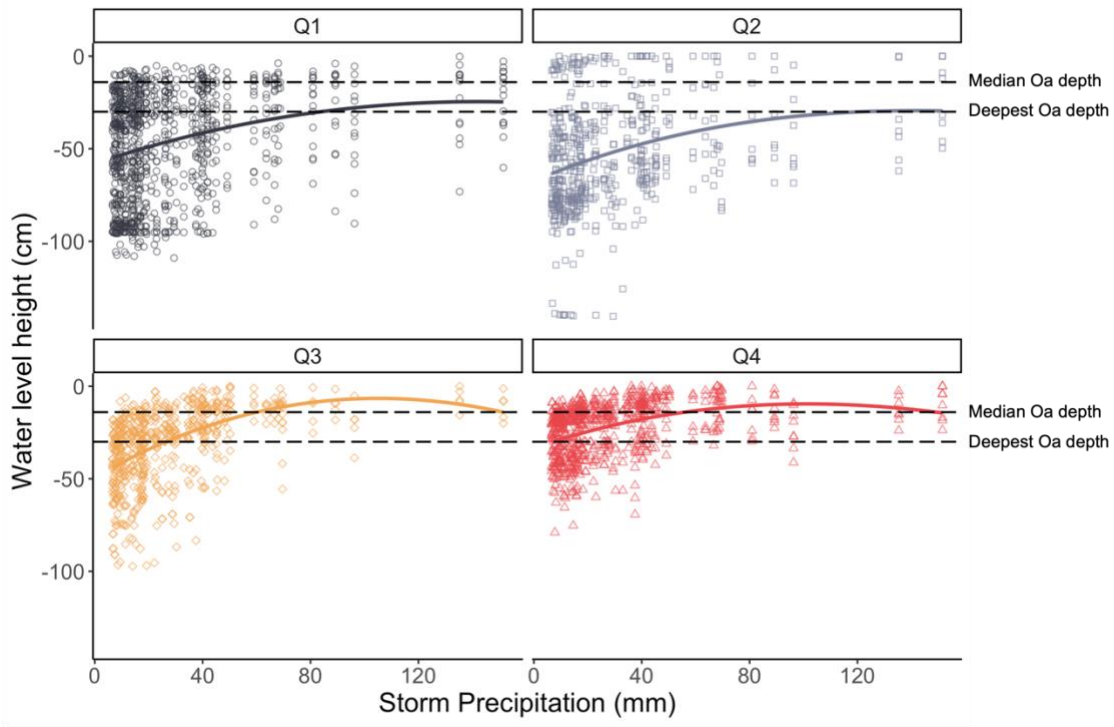

Figure 7. Peak groundwater responses for all storm events characterized in this study across increasing storm precipitation. Trend lines within each panel are LOESS (locally weighted smoothing) lines. Dotted black horizontal lines denote the median and lower depths of the organic horizon, which was calculated from the lower depths of Oa horizons in 36 soil pits described in the catchment (Fig. 1).

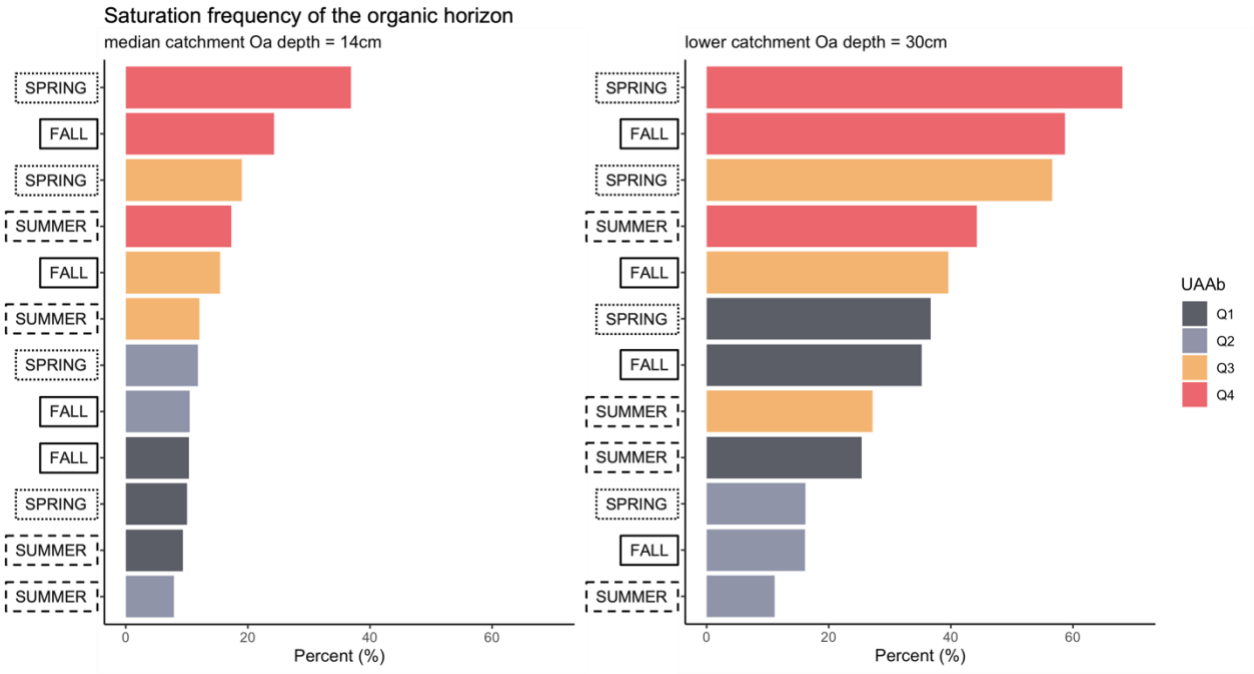

Figure 8. Saturation frequency of organic horizons for all UAAb well groups (Q1-Q4) for storm events across all snow-free seasons (May-Nov). Saturation frequency was calculated as the number times the peak depth of the water table crossed over the threshold of the median catchment Oa horizon (14 cm) and deepest catchment Oa horizon (30 cm), divided by the total number of groundwater responses.

Table 2. Overall organic horizon saturation frequency and mean DOC concentrations for each well group. Lower case letters next to DOC concentrations denote significant differences between well groups ($p < 0.05$).

UAAb	O-horizon Saturation Frequency		Mean DOC concentration, mg/L (n = 261)
	Median Oa depth 14 cm	Deepest Oa depth 30 cm	
Q1	11%	36%	2.8[a]
Q2	12%	20%	2.2[a]
Q3	22%	58%	9.5[b]
Q4	32%	69%	13.5[c]

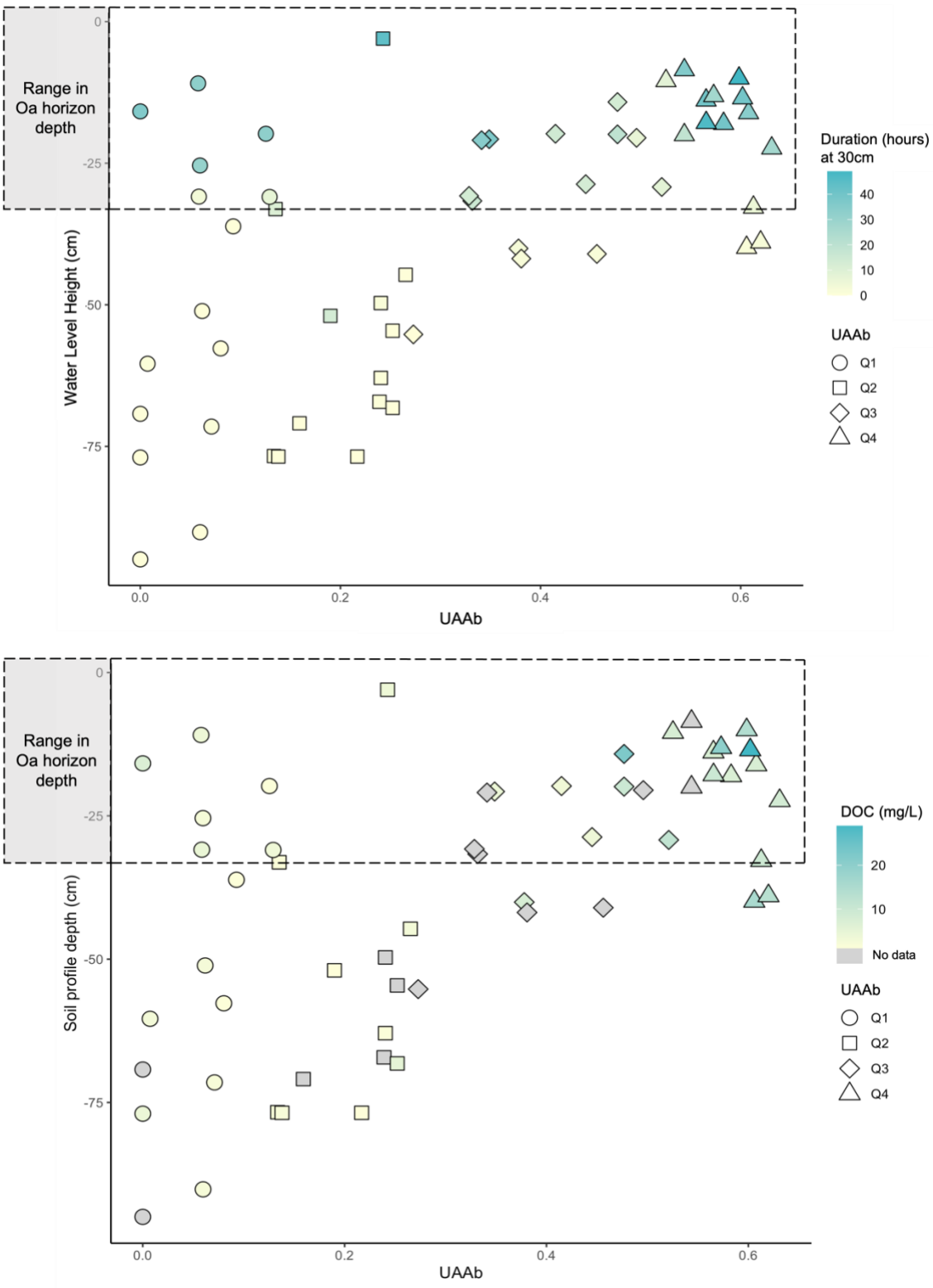

Figure 9. Median peak water level reached across all storm events for each well. Shapes indicate which well group (Q1-Q4) each well classified as. Top panel: shapes are colored by the average duration of time water levels sat at or above 30 cm (deepest Oa horizon

lower boundary). Bottom panel: shapes are colored by average DOC concentration (mg/L) for all groundwater samples taken between the months of May and November. Gray colors indicate that no groundwater chemistry data was available for that well.

Discussion

Organic horizon saturation defined by catchment structure

In this study, distinct groundwater responses to storm events were observed at different landscape positions, defined by bedrock-weighted upslope accumulated area (UAAb). The UAAb metric is representative of and correlates with many other terrain properties in this catchment such as elevation (r_s = 0.59), upslope topographic wetness (r_s = -0.41), and known hillslope gradients in tree cover type. Because of the geomorphology of this region, wells located nearest bedrock outcrops are typically close to ridges and soils are shallower to bedrock with small drainage areas (high UAAb values), although in other catchments these shallow soils can occur at lower elevations. Conversely, wells further from bedrock outcrops are generally near perennial streams and are deeper soils with larger drainage areas (low UAAb values). In general, wells nearest bedrock outcrops interacted with the organic horizon most frequently and for the largest proportion of time annually compared to all other groups. This was unsurprising, since the ratio of mineral soil thickness to organic soil thickness is small, and only a relatively small rise of the water table during an event is needed to reach breach the lower Oa horizon depths. It could be expected then that a decrease in UAAb might correspond with a linear decrease in water table height and/or duration; however, this was not always the case (Fig 6., Fig. 9). In fact, many of the response metrics displayed a slight U-shaped behavior across the UAAb well groups (Fig. 6, Fig. 9), where water levels in several locations furthest from bedrock outcrops (Q1) were also frequently high into the organic horizons during an event. Using the UAAb metric was critical for identifying this divergence in groundwater behavior.

There is a basic understanding at this site that the shallow transient water table forms episodically in soils near ridges mainly during storm events and snowmelt periods, and water is moved downslope with lateral subsurface flow as the water storage capacity

is exceeded (Gannon et al., 2017). For this study, all wells in groups Q4 and many in Q3 fall into this category. As soils deepen in backslope positions, the water table exists deeper in the solum only rises to shallow depths during periods when the catchment is exceptionally wet. Most wells in Q2 were identified as similar soil types as these, which on average interacted with the organic horizons less frequently and for the least amount of time. Further downslope, near streams, an increase in flow convergence and drainage area promotes a seasonal or perennial water table, which can often result in whole-solum saturation during storm event periods. Soils here are often more intricately connected to the stream network, which could largely explain why many soils in group Q1 (low UAAb) were most responsive to rainfall (Fig. 5b), and frequently interacted with organic horizons (Fig. 9).

While the slight U shape behavior in groundwater responses across UAAb values (high water tables in soils closest and furthest from streams) does a fair job at explaining topographic controls on organic horizon saturation dynamics, it falls short in explaining spatial patterns of shallow groundwater dissolved organic carbon (DOC) chemistry known at this site. In theory, frequent and longer soil-water interaction time in organic horizons would increase the retrieval of additional C-inputs to groundwater solutions across the catchment, so one might expect DOC concentrations to be high near ridges and close to streams. However, several other studies have found DOC concentrations in shallow groundwater was markedly higher in soils near ridges and decreases laterally downslope, with the lowest concentrations near streams (Zimmer et al., 2013; Gannon et al., 2015; Bailey et al., 2019). Results from this study found similar spatial trends in groundwater DOC concentrations, with the lowest DOC in the stream-adjacent UAAb groups (Table 2).

Deviations in the influence of organic horizon saturation on DOC concentrations are likely due to several reasons. First, known spatial variations in vegetation type and soil O horizon chemistry exist in this region. Higher elevations in Watershed 3 are dominated by coniferous tree species that transition to more deciduous-dominant lower on the landscape. Tree litter from conifers are known to have a higher C:N ratio and slower decomposition rates, attributed by higher lignin:N content (Preston et al., 2000; Krishna and Mohan, 2017). In addition, conifer litter generates more acidic organic

compounds (e.g., phenolic acids) as leachates and decomposition products, which generally increases overall DOC solubility (Blaschke, 1979). In an adjacent watershed at HBEF, water draining from Oa horizons in more coniferous-dominated portions of the landscape was shown to have significantly higher DOC concentrations than Oa horizons in lower portions of the landscape, a pattern that has been linked to elevational differences in litter input C chemistry and solubility (Dittman et al., 2007; LoRusso et al., 2021).

Secondly, this study used uniform Oa horizon depths (median 14 cm, bottom 30 cm) to assess organic horizon saturation across the entire catchment. Bailey et al. (2014) found that Oa depth was thickest in soils near bedrock zones (mean = 20.8 cm) and decreased in soil types commonly found closer to streams (mean = 3.9 cm). Using unique O horizon depths for each well location would likely shift O-horizon saturation frequency estimates, such as increased frequency in wells with higher UAAb values and decreasing frequency in lower UAAb values. Nonetheless, several wells with smaller UAAb values, lower on the landscape, consistently saturated near to the soil surface (<10 cm) during storm events (e.g., D1, I7, I8, K1). For these wells, DOC concentrations were still generally low, compared to upslope wells (Fig. 9). While soils in lower landscape positions likely do experience episodic saturation into the organic horizon, water tables persist longest in the portion of the soil profile that are Bh horizons, where the predominant pool of soil carbon is complexed as stable amorphous organometallic compounds (Bourgault et al., 2015), which is less mobile than DOC.

Lastly, the divergence of shallow horizon saturation dynamics and soil solution DOC concentrations across landscape positions suggests there are additional sources of DOC to mineral soils, other than just accessing stored O horizon DOC in soils at each location. Higher areas of the watershed, near ridges, are dominated by outcrops interlaced with shallow soils that are predominantly organic horizons laying directly on top of bedrock (Fraser et al., 2020). Water draining from bedrock-associated organic soils are the highest for all soils in the catchment (Bailey et al., 2019). During storm events, the transient water table in mineral soils nearest bedrock outcrop zones in the catchment (i.e., group Q4) raises highest into the shallow soil profile, likely becoming hydrologically connected to draining upslope organic soils as they drain. Organic soil enhances the rapid

transmission of water due to their porous nature (high saturated hydraulic conductivity), which could enhance preferential flow over mineral soil. Therefore, DOC concentrations in these portions of the landscape are likely driven by both local (O-horizon leaching) and upslope (draining organic soil) sources during periods of high hydrologic connectivity (Gannon et al., 2015).

Presented results and interpretations compliment previous work at HBEF, where known spatial patterns in soil morphology and hydrology vary with topography. Mineral soils nearest bedrock outcrops have been described as most elementally-depleted (dominated by eluvial horizons), where is has been assumed that the frequency flushing of groundwater rich in organic acidity promotes enhanced mineral weathering rates (Bailey et al., 2019; Bower et al., 2023). Additionally, during storm events when the stream network expands upslope, it's likely these soils act as major contributing areas for rapid DOC delivery to streams, which is known to be highest in the furthest reaches of the watershed stream network (Bailey et al., 2019; Zimmer et al., 2013).

The importance of seasonality for DOC mobilization

For storms outside of snowpack season, spring and fall months were the most important time periods for organic horizon saturation across all well groups. Fall and spring organic horizon saturation occurred most frequently in soils with high UAAb values (high elevation, near bedrock outcrops). In comparison, for the same landscape position, organic horizon saturation occurred for less than half of summer storm events.

During the snow-free months, soils across the catchment are most saturated in the spring and fall, albeit for different reasons. Throughout the early spring months, soil water content is still high from antecedent snowmelt, even as the evapotranspiration rates begin to increase. During snowmelt periods, any labile DOC in the organic horizons is likely flushed out (Demers et al., 2010). Dittman et al. (2007) attribute observed low Oa solution DOC concentrations in the early spring to this "dilution phenomenon." Increased hydrologic fluxes (high saturation frequency on already moist soil) during the snow-free spring could indicate that solutions in the Oa horizon would still be relatively dilute, even though hydrologic export remains high.

As temperatures raise in the summer months and evapotranspiration increases, soils dry out and the water table decreases as rain events are not large enough to overcome moisture deficits by vegetation water demand (Campbell et al., 2011; Shanley et al., 2016). During this time, organic matter decomposition rates by enhanced microbial cycling is at an annual high. Soil solutions in the organic horizons during late summer into early fall consequently begin to accumulate C, which has been shown as distinct seasonal increases in Oa horizon DOC concentrations (Dittman et al., 2007, Fuss et al., 2011). During fall, evapotranspiration rates decrease, and soil water content increases once again. High soil moisture contents and decreased evapotranspiration rates generally promote the formation and persistence of a shallower water table. It is likely that these early fall storm events, following low-flow summers, flush out large amounts of stored C and soluble acids from the O horizon.

Differences in hydrologic controls and biologic activity suggest that drivers of DOC mobilization vary seasonally. Large early-fall storm events are likely discrete "pulse" moments for enhanced DOC mobilization annually, whereas increased high catchment wetness and dilute DOC concentrations in the spring suggest prolonged periods of DOC leaching from organic horizons. In either case, it is plausible to suggest that spring and fall events likely promote mobilization of C from the forest floor to mineral soils, providing insight to when, annually, biogeochemical processes enhanced by organic acidity might occur most frequently, especially higher in the catchment.

Conclusions and implications

At Hubbard Brook Experimental Forest, interactions of shallow groundwater with soil organic horizons varies spatially across the catchment. Water levels in positions highest in the landscape with drainage areas dominated by bedrock outcrops and shallow soils (high UAAb values) consistently reached highest into the soil profile, surpassing the Oa horizon boundary. Groundwater DOC concentrations were also greatest in these landscape positions. While several wells in lower catchment positions (small UAAb values) also frequently rose to shallower portions of the soil profile, DOC concentrations in groundwater chemistry here were lowest. It is likely that the physical mechanism of groundwater reaching organic horizons enhances DOC mobility through the leaching of

C from the O horizons (local source) and by increased hydrologic connectivity to organic soils surrounding bedrock outcrops (upslope source). Minimizing disturbance activities in higher areas of the catchment could be crucial for mediating DOC mobilization to streams and downslope C-sequestration through the formation of stable organometallic complexes (Jandl et al., 2007). Therefore, streamside management may not be as important as in shallow-to-bedrock portions of the landscape, which may be underrecognized contributors to catchment C-fluxes.

The tendency and frequency at which organic horizons became saturated was magnified by rainfall amount for all landscape positions. Seasonal differences in catchment wetness were likely a major driver in organic horizon saturation frequency, which occurred most often during the spring and fall months. Predicted alterations of the hydrologic cycle across the northeast with climate change has large implications for the timing and magnitude of flushing events and DOC mobilization. For example, decreased snowpack and an increase in freeze-thaw cycles could increase spring soil DOC concentrations through the physical degradation of SOM. This could enhance additional nutrient losses and metal export, which are already highest during the spring in this region. Additionally, large storm events (e.g., fall hurricanes, summer thunderstorms) are predicted to increase in magnitude and frequency (Hicke et al., 2022) which could shift the timing of late summer and early fall DOC mobilization events when soil C concentrations are highest, annually. Future research should examine correlations between DOC concentrations in organic horizons and groundwater chemistry with saturation frequency under varying storm intensities and antecedent conditions.

References

Anderson, M.G. and Burt, T.P., 1990. Subsurface runoff. *Process studies in hillslope hydrology.*, pp.365-400.

Anderson, M.G. and Burt, T.P., 1978. The role of topography in controlling throughflow generation. *Earth Surface Processes*, *3*(4), pp.331-344.

Bailey, S.W., Brousseau, P.A., McGuire, K.J. and Ross, D.S., 2014. Influence of landscape position and transient water table on soil development and carbon distribution in a steep, headwater catchment. *Geoderma*, *226*, pp.279-289.

Bailey, S.W., McGuire, K.J., Ross, D.S., Green, M.B. and Fraser, O.L., 2019. Mineral weathering and podzolization control acid neutralization and streamwater chemistry gradients in upland glaciated catchments, northeastern United States. *Frontiers in Earth Science*, *7*, p.63.

Bailey, S.W., J.P. Gannon, K.J. McGuire, L.H. Pardo, and A.M. Pennino. 2023. Hubbard Brook Experimental Forest: Watershed 3 Subsurface Water Chemistry ver 3. Environmental Data Initiative. https://doi.org/10.6073/pasta/d82538ddccb6b97906050e6e45cb816a (Accessed 2023-03-14).

Benton, J.R., McGuire, K.J. and Schreiber, M.E., 2022. Subsurface permeability contrasts control shallow groundwater flow dynamics in the critical zone of a glaciated, headwater catchment. *Hydrological Processes*, 36(9).

Blaschke, H., 1979. Leaching of water-soluble organic substances from coniferous needle litter. Soil Biology and Biochemistry, 11(6), pp.581-584.

Bourgault, R.R., Ross, D.S. and Bailey, S.W., 2015. Chemical and morphological distinctions between vertical and lateral podzolization at Hubbard Brook. *Soil Science Society of America Journal*, *79*(2), pp.428-439.

Bourgault, R.R., Ross, D.S., Bailey, S.W., Perdrial, N. and Bower, J., 2022. Groundwater input drives large variance in soil manganese concentration and reactivity in a forested headwater catchment. *Soil Science Society of America Journal*, *86*(6), pp.1553-1570.

Bower et al., 2023. Geoderma. *In review.*

Campbell, J.L., Driscoll, C.T., Pourmokhtarian, A. and Hayhoe, K., 2011. Streamflow responses to past and projected future changes in climate at the Hubbard Brook Experimental Forest, New Hampshire, United States. *Water Resources Research*, *47*(2).

Demers, J.D., Driscoll, C.T. and Shanley, J.B., 2010. Mercury mobilization and episodic stream acidification during snowmelt: Role of hydrologic flow paths, source areas, and supply of dissolved organic carbon. *Water Resources Research*, *46*(1).

Detty, J.M. and McGuire, K.J., 2010. Topographic controls on shallow groundwater dynamics: implications of hydrologic connectivity between hillslopes and riparian zones in a till mantled catchment. *Hydrological Processes*, 24(16), pp.2222-2236.

Dittman, J.A., Driscoll, C.T., Groffman, P.M. and Fahey, T.J., 2007. Dynamics of nitrogen and dissolved organic carbon at the Hubbard Brook Experimental Forest. *Ecology*, *88*(5), pp.1153-1166.

Doble, R.C. and Crosbie, R.S., 2017. Current and emerging methods for catchment-scale modelling of recharge and evapotranspiration from shallow groundwater. *Hydrogeology Journal*, *25*(1), p.3.

Drever, J. I., and Stillings, L.L. "The role of organic acids in mineral weathering." Colloids and Surfaces A: physicochemical and engineering aspects 120, no. 1-3 (1997): 167-181.

Drever, J.I. and Vance, G.F., 1994. Role of soil organic acids in mineral weathering processes. *Organic Acids in Geological Processes*, pp.138-161.

Fraser, O.L., Bailey, S.W., Ducey, M.J. and McGuire, K.J., 2020. Predictive modeling of bedrock outcrops and associated shallow soil in upland glaciated landscapes. *Geoderma*, *376*.

Fröberg, M., Berggren, D., Bergkvist, B., Bryant, C. and Mulder, J., 2006. Concentration and fluxes of dissolved organic carbon (DOC) in three Norway spruce stands along a climatic gradient in Sweden. *Biogeochemistry*, 77, pp.1-23.

Fuss, C.B., Driscoll, C.T., Johnson, C.E., Petras, R.J. and Fahey, T.J., 2011. Dynamics of oxidized and reduced iron in a northern hardwood forest. *Biogeochemistry*, *104*, pp.103-119.

Gannon, J.P., Bailey, S.W. and McGuire, K.J., 2014. Organizing groundwater regimes and response thresholds by soils: A framework for understanding runoff generation in a headwater catchment. *Water Resources Research*, 50(11), pp.8403-8419.

Gannon, J.P., Bailey, S.W., McGuire, K.J. and Shanley, J.B., 2015. Flushing of distal hillslopes as an alternative source of stream dissolved organic carbon in a headwater catchment. *Water Resources Research*, *51*(10), pp.8114-8128.

Guggenberger, G., Zech, W. and Schulten, H.R., 1994. Formation and mobilization pathways of dissolved organic matter: evidence from chemical structural studies

of organic matter fractions in acid forest floor solutions. *Organic Geochemistry*, 21(1), pp.51-66.

Gillin, C.P., Bailey, S.W., McGuire, K.J. and Gannon, J.P., 2015. Mapping of hydropedologic spatial patterns in a steep headwater catchment. *Soil Science Society of America Journal*, *79*(2), pp.440-453.

Godsey, S.E., Kirchner, J.W. and Clow, D.W., 2009. Concentration–discharge relationships reflect chemostatic characteristics of US catchments. *Hydrological Processes: An International Journal*, *23*(13), pp.1844-1864.

Hornberger, G.M., Bencala, K.E. and McKnight, D.M., 1994. Hydrological controls on dissolved organic carbon during snowmelt in the Snake River near Montezuma, Colorado. *Biogeochemistry*, *25*, pp.147-165.

Huber, C., Filella, M. and Town, R.M., 2002. Computer modelling of trace metal ion speciation: practical implementation of a linear continuous function for complexation by natural organic matter. *Computers & Geosciences*, *28*(5), pp.587-596.

Inamdar, S., Rupp, J. and Mitchell, M., 2009. Groundwater flushing of solutes at wetland and hillslope positions during storm events in a small, glaciated catchment in western New York, USA. *Hydrological Processes: An International Journal*, *23*(13), pp.1912-1926.

Jandl, R., Lindner, M., Vesterdal, L., Bauwens, B., Baritz, R., Hagedorn, F., Johnson, D.W., Minkkinen, K. and Byrne, K.A., 2007. How strongly can forest management influence soil carbon sequestration?. *Geoderma*, *137*(3-4), pp.253-268.

Jencso, K.G., McGlynn, B.L., Gooseff, M.N., Wondzell, S.M., Bencala, K.E. and Marshall, L.A., 2009. Hydrologic connectivity between landscapes and streams: Transferring reach-and plot-scale understanding to the catchment scale. *Water Resources Research*, 45(4).

Kalbitz, K., Solinger, S., Park, J.H., Michalzik, B. and Matzner, E., 2000. Controls on the dynamics of dissolved organic matter in soils: a review. *Soil Science*, *165*(4), pp.277-304.

Krishna, M.P. and Mohan, M., 2017. Litter decomposition in forest ecosystems: a review. *Energy, Ecology and Environment*, *2*, pp.236-249.

Lawrence, C., Harden, J. and Maher, K., 2014. Modeling the influence of organic acids on soil weathering. *Geochimica et Cosmochimica Acta*, *139*, pp.487-507.

LoRusso, N.A., Bailey, S.W., Zeng, T., Montesdeoca, M. and Driscoll, C.T., 2021. Dissolved Organic Matter Dynamics in Reference and Calcium Silicate-Treated Watersheds at Hubbard Brook Experimental Forest, NH, USA. *Journal of Geophysical Research: Biogeosciences*, *126*(7).

Lin, H., 2003. Hydropedology: Bridging disciplines, scales, and data. *Vadose Zone Journal*, *2*(1), pp.1-11.

Lundström, U.S., van Breemen, N. and Bain, D., 2000. The podzolization process. A review. *Geoderma*, *94*(2-4), pp.91-107.

Ma, Y.J., Li, X.Y., Guo, L. and Lin, H., 2017. Hydropedology: Interactions between pedologic and hydrologic processes across spatiotemporal scales. *Earth-science Reviews*, *171*, pp.181-195.

McClain, M.E., Boyer, E.W., Dent, C.L., Gergel, S.E., Grimm, N.B., Groffman, P.M., Hart, S.C., Harvey, J.W., Johnston, C.A., Mayorga, E. and McDowell, W.H., 2003. Biogeochemical hot spots and hot moments at the interface of terrestrial and aquatic ecosystems. *Ecosystems*, pp.301-312.

McDowell, W.H. and Likens, G.E., 1988. Origin, composition, and flux of dissolved organic carbon in the Hubbard Brook Valley. *Ecological Monographs*, *58*(3), pp.177-195.

McGlynn, B.L. and McDonnell, J.J., 2003a. Role of discrete landscape units in controlling catchment dissolved organic carbon dynamics. *Water Resources Research*, *39*(4).

McGlynn, B.L. and McDonnell, J.J., 2003b. Quantifying the relative contributions of riparian and hillslope zones to catchment runoff. *Water Resources Research*, *39*(11).

Neff, J.C. and Asner, G.P., 2001. Dissolved organic carbon in terrestrial ecosystems: synthesis and a model. *Ecosystems*, 4, pp.29-48.

Penna, D., van Meerveld, H.J., Oliviero, O., Zuecco, G., Assendelft, R.S., Dalla Fontana, G. and Borga, M.A.R.C.O., 2015. Seasonal changes in runoff generation in a small forested mountain catchment. *Hydrological Processes*, *29*(8), pp.2027-2042.

Preston, C.M., Trofymow, J.A. and Working Group, T.C.I.D.E., 2000. Variability in litter quality and its relationship to litter decay in Canadian forests. *Canadian Journal of Botany*, *78*(10), pp.1269-1287.

Qualls, R.G., Haines, B.L. and Swank, W.T., 1991. Fluxes of dissolved organic nutrients and humic substances in a deciduous forest. *Ecology*, *72*(1), pp.254-266.

Raulund-Rasmussen, K., Borggaard, O.K., Hansen, H.C.B. and Olsson, M., 1998. Effect of natural organic soil solutes on weathering rates of soil minerals. *European Journal of Soil Science*, *49*(3), pp.397-406.

Rinderer, M., van Meerveld, I., Stähli, M. and Seibert, J., 2016. Is groundwater response timing in a pre-alpine catchment controlled more by topography or by rainfall?. *Hydrological Processes*, *30*(7), pp.1036-1051.

Seibert, J. and McGlynn, B.L., 2007. A new triangular multiple flow direction algorithm for computing upslope areas from gridded digital elevation models. *Water Resources Research*, *43*(4).

Shanley, J.B., Sebestyen, S.D., McDonnell, J.J., McGlynn, B.L. and Dunne, T., 2015. Water's Way at Sleepers River watershed–revisiting flow generation in a post-glacial landscape, Vermont USA. *Hydrological Processes*, *29*(16), pp.3447-3459.

Shanley, J.B., Chalmers, A.T., Mack, T.J., Smith, T.E. and Harte, P.T., 2016. Groundwater level trends and drivers in two northern New England glacial aquifers. *JAWRA Journal of the American Water Resources Association*, *52*(5), pp.1012-1030.

Sidle, R.C., Tsuboyama, Y., Noguchi, S., Hosoda, I., Fujieda, M. and Shimizu, T., 2000. Stormflow generation in steep forested headwaters: a linked hydrogeomorphic paradigm. *Hydrological Processes*, *14*(3), pp.369-385.

Singh, N.K., Emanuel, R.E., Nippgen, F., McGlynn, B.L. and Miniat, C.F., 2018. The relative influence of storm and landscape characteristics on shallow groundwater responses in forested headwater catchments. *Water Resources Research*, *54*(12), pp.9883-9900.

Swank, W.T. and Douglass, J.E., 1974. Streamflow greatly reduced by converting deciduous hardwood stands to pine. *Science*, *185*(4154), pp.857-859.

Tang, W. and Carey, S.K., 2017. Hyd R un: a MATLAB toolbox for rainfall–runoff analysis. *Hydrological Processes*, 31(15), pp.2670-2682.

Tromp-van Meerveld, H.J. and McDonnell, J.J., 2006. Threshold relations in subsurface stormflow: 1. A 147-storm analysis of the Panola hillslope. *Water Resources Research*, *42*(2).

Welsch, D.L., Kroll, C.N., McDonnell, J.J. and Burns, D.A., 2001. Topographic controls on the chemistry of subsurface stormflow. *Hydrological Processes*, *15*(10), pp.1925-1938.

Zimmer, M.A., Bailey, S.W., McGuire, K.J. and Bullen, T.D., 2013. Fine scale variations of surface water chemistry in an ephemeral to perennial drainage network. *Hydrological Processes*, *27*(24), pp.3438-3451.

Appendix C

Table C1. Precipitation information for each storm for when a groundwater level metrics were calculated during the snow-free months.

Start	End	Total Precipitation (mm)	Event Duration (hr)	Max Hourly Intensity (mm/hr)	Whole Storm Intensity (mm/hr)
7/6/11 16:30	7/6/11 20:45	14.0	4.3	9.4	3.3
7/8/11 20:15	7/9/11 2:45	13.5	6.5	11.1	2.1
7/25/11 20:00	7/26/11 1:45	8.2	5.8	2.6	1.4
7/29/11 15:00	7/29/11 22:00	11.7	7.0	4.2	1.7
8/6/11 22:00	8/7/11 12:15	14.6	14.3	2.6	1.0
8/9/11 18:00	8/10/11 21:30	29.4	27.5	3.8	1.1
8/14/11 4:30	8/16/11 12:15	96.3	55.8	16.1	1.7
8/21/11 14:45	8/22/11 2:30	43.7	11.8	10.5	3.7
8/25/11 11:45	8/25/11 22:30	16.1	10.8	13.5	1.5
8/27/11 19:00	8/29/11 1:00	151.5	30.0	17.5	5.1
9/4/11 19:30	9/6/11 7:00	45.0	35.5	10.2	1.3
9/7/11 2:15	9/8/11 4:00	26.0	25.8	2.9	1.0
9/15/11 7:00	9/15/11 17:15	15.2	10.3	8.9	1.5
9/22/11 6:15	9/22/11 20:45	19.2	14.5	6.3	1.3
9/23/11 21:00	9/24/11 11:45	9.9	14.8	2.6	0.7
9/29/11 2:45	9/29/11 22:45	39.9	20.0	7.1	2.0
9/30/11 18:00	10/2/11 22:30	80.9	52.5	19.8	1.5
10/13/11 6:00	10/13/11 11:00	9.4	5.0	4.1	1.9
10/14/11 7:15	10/15/11 2:30	49.1	19.3	8.6	2.6
10/19/11 14:30	10/20/11 6:15	10.8	15.8	3.6	0.7
10/27/11 1:00	10/27/11 20:00	11.4	19.0	1.8	0.6
10/29/11 17:15	10/30/11 8:00	15.8	14.8	2.8	1.1
11/10/11 14:15	11/11/11 5:30	16.9	15.3	5.8	1.1
11/14/11 19:45	11/15/11 0:30	7.4	4.8	3.4	1.6
11/16/11 16:15	11/16/11 23:15	9.4	7.0	1.8	1.3
11/23/11 0:00	11/23/11 12:15	37.5	12.3	5.8	3.1
11/29/11 13:30	11/30/11 5:45	36.2	16.3	9.3	2.2
5/1/12 3:15	5/1/12 14:00	21.0	10.8	3.4	2.0
5/4/12 0:30	5/4/12 16:15	16.5	15.8	6.0	1.0
5/8/12 4:45	5/9/12 1:00	63.6	20.3	7.2	3.1
5/9/12 14:00	5/10/12 9:15	14.8	19.3	3.1	0.8
5/14/12 8:15	5/16/12 0:00	41.8	39.8	3.9	1.1
5/16/12 19:00	5/16/12 23:00	7.5	4.0	5.9	1.9
5/25/12 3:00	5/25/12 17:00	8.6	14.0	2.0	0.6

5/28/12 23:15	5/29/12 21:00	59.0	21.8	17.5	2.7
6/2/12 5:15	6/4/12 21:30	66.7	64.3	9.9	1.0
6/6/12 6:30	6/7/12 0:00	8.7	17.5	3.3	0.5
6/8/12 14:15	6/8/12 21:00	8.0	6.8	4.7	1.2
6/12/12 19:15	6/13/12 9:00	41.9	13.8	4.8	3.0
6/25/12 1:30	6/25/12 19:00	40.4	17.5	22.6	2.3
7/4/12 2:45	7/4/12 18:45	17.1	16.0	9.1	1.1
7/17/12 8:15	7/18/12 0:30	7.8	16.3	2.4	0.5
7/23/12 20:30	7/24/12 17:00	23.0	20.5	5.4	1.1
7/26/12 18:15	7/27/12 7:15	11.1	13.0	5.4	0.9
7/28/12 16:00	7/28/12 18:45	11.4	2.8	4.6	4.1
7/29/12 13:00	7/29/12 15:00	10.8	2.0	7.0	5.4
8/1/12 22:45	8/1/12 23:30	9.6	0.8	9.6	12.8
8/5/12 14:30	8/5/12 22:30	13.8	8.0	9.1	1.7
8/9/12 19:15	8/11/12 0:15	135.3	29.0	43.4	4.7
8/15/12 4:45	8/15/12 17:30	7.7	12.8	4.8	0.6
8/27/12 17:30	8/28/12 4:15	33.0	10.8	8.7	3.1
9/2/12 3:45	9/2/12 7:15	6.9	3.5	4.7	2.0
9/4/12 5:00	9/5/12 7:45	30.3	26.8	4.1	1.1
9/8/12 15:00	9/9/12 0:15	22.9	9.3	10.4	2.5
9/18/12 10:30	9/19/12 3:45	89.2	17.3	12.1	5.2
9/22/12 22:30	9/23/12 2:15	7.2	3.8	4.4	1.9
9/28/12 9:15	9/29/12 6:15	14.0	21.0	2.6	0.7
9/29/12 22:30	10/1/12 11:45	13.0	37.3	1.6	0.3
10/3/12 6:30	10/4/12 14:00	19.1	31.5	10.1	0.6
10/7/12 21:00	10/8/12 1:15	6.6	4.3	2.4	1.6
10/10/12 9:00	10/11/12 6:45	9.6	21.8	3.1	0.4
10/14/12 0:15	10/14/12 13:30	9.8	13.3	2.8	0.7
10/19/12 8:30	10/20/12 4:00	39.8	19.5	6.3	2.0
10/29/12 16:30	10/31/12 10:15	68.8	41.8	17.1	1.6
11/13/12 4:00	11/13/12 12:00	16.1	8.0	3.9	2.0
5/8/13 18:00	5/9/13 15:30	10.3	21.5	3.6	0.5
5/11/13 2:00	5/11/13 21:00	26.3	19.0	8.7	1.4
5/19/13 16:45	5/20/13 8:45	22.1	16.0	4.0	1.4
5/21/13 20:15	5/22/13 3:15	14.3	7.0	9.2	2.0
5/22/13 16:45	5/24/13 7:00	11.4	38.3	2.6	0.3
5/24/13 19:45	5/26/13 4:30	27.3	32.8	3.6	0.8
5/29/13 4:45	5/29/13 14:15	8.2	9.5	3.4	0.9
6/2/13 14:00	6/2/13 21:30	27.9	7.5	20.4	3.7
6/6/13 20:30	6/8/13 4:15	26.1	31.8	2.6	0.8
6/10/13 19:00	6/12/13 9:45	39.2	38.8	6.3	1.0

6/22/13 16:15	6/23/13 18:00	14.5	25.8	3.6	0.6
6/24/13 15:15	6/24/13 23:30	18.2	8.3	13.7	2.2
6/28/13 2:30	6/29/13 17:30	38.3	39.0	11.5	1.0
7/1/13 17:45	7/2/13 23:00	68.0	29.3	13.7	2.3
7/7/13 22:15	7/8/13 22:30	14.1	24.3	4.8	0.6
7/10/13 4:15	7/10/13 18:00	18.7	13.8	4.6	1.4
7/17/13 20:00	7/17/13 23:30	16.9	3.5	12.3	4.8
7/23/13 1:15	7/23/13 15:00	39.5	13.8	12.4	2.9
5/1/19 14:15	5/3/19 23:00	34.6	56.8	5.0	0.6
5/7/19 10:45	5/7/19 17:45	10.6	7.0	2.4	1.5
5/9/19 19:30	5/10/19 14:30	36.6	19.0	5.1	1.9
5/13/19 19:30	5/14/19 6:15	6.8	10.8	1.5	0.6
5/17/19 4:15	5/17/19 19:15	6.8	15.0	3.1	0.5
5/19/19 17:30	5/20/19 19:15	29.7	25.8	9.5	1.2
5/23/19 16:45	5/24/19 6:30	17.2	13.8	6.3	1.3
5/25/19 19:15	5/26/19 4:00	17.4	8.8	8.9	2.0
5/28/19 10:00	5/28/19 23:30	23.0	13.5	3.6	1.7
6/4/19 19:45	6/6/19 6:15	40.8	34.5	4.1	1.2
6/10/19 23:00	6/11/19 10:30	39.8	11.5	7.3	3.5
6/20/19 4:00	6/22/19 0:30	45.4	44.5	9.7	1.0
6/25/19 10:45	6/26/19 5:30	18.0	18.8	4.9	1.0
6/26/19 20:15	6/26/19 22:30	9.3	2.3	7.9	4.1
6/29/19 19:30	6/30/19 17:15	14.5	21.8	4.9	0.7
7/6/19 14:00	7/6/19 15:45	10.7	1.8	9.9	6.1
7/11/19 14:30	7/12/19 2:00	69.6	11.5	22.4	6.1
7/22/19 11:30	7/23/19 8:15	14.5	20.8	1.8	0.7
7/28/19 19:30	7/28/19 22:15	7.2	2.8	3.6	2.6
7/30/19 19:00	8/1/19 2:45	29.7	31.8	17.0	0.9
8/7/19 16:15	8/8/19 13:15	40.7	21.0	31.2	1.9
8/16/19 1:30	8/16/19 8:30	6.7	7.0	4.1	1.0
8/21/19 9:45	8/22/19 3:30	27.4	17.8	8.7	1.5
8/28/19 17:15	8/29/19 2:30	35.2	9.3	13.0	3.8
9/2/19 0:45	9/3/19 0:15	48.1	23.5	7.2	2.0
9/10/19 22:45	9/11/19 6:45	9.8	8.0	3.6	1.2
9/23/19 18:45	9/23/19 22:00	11.7	3.3	4.1	3.6
9/26/19 12:30	9/26/19 17:30	9.3	5.0	3.1	1.9
9/30/19 23:00	10/1/19 7:30	8.5	8.5	3.1	1.0
10/1/19 20:45	10/2/19 3:45	6.6	7.0	3.6	0.9
10/3/19 20:45	10/4/19 5:15	7.8	8.5	1.9	0.9
10/6/19 14:15	10/8/19 1:00	17.4	34.8	2.8	0.5
10/16/19 19:30	10/17/19 20:30	25.0	25.0	4.1	1.0

10/22/19 19:30	10/23/19 7:30	18.3	12.0	3.6	1.5
10/27/19 5:15	10/30/19 2:15	45.2	69.0	4.3	0.7
10/30/19 22:30	11/1/19 7:45	50.2	33.3	7.6	1.5
11/7/19 12:45	11/8/19 19:30	7.4	30.8	1.2	0.2
11/11/19 7:30	11/12/19 11:15	17.5	27.8	2.1	0.6
11/18/19 23:15	11/19/19 18:00	17.7	18.8	6.1	0.9
11/22/19 0:00	11/22/19 17:30	8.2	17.5	2.6	0.5
11/24/19 6:15	11/24/19 22:15	28.8	16.0	6.4	1.8
11/27/19 17:15	11/28/19 12:45	22.4	19.5	4.7	1.1
5/8/20 22:45	5/9/20 8:45	13.6	10.0	2.9	1.4
5/11/20 13:30	5/12/20 2:30	11.1	13.0	4.8	0.9
5/15/20 17:45	5/16/20 1:00	12.8	7.3	6.4	1.8
5/29/20 19:30	5/30/20 0:00	7.0	4.5	3.3	1.6
6/28/20 14:30	7/2/20 4:45	81.0	86.3	34.5	0.9
7/8/20 13:45	7/9/20 6:00	8.0	16.3	3.0	0.5
7/11/20 0:30	7/11/20 11:45	22.3	11.3	4.4	2.0
7/14/20 5:15	7/14/20 8:45	30.1	3.5	17.3	8.6
7/17/20 1:45	7/17/20 12:00	10.7	10.3	3.3	1.0
7/22/20 22:15	7/23/20 19:15	8.6	21.0	4.6	0.4
8/4/20 9:00	8/4/20 22:00	22.1	13.0	6.1	1.7

Research Conclusions

While there has been a substantial decline in acid deposition following the 1990 Amendments to the Clean Air Act, forests across the northeastern US still see effects from chronic acidification on soil nutrient pools and surface water chemistry. While overall precipitation inputs of acidity have decreased, seasonal shifts in water flow paths and sources of organic acidity through soil can regulate episodic stream water acidification during hydrologic events. At the same time, increases in solution acidity and soil-water interactions enhances mineral weathering reactions, which are important for the replenishment of nutrients, especially in base-poor ecosystems. However, weathering inputs are difficult to measure since overall soil nutrient fluxes from biotic cycling and ion-exchange processes happen at much more rapid paces.

The influence of catchment structure on the distribution of soil moisture across landscapes is widely recognized. Yet, it is still not well quantified where, when, and how subsurface flow affects chemical weathering processes. Often, signals of mineral weathering are inferred from stream export chemistry, and sources are usually partitioned into deeper or shallower flow path contributions. Deeper subsurface flow paths, lower in the regolith, which are highly concentrated in weathering nutrients due to increased water residence time with reactive minerals whereas waters draining from shallow soils are more enriched in organic acids. However, in steep mountainous landscapes, depth to bedrock and solution chemistry is highly variable along hillslopes, therefore there is likely a lot more intra-watershed variability in chemical weathering processes within the shallow zone itself than previously thought. While evidence of this has been observed through differences in soil development (extent of long-term mineral weathering alteration) across catchments, current weathering processes driven by differences in subsurface flow dynamics in the shallow subsoil are still not well understood.

This dissertation focused on the effects of subsurface flow on the mobilization and distribution of dissolved organic carbon (DOC) and weatherable solutes to explain spatial patterns in chemical weathering in a forested headwater catchment.

Results from these dissertation chapters conclude the following:

(1) Annual fluxes of weatherable elements (Ca^{2+}, Mg^{2+}, Na^{+}) in the shallow soil zone systematically varied with groundwater saturation frequency (the number of times soils saturated and drained), DOC concentrations, and whole-profile elemental depletion. This likely reflects the influence of subsurface flow dynamics and solution chemistry on present-day and historical mineral weathering patterns across the catchment.
(2) Annual and event-based subsurface flow dynamics were not uniform in this catchment and varied predictably with surface topography and upslope drainage characteristics.
(3) During storm events, peak water level height reached in the soil profile best explains DOC groundwater concentrations, providing a flushing mechanism for DOC mobility in which rising water tables intercept and drain shallower portions of the soil profile enriched in C. At higher portions in the landscape, shallower water tables are likely hydrologic connected to upslope organic soils surrounding bedrock outcrops, which have high permeability and limited water storage, which can rapidly drain downslope to mineral soils. This helps explain observed spatial deviations in DOC concentrations and saturation frequency across the catchment.
(4) Saturation of the organic horizon was greatest during the spring and fall months, especially in portions of the landscape closest to bedrock outcrops and shallow organic soils, which could identify key moments and catchment positions for enhanced DOC mobilization through the shallow soil zone.

Conclusions from this body of research underscores the importance of long-term, spatially extensive studies for understanding variability in hydrological and biogeochemical processes across catchments. It is evident from this work, and many others, that catchment structure plays an important role in mediating subsurface flow dynamics. This study extends what is previously known to suggest that hydrologic variability in the shallow soil zone is what controls the mobilization and transport of

organic acids and ultimately drives the spatial structure of chemical weathering processes within a catchment.

Using similar approaches to research and monitoring will likely be critical for understanding ecosystem responses to the alteration and intensification of hydrologic cycles and land use changes across the northeast. Therefore, investigating relationships between the timing and/or magnitude of extreme precipitation events on base cation weathering rates could be an important future area of research in regions that have been altered by chronic acidification.